Tunable Heparan Sulfate Glycomimetics for Modulating Chemokine Activity

Thesis by
Gloria J. Sheng

In Partial Fulfillment of the Requirements for the Degree
of
Doctor of Philosophy

CALIFORNIA INSTITUTE OF TECHNOLOGY
Pasadena, California
2014
(Defended July 30, 2013)

In memory of Long Phan

ACKNOWLEDGEMENTS

I owe my deepest gratitude to those who have provided me with support, mentorship, and friendship throughout the years. First, I would like to thank my adviser Linda Hsieh-Wilson for her guidance and motivation. Thank you for believing in me and providing me with many hands-on opportunities to further my scientific development. I have learned many important lessons, such as never backing down against a difficult reviewer. Without your investment in my personal growth, I would not have found the courage to apply my scientific training to a new career in medicine. I look forward to opportunities for clinical collaborations with your group in the future.

I would also like to thank the members of my committee, Dennis Dougherty, Frances Arnold, and Sarkis Mazmanian. Thank you for your unwavering support all throughout graduate school. I could not have asked for a more enthusiastic group of professors to serve on my committee. You have all provided me with lots of useful advice and scientific insight, and I always looked forward to our interactions.

My research endeavors would not have been possible without the wonderful staff in the Chemistry department. To Anne Penney, Agnes Tong, Joe Drew, Mona Shahgholi, Scott Ross, David Vander Velde, Susan Mucha, and Joelle Radford, I owe you all my deepest gratitude. Thank you for your hard work and positive interactions throughout the day.

I am extremely grateful to have met Joe Shepherd, Felicia Hunt, Anneila Sargent, and John Dabiri and to have had the opportunity to work with them on various projects addressing quality of life and work-life balance at Caltech. Thank you for being so receptive to student ideas and dedicating many hours of your time to organizing the Student-Faculty Colloquium. It was truly a pleasure to work with each of you.

Though I did not successfully convince any of my family members to move out to the West Coast, they have provided me with unconditional love and Facebook likes from afar. Mom and Dad, thank you for your endless words of encouragement. I am grateful to have your unwavering support of my ever-changing life decisions. Your emails are quite strange, but they make me laugh and remind me of what it is like to be home again. Grandpa and grandma, thank you for imparting your spiritual wisdom throughout the years. I have benefited so much from your teachings and hope that I am able to make you very proud. Aunt Hosanna, Uncle Matthew, Aunt Sarah, you have all been incredible mentors to me. Thank you for teaching me the importance of self-discipline and work ethic; the summers that I spent with you as a child have undeniably shaped me into the person that I am today. Laura Kuah, Michelle Kuah, Josh Sheng, and Jed Sheng, having you as cousins has definitely compensated for the fact that I dislike being an only child. Thank you for all the vacations, shopping hauls, laser tag and video game sessions, and inside jokes on repeat. You guys understand my sense of humor (and its precise genetic basis) better than anyone else. I cannot wait to return to the East Coast and spend more time with each of you.

The wonderful and brilliant people that I have met at Caltech will largely define my memories from here. Elisabeth Wang, Elizabeth Jensen, and Betty (ElizaBetty) Wong, thank you for being so kind and thoughtful, and bringing so much laughter and meaning to my graduate school experience. Paul Nelson, thank you for the many hours of sleep and Quake (but not math) that you gave up for me. You always invented creative ways to keep my imagination alive during our most monotonous of times at Caltech. I am grateful to always have you as my biggest supporter and number one fan; I am yours as well. Emzo De Los Santos, Naeem Husain, Sandy Nandagopal, and Naomi Kreamer, thank you for your endless compassion and loyalty, and all the amazing times we shared together. I am extremely grateful for your friendships. Jeff Holder, David Yeaton-Massey, and Terry Gdoutos, thank you for your refreshing honesty. You are amazing listeners; I am glad to be able to count on

you for advice and perspective. Allen Hong and Matt Winston, thank you for being my confidants from the very first day of graduate school. We have been through a lot together, but I know that we will look back at our Caltech experiences with a special fondness and nostalgia. Landry Fokoua, Chris Marotta, Hanqing Li, and Ryan Henning, thank you for the many enjoyable conversations; you know exactly how to brighten up my day. Jerzy Szablowski, thank you for always bringing me ice cream on a moment's notice. Thibaud Talon, Andreï Pissarenko, Thibault Flinois, Sirgay Monaco, Murat Koloğlu, Matt Fishman, Valérie Payré, Julia Pitzer, and Victor Luo, thank you for bringing in the sunshine, literally and metaphorically, to my last summer in graduate school.

Finally, I would like to thank the Linda Hsieh-Wilson group for fostering a positive and stimulating research environment. I have gained something unique from each member of the group and so it is literally impossible to express the depth of my appreciation here. In my partial attempt to do so: Young In Oh and Mike Chang, thank you for being my earliest mentors at Caltech and paving the way for my work. I have learned so much from both of you, and will always be thankful for your friendship and support. Peter Clark, Jessica Rexach, and Jessica Dweck, thank you for the many late conversations about science and life outside of science. Abigail Pulsipher, Shannon Stone, Jeanluc Chaubard, Gregory Miller, and Kuang-Wei Yang, thank you for being the best listeners. Research always has its very unique set of challenges and you guys have offered me wonderful insights on how to understand and tackle them. Matt Griffin, Claude Rogers, Josh Brown, Andrew Wang, Sheldon Cheung, and Chithra Krishnamurthy, thank you for providing scientific advice on how to navigate through biological experiments. I would have struggled a lot on my own if it were not for your willingness to help. To all members of the Hsieh-Wilson lab, past and present: you are an incredible group of talented and fearless scientists, and it has truly been an honor to work with each of you.

ABSTRACT

Heparan sulfate (HS) glycosaminoglycans participate in critical biological processes by modulating the activity of a diverse set of protein binding partners. Such proteins include all known members of the chemokine superfamily, which are thought to guide the migration of distinct subsets of immune cells through their interactions with HS proteoglycans on endothelial cell surfaces. Animal-derived heparin polysaccharides have been shown to reduce inflammation levels through the inhibition of HS-chemokine interactions; however, the clinical usage of heparin as an anti-inflammatory drug is hampered by its anticoagulant activity and potential risk for side effects, such as heparin-induced thrombocytopenia (HIT).

Here, we describe an expedient, divergent synthesis to prepare defined glycomimetics of HS that recapitulate the macromolecular structure and biological activity of natural HS glycosaminoglycans. Our synthetic approach uses a core disaccharide precursor to generate a library of four differentially sulfated polymers. We show that a trisulfated glycopolymer antagonizes the chemotactic activities of pro-inflammatory chemokine RANTES with similar potency as heparin polysaccharide, without potentiating the anticoagulant activities of antithrombin III. The same glycopolymer also inhibited the homeostatic chemokine SDF-1 with significantly more efficacy than heparin. Our work offers a general strategy for modulating chemokines and dissecting the pleiotropic functions of HS/heparin through the presentation of defined sulfation motifs within multivalent polymeric scaffolds.

TABLE OF CONTENTS

LIST OF ABBREVIATIONS

APTT	Activated Partial Thromboplastin Time
ATIII	Antithrombin III
CS	Chondroitin Sulfate
DBU	1,8-Diazabicycloundec-7-ene
DCE	Dichloroethane
DIPEA	*N*,*N*-Diisopropylethylamine
DS	Dermatan Sulfate
EC_{50}	Half-Maximal Effective Concentration
ELISA	Enzyme-Linked Immunosorbent Assay
FIIa	Factor IIa
FBS	Fetal Bovine Serum
FGF	Fibroblast Growth Factor
FXa	Factor Xa
GDNF	Glial cell line-Derived Neurotrophic Factor
GlcA	D-Glucuronic Acid
GlcN	Glucosamine
GlcNAc	*N*-Acetylglucosamine
GPCR	G-Protein Coupled Receptor
GPI	Glycosylphosphatidylinositol
Gro-α	Growth Related Oncogene-α
HBSS	Hank's Balanced Salt Solution
HIT	Heparin-Induced Thrombocytopenia
HRP	Horseradish Peroxidase
HS	Heparan Sulfate
IC_{50}	Half-Maximal Inhibitory Concentration
IdoA	L-Iduronic Acid
IL-8	Interleukin-8
NA	*N*-Acetylated
NS	*N*-Sulfated
NSI	Non-Syncitum-Inducing
PBS	Phosphate-Buffered Saline
PDGF	Platelet-Derived Growth Factor
PE	Phycoerythrin
PES	Polyethersulfone
PF-4	Platelet Factor 4
PMB	*para*-Methoxybenzylether
PT	Prothrombin Time
RANTES	Regulated on Activation, Normal T cell Expressed and Secreted
ROMP	Ring-Opening Metathesis Polymerization
SEC-MALS	Size Exclusion Chromatography Multi-Angle Light Scattering
SEM	[2-(Trimethylsilyl)Ethoxy]Methyl Acetal
SDF-1	Stromal cell-Derived Factor 1
TLC	Thin-Layer Chromatography
TMB	3,3',5,5'-Tetramethylbenzidine
TMSOK	Potassium Trimethylsilanolate

TMSOTf	Trimethylsilyl Trifluoromethanesulfonate
TBAI	Tetrabutylammonium Iodide
TBS	*tert*-Butyldimethylsilyl
TBSOTf	*tert*-Butyldimethylsilyl Trifluoromethanesulfonate
VEGF	Vascular Endothelial Growth Factor

C h a p t e r 1

HEPARAN SULFATE AND HEPARIN POLYSACCHARIDES

Structural Features of Heparan Sulfate Proteoglycans

Heparan sulfate (HS) proteoglycans are cell surface and extracellular matrix macromolecules that comprise a core protein to which HS glycosaminoglycan (GAG) chains are covalently linked. Their remarkable structural diversity and ubiquitous expression allows them to regulate a wide variety of normal and pathophysiological activities, including development, blood coagulation, metastasis, angiogenesis, and inflammation.[1] HS proteoglycans can be classified into three families based on their core protein structure: membrane-spanning proteoglycans (syndecans, betaglycans, CD44v3), glycosylphosphatidylinositol (GPI)-linked proteoglycans (glypicans), and secreted extracellular matrix proteoglycans (perlecan, agrin, collagen XVII). Hematopoietic stem cells also carry an intracellular proteoglycan known as serglycin, which is important for the retention of several inflammatory mediators in storage granules and secretory vesicles. Some HS proteoglycans are hybridized with chondroitin sulfate (CS) and/or dermatan sulfate (DS) chains, resulting in even greater diversification of their biological activities. Notably, all major forms of HS proteoglycans are evolutionarily conserved from vertebrates to *Drosophilia* and *C. elegans*, thereby enabling their functional and genetic analyses in model organism systems.[2]

The structural complexity of HS proteoglycans arises largely from heterogeneous sugar chains that decorate the core protein. HS chains are assembled by the three-step sequential action (initiation, polymerization, and elaboration) of glycosyltransferase and modification enzymes found in the Golgi (Figure 1). Nascent HS polysaccharides arise from the stepwise addition of D-glucuronic acid (GlcA) and *N*-acetylglucosamine (GlcNAc) units to the reducing end of an initiating tetrasaccharide linker (xylose-galactose-galactose-uronic acid), generating a backbone of 40-300 units in length.[3]

Further modifications are then made at distinct sites along the polysaccharide chain, which include *N*-deacetylation and *N*-sulfonation of GlcNAc, C5 epimerization of GlcA to L-iduronic acid (IdoA), and *O*-sulfonation at the 2-*O* position of IdoA or GlcA and the 6-*O* or 3-*O* positions of GlcNAc. Importantly, the overall organization of the anionic sulfate and carboxyl groups dictate the precise location of the ligand-binding sites, and their addition to the chain is regulated by cell type and the presence of specific growth factors in the extracellular environment.[4]

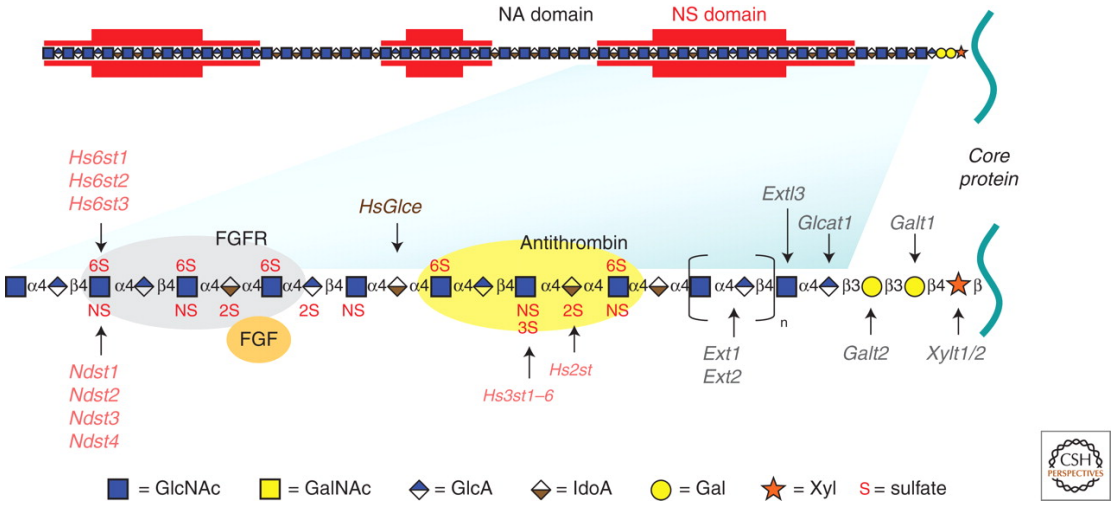

Figure 1. Macromolecular organization and fine structure of heparan sulfate (HS) and heparin. Biosynthesis is initiated by the addition of xylose to serine residues on the core protein. Extl3 attaches the first N-acetyl-D-glucosamine (GlcNAc), and then an enzyme complex comprised of Ext1 and Ext2 adds repeating units of GlcA and GlcNAc to the nascent chain. Late-stage processing of the chain includes deacetylation and *N*-sulfonation of GlcNAc by *N*-deacetylase-*N*-sulfotransferase (Ndst), C5 epimerization of D-glucoronic acid (GlcA) to L-iduronic acid (IdoA) by C5 epimerase (HsGlce), and a series of *O*-sulfonation modifications by uronyl 2-*O*-sulfotransferase (Hs2st), glucosaminyl 6-*O*-sulfotransferases (Hs6st1-3), and glucosaminyl 3-*O*-sulfotransferases (Hs3st1, 2, 3a, 3b, 4, 5, 6). Modifications generally occur within *N*-sulfated (NS) domains, which are interspersed by unmodified *N*-acetylated (NA) domains. Adapted from [3].

The anticoagulant drug heparin, purified from the secretory granules of mast cells, shares many of the structural features of HS; in fact, the two species are referred to interchangeably in the chemical literature.[5] Like HS, heparin is comprised of alternating units of glucosamine and uronic acid, and can undergo epimerization, *N*-sulfonation, and *O*-sulfonation at the same positions. On average, heparin contains 2.3 sulfate groups per disaccharide unit, while HS possesses 0.8 sulfate groups.[3]

Thus, heparin exhibits higher overall levels of *N*-sulfation and has greater conversion of GlcA to IdoA, which facilitates elaborations such as 6-*O*-sulfonation of glucosamine residues and 2-*O*-sulfonation of uronic acid residues.[6] As a result, trisulfated disaccharide IdoA2S-GlcNS6S is the major repeating unit found within heparin polysaccharides and constitutes the majority of the *N*-sulfated (NS) domains. In contrast, HS chains have large clusters of unmodified GlcNAc and GlcA residues that form the *N*-acetylated (NA) domains (Figure 1). These domains are interspersed by NS and mixed NS/NA clusters, both of which enable HS proteoglycans to recognize multiple types of protein ligands.

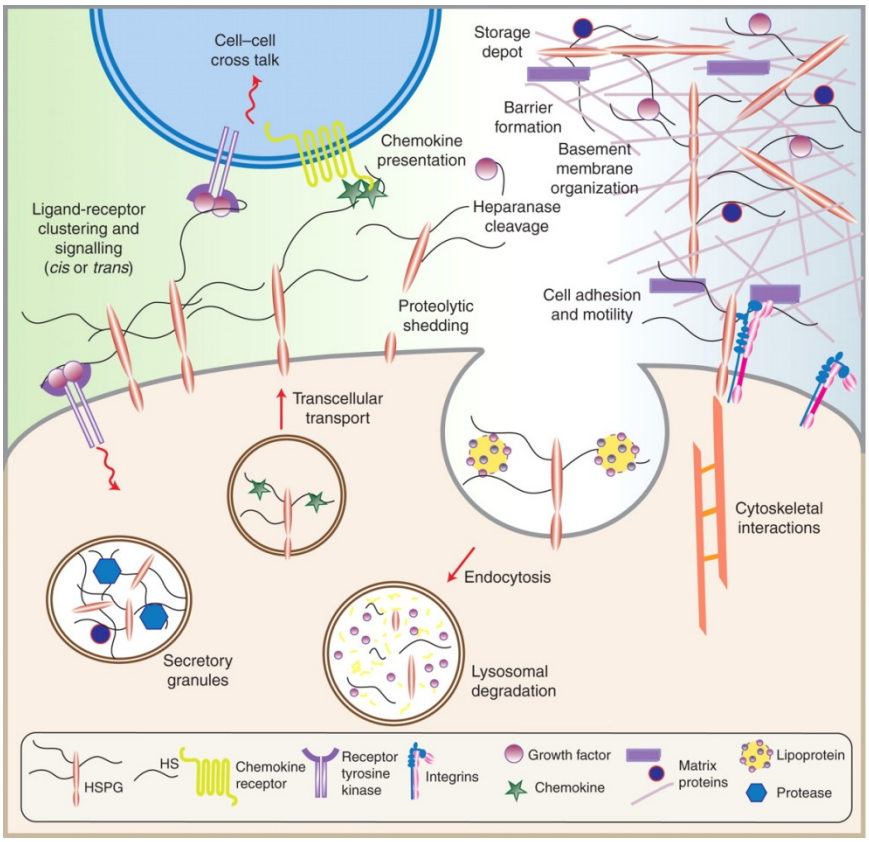

Figure 2. Multiple activities of HS proteoglycans in cells and tissues. HS proteoglycans are involved in ligand presentation and sequestration, receptor activation, clustering, and signaling, receptor-mediated endocytosis, cell adhesion and motility, and cytoskeleton interactions. Adapted from [3] and [7].

HS proteoglycans participate in multiple biological processes through modulating the activities of diverse protein binding partners, including cytokines, chemokines, growth factors, protease and protease inhibitors, and extracellular matrix factors (Figure 2).[3] For a more detailed review of the physiological roles of HS proteoglycans and their protein interactions, please refer to Bishop *et al.*[7] Briefly, such interactions generate a depot of regulatory factors that are essentially liberated by the degradation of HS chains or the removal of their sulfate modifications by either heparanase or 6-*O*-endoglucosamine-sulfatase (Sulf), respectively.[8] HS proteoglycans can also serve as coreceptors in ligand-receptor interactions by presenting ligands in a more active configuration to their cognate receptors, lowering the threshold required for receptor signaling and activation, and altering the duration of signaling cascades.[9] Similarly, they can act as the primary receptors for the clearance of bound ligands, which is particularly relevant to lipoprotein metabolism in the liver and the etiology of hypertriglyceridemia.[10] Finally, HS proteoglycans have been shown to promote the formation of long-range gradients, such as morphogen gradients that are required for cell differentiation during development[11] and chemokine gradients that are utilized for the recruitment and homing of specific leukocyte populations.[12]

Specificity of Heparan Sulfate and Heparin-Binding Ligands

Glycan-binding proteins (also known as lectins) typically have a carbohydrate recognition domain of defined protein folds and/or sequence motifs that designates their membership in one of many conserved gene families.[13] However, HS-binding proteins are a noted exception to this paradigm, as they do not require a common fold and/or sequence motif for carbohydrate interactions. Instead, HS-binding proteins display positively-charged amino acids on both their external surfaces and shallow grooves, often within noncontiguous clusters, that make key electrostatic contacts with the

sulfated regions of HS chains. Hydrogen bonds, van der Waal forces, and hydrophobic effects have been shown to further stabilize these interactions.[14] In contrast to these common peptide sequences, defined sugar motifs that engage proteins have only been identified for a small subset of cases. The best-studied example to date is the high affinity interaction between heparin and antithrombin III (ATIII), a complex which is able to reduce the risk of blood clots by potentiating ATIII activity in the coagulation cascade. Through a series of structure-function analyses, a specific glucosaminyl 3-*O*-sulfated pentasaccharide ($GlcNAc6SO_3$-GlcA-$GlcNSO_3$,3,$6SO_3$-$IdoA2SO_3$-$GlcNSO_3$,$6SO_3$)[15] has been identified as the minimal epitope required for this interaction. A methylated form of this pentasaccharide is now commercially distributed as the drug Arixtra (GlaxoSmithKline) as a safer alternative to heparin for the treatment of thrombosis.[16]

While most ligands do not require uronyl 3-*O* sulfation, the study of heparin-ATIII interactions has instigated the search for other HS/heparin motifs that can engage specific protein binding partners. This pursuit has proven to be technically demanding, given the heterogeneity of the macromolecular organization (sulfated and non-sulfated domains, chain length) and fine structure (sulfation motifs, monosaccharide identity, glycosidic linkage type) of HS/heparin polysaccharides. However, using a combined approach of fractionation, sequencing, and mass spectrometry, the requisite fragments of sulfated oligosaccharides have been identified for some ligands, including fibroblast growth factor 2 (FGF2),[17] vascular endothelial growth factor (VEGF),[18] platelet-derived growth factor (PDGF),[19] platelet factor 4 (PF4),[20] and L-selectin.[21] Extracellular Sulf enzymes have also been shown to regulate the activity of several growth factors (e.g. FGF2, FGF4, GDNF, Wnt) *in vivo*, suggesting a potential role for glucosaminyl 6-*O*-sulfation in these growth factor interactions.[22] Mapping the exact HS sequences necessary for these interactions to occur, however, still remains an area of active investigation.

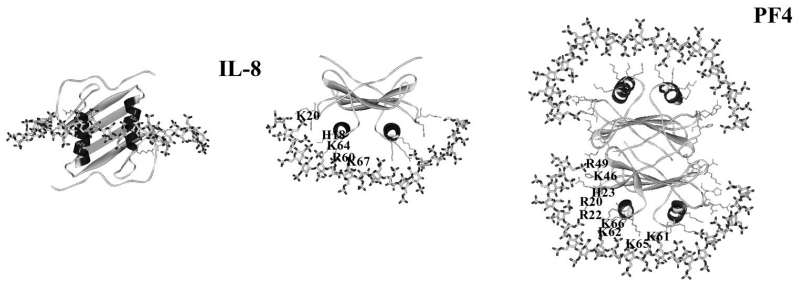

Figure 3. Representation of the lowest energy models for the molecular docking of HS/heparin interactions with IL-8 and PF4 oligomers. Proteins are represented by ribbons, except for side chains that are directly involved in polysaccharide interactions; HS/heparin polysaccharides are represented by sticks. Adapted from [25].

The macromolecular arrangement of sulfated and non-sulfated domains plays a key role in ligand engagement, especially for the formation of higher-order oligomers. This paradigm has been closely examined for the chemokine superfamily, a set of small (8-10 kDa) secreted proteins that signal through G-protein coupled receptors (GPCRs) on cell surfaces.[23] The binding of chemokines to HS chains permits their local retention on the endothelium and facilitates their formation of oligomers that may be required for *in vivo* activity.[24] To date, no co-crystal structures have been reported for complexes of HS polysaccharides and chemokines. However, molecular docking predicts that NS regions are able to force the polysaccharide into a horseshoe configuration to make critical contacts with distal antiparallel α-helices in the chemokine dimer (Figure 3).[25] In further support of this model, biochemical studies have shown that the dimerization of IL-8 (interleukin-8) necessitates a 22-24mer comprised of two NS blocks separated by an unsulfated block of ~14 monosaccharides; in the absence of a sufficiently long NA sequence to flank the S domains, dimerization of IL-8 is unable to occur.[26] This horseshoe arrangement for HS/heparin chains is also thought to facilitate the oligomerization of the antigenic PF4 tetramer involved in heparin-induced thrombocytopenia (HIT).[27] However, definitive evidence for the oligomerization of proteins as a result of HS/heparin spatial reorganization has yet to be uncovered.

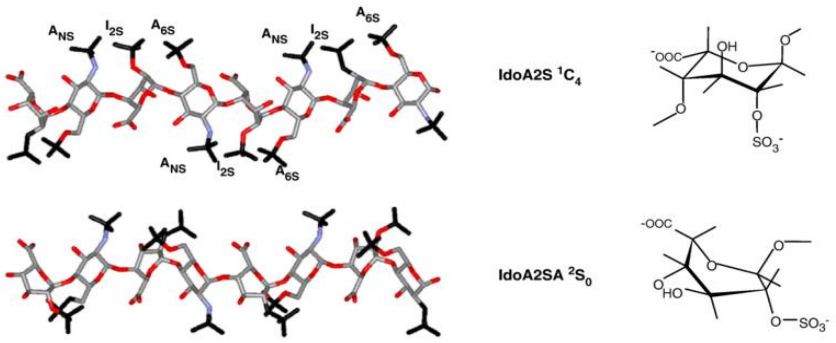

Figure 4. Energy-minimized structures of HS/heparin polysaccharide chains containing the $^{1}C_{4}$ (chair) or $^{2}S_{0}$ (skew-boat) IdoA conformer. Adapted from [29].

Nonsulfated NA domains are generally believed to confer greater flexibility to the polysaccharide and facilitate ligand binding. In contrast, closely spaced sulfated groups in NS domains are expected to produce a stiffer chain due to charge repulsion. This concept has been further explored using ^{15}N NMR and molecular simulations on N-acetyl (K5) heparosan, both of which strongly indicate that nonsulfated chains behave as disordered random coils.[28] Recent evidence also points to a special role for IdoA residues to provide additional conformational plurality to the polysaccharide. Within HS/heparin chains, IdoA typically exists in equilibrium in either the $^{1}C_{4}$ (chair) or $^{2}S_{0}$ (skew-boat) conformation (Figure 4). Protein binding interactions drive the equilibrium towards one of the two conformers in solution, as observed for ATIII-bound heparin oligosaccharides that predominantly contain $^{2}S_{0}$.[29] Consequently, conformationally-locked derivatives of HS/heparin unable to form the $^{2}S_{0}$ conformer have reduced affinities for ATIII.[30] The IdoA conformer equilibrium is also affected by *O*-sulfation status of neighboring GlcA units, suggesting that the optimization of protein contacts for these interactions is a highly dynamic process involving the regulation of multiple heparin/HS biosynthesis and remodeling enzymes.[31]

Heparin-Based Therapeutics in Inflammatory Disease

Unfractionated heparin and its derivatives (in particular, low molecular weight heparin and Arixtra) serve as some of the most important anticoagulants in the clinic today.[32] These drugs are widely utilized in the prevention and treatment of venous thrombosis and pulmonary embolism, as well as for the management of arterial thrombosis in patients with acute myocardial infarction.[33] While heparin has primarily been exploited for its anticoagulant properties, it has long been known to also possess strong anti-inflammatory activity, which is not surprising given its ability to target a large number of ligands such as chemokines, cytokines, growth factors, and metalloproteinases.[34] After heparin was first introduced as an anticoagulant in the clinic, multiple studies emerged describing a noticeable improvement in asthma symptoms for patients on intravenous heparin therapy.[35] More recently, controlled trials with heparin[36] and low molecular weight derivative enoxaparin[37] have shown that the inhaled form of this polysaccharide can inhibit the bronchoconstrictive response for exercise-induced asthma patients. Furthermore, heparin treatment is also known to promote healing in cases of ulcerative colitis,[38] myocardia ischemia-reperfusion injuries,[39] and burn injuries.[40]

While there is great potential for heparin as an anti-inflammatory agent, its practical application for the treatment of acute and chronic inflammatory diseases is limited by its anticoagulant activity and high risk for complications, such as heparin-induced thrombocytopenia (HIT).[41] Even mimetics of heparin with reduced anticoagulant activities can be potentially dangerous, such as in the case of PI-88 (Progen Pharmaceuticals), an anti-tumor drug that exhibited serious bleeding for some patients during Phase II trials.[42] Considerable efforts have been devoted to the preparation of completely non-anticoagulant derivatives that are still able to retain the anti-inflammatory properties of heparin. This is a challenging task, as one third of endogenous heparin chains contain the pentasaccharide sequence that activates ATIII, and active glucosaminyl 3-*O*-sulfate groups are difficult to remove in the presence of other sulfate modifications. For example, the chemical procedure used to desulfate

at this specific position also removes uronyl 2-*O* sulfates. Simultaneous loss of both modifications mitigates the anti-inflammatory properties of the polysaccharide, as shown in animal models of thioglycollate-induced peritonitis and oxazolone-induced delayed-type hypersensitivity.[43] The *de novo* synthesis of non-3-*O*-sulfated heparin compounds is not a reasonable alternative to pursue[44] given the number of stereoselective glycosylation reactions and regioselective sulfate modifications that would be necessitated by such preparations. Despite the inherent challenges of dissecting the anti-inflammatory properties of HS/heparin from its undesired anticoagulant properties, the production of such agents would allow for global modulation of the immune response through the ability to target multiple proteins in the inflammatory cascade.

The development of HS/heparin analogs with novel and sometimes unpredictable properties offers a unique solution towards resolving this goal. One approach to designing HS/heparin mimetics is to amplify the bioactive sequences using a multivalent scaffold, such as hyperbranched dendrimers of defined structure and molecular weight. This strategy was utilized by Seeberger and coworkers to conjugate amine-functionalized heparin oligosaccharides to a carboxylic acid-containing dendrimer core (Figure 5).[45] The authors found that synthetic glycodendrimers not only bound to FGF-2 more effectively than monovalent heparin oligosaccharides, but also potentiated mitogen-activated kinase signaling for the ligand. The glycodendrimers were similarly effective at disrupting the migration of splenocyte and lymph node cells towards pro-inflammatory chemokine (CCL21) gradients, but not homeostatic chemokine (CXCL12 and CCL19) gradients *in vitro*.[46] Given the pleiotropic functions of HS/heparin polysaccharides, it is not surprising that these mimetics showed robust activity in multiple biological contexts. While the anticoagulant activity of these compounds was not studied, such experiments in the future would allow one to determine if synthetic glycodendrimers could be utilized as anti-inflammatory agents *in vivo*.

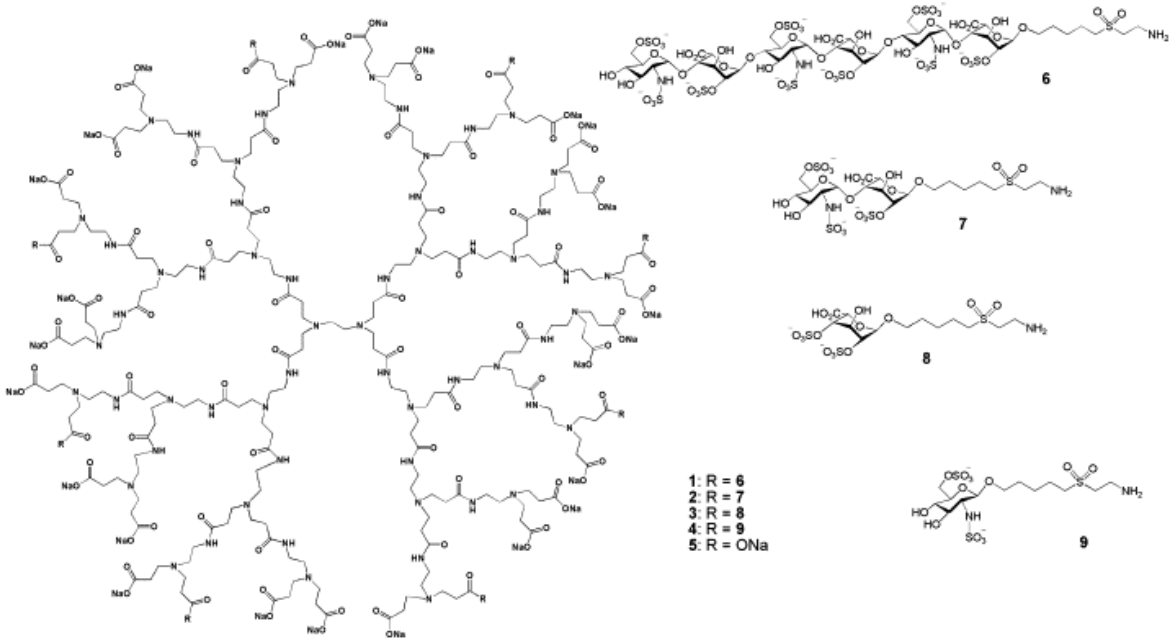

Figure 5. Glycodendrimer structures conjugated with amine-functionalized heparin oligosaccharides. Adapted from [45].

A second strategy towards obtaining non-anticoagulant, anti-inflammatory mimetics is to conduct a high-throughput screen on a large library of compounds using these defined criteria. For example, Progen Pharmaceuticals recently developed a new series of homogenously sulfated, single entity sugars attached to an aglycone lipophilic moiety (PG500) based on the chemical structure of the original PI-88 drug.[47] The new series of compounds was first screened for potential anticoagulant activity in human plasma, and any compound that altered the activated partial thromboplastin (PT) time for blood clotting was eliminated from further testing. Next, the anti-angiogenesis and anti-metastasis activities of the remaining compounds were evaluated using *in vivo* tumor growth and proliferation assays. Several PG500 compounds exhibited strong inhibitory activity against the most aggressive types of tumors. Not surprisingly, the same hits targeted FGF1, FGF2, and VEGF with exceptional potency, suggesting that the *in vivo* efficacy of a drug within a tumor niche is correlated with its *in vitro* binding preferences. While compounds in the PG500 series have not been tested for

anti-inflammatory activity, it is reasonable to predict that several of the compounds with low anti-coagulant activity would also be effective in *in vivo* animal models of inflammation and injury.

REFERENCES

[1] M. Bernfield, M. Gotte, P. W. Park, O. Reizes, M. L. Fitzgerald, J. Lincecum, M. Zako, *Annual review of biochemistry* **1999**, *68*, 729-777.

[2] J. D. Esko, S. B. Selleck, *Annual review of biochemistry* **2002**, *71*, 435-471.

[3] S. Sarrazin, W. C. Lamanna, J. D. Esko, *Cold Spring Harbor perspectives in biology* **2011**, *3*.

[4] M. Kato, H. Wang, M. Bernfield, J. T. Gallagher, J. E. Turnbull, *The Journal of biological chemistry* **1994**, *269*, 18881-18890.

[5] W. H. Burgess, T. Maciag, *Annual review of biochemistry* **1989**, *58*, 575-606.

[6] U. Lindahl, M. Kusche-Gullberg, L. Kjellen, *The Journal of biological chemistry* **1998**, *273*, 24979-24982.

[7] J. R. Bishop, M. Schuksz, J. D. Esko, *Nature* **2007**, *446*, 1030-1037.

[8] G. K. Dhoot, M. K. Gustafsson, X. Ai, W. Sun, D. M. Standiford, C. P. Emerson, Jr., *Science* **2001**, *293*, 1663-1666.

[9] R. V. Iozzo, J. J. Zoeller, A. Nystrom, *Molecules and cells* **2009**, *27*, 503-513.

[10] E. M. Foley, J. D. Esko, *Progress in molecular biology and translational science* **2010**, *93*, 213-233.

[11] Y. Takei, Y. Ozawa, M. Sato, A. Watanabe, T. Tabata, *Development* **2004**, *131*, 73-82.

[12] L. Wang, M. Fuster, P. Sriramarao, J. D. Esko, *Nature immunology* **2005**, *6*, 902-910.

[13] A. Varki, M. E. Etzler, R. D. Cummings, J. D. Esko, in *Essentials of Glycobiology*, 2nd ed. (Eds.: A. Varki, R. D. Cummings, J. D. Esko, H. H. Freeze, P. Stanley, C. R. Bertozzi, G. W. Hart, M. E. Etzler), Cold Spring Harbor (NY), **2009**.

[14] I. Capila, R. J. Linhardt, *Angew Chem Int Ed Engl* **2002**, *41*, 391-412.

[15] S. T. Olson, I. Bjork, R. Sheffer, P. A. Craig, J. D. Shore, J. Choay, *The Journal of biological chemistry* **1992**, *267*, 12528-12538.

[16] J. M. Walenga, W. P. Jeske, M. M. Samama, F. X. Frapaise, R. L. Bick, J. Fareed, *Expert opinion on investigational drugs* **2002**, *11*, 397-407.

[17] S. Guimond, M. Maccarana, B. B. Olwin, U. Lindahl, A. C. Rapraeger, *The Journal of biological chemistry* **1993**, *268*, 23906-23914.

[18] S. Soker, D. Goldstaub, C. M. Svahn, I. Vlodavsky, B. Z. Levi, G. Neufeld, *Biochemical and biophysical research communications* **1994**, *203*, 1339-1347.

[19] E. Feyzi, F. Lustig, G. Fager, D. Spillmann, U. Lindahl, M. Salmivirta, *The Journal of biological chemistry* **1997**, *272*, 5518-5524.

[20] M. Maccarana, U. Lindahl, *Glycobiology* **1993**, *3*, 271-277.

[21] K. Norgard-Sumnicht, A. Varki, *The Journal of biological chemistry* **1995**, *270*, 12012-12024.

[22] S. Wang, X. Ai, S. D. Freeman, M. E. Pownall, Q. Lu, D. S. Kessler, C. P. Emerson, Jr., *Proceedings of the National Academy of Sciences of the United States of America* **2004**, *101*, 4833-4838.

[23] H. Lortat-Jacob, *Current opinion in structural biology* **2009**, *19*, 543-548.

[24] A. E. Proudfoot, T. M. Handel, Z. Johnson, E. K. Lau, P. LiWang, I. Clark-Lewis, F. Borlat, T. N. Wells, M. H. Kosco-Vilbois, *Proceedings of the National Academy of Sciences of the United States of America* **2003**, *100*, 1885-1890.

[25] H. Lortat-Jacob, A. Grosdidier, A. Imberty, *Proceedings of the National Academy of Sciences of the United States of America* **2002**, *99*, 1229-1234.

[26] E. Krieger, E. Geretti, B. Brandner, B. Goger, T. N. Wells, A. J. Kungl, *Proteins* **2004**, *54*, 768-775.

[27] S. E. Stringer, J. T. Gallagher, *The Journal of biological chemistry* **1997**, *272*, 20508-20514.

[28] M. Mobli, M. Nilsson, A. Almond, *Glycoconjugate journal* **2008**, *25*, 401-414.

[29] M. Guerrini, S. Guglieri, B. Casu, G. Torri, P. Mourier, C. Boudier, C. Viskov, *The Journal of biological chemistry* **2008**, *283*, 26662-26675.

[30] S. K. Das, J. M. Mallet, J. Esnault, P. A. Driguez, P. Duchaussoy, P. Sizun, J. P. Herault, J. M. Herbert, M. Petitou, P. Sinay, *Chemistry* **2001**, *7*, 4821-4834.

[31] K. J. Murphy, N. McLay, D. A. Pye, *Journal of the American Chemical Society* **2008**, *130*, 12435-12444.

[32] Y. Xu, S. Masuko, M. Takieddin, H. Xu, R. Liu, J. Jing, S. A. Mousa, R. J. Linhardt, J. Liu, *Science* **2011**, *334*, 498-501.

[33] *The New England journal of medicine* **1989**, *320*, 1014-1015.

[34] U. Lindahl, *Thrombosis and haemostasis* **2007**, *98*, 109-115.

[35] E. J. Bardana, M. J. Edwards, B. Pirofsky, *Ann Allergy* **1969**, *27*, 108-&.

[36] T. Ahmed, J. Garrigo, I. Danta, *New Engl J Med* **1993**, *329*, 90-95.

[37] T. Ahmed, B. J. Gonzalez, I. Danta, *Am J Respir Crit Care Med* **1999**, *160*, 576-581.

[38] R. C. Evans, V. S. Wong, A. I. Morris, J. M. Rhodes, *Alimentary pharmacology & therapeutics* **1997**, *11*, 1037-1040.

[39] V. H. Thourani, S. S. Brar, T. P. Kennedy, L. R. Thornton, J. A. Watts, R. S. Ronson, Z. Q. Zhao, A. L. Sturrock, J. R. Hoidal, J. Vinten-Johansen, *American journal of physiology. Heart and circulatory physiology* **2000**, *278*, H2084-2093.

[40] M. J. Saliba, Jr., *Burns : journal of the International Society for Burn Injuries* **2001**, *27*, 349-358.

[41] T. E. Warkentin, J. G. Kelton, *Annual review of medicine* **1989**, *40*, 31-44.

[42] K. D. Lewis, W. A. Robinson, M. J. Millward, A. Powell, T. J. Price, D. B. Thomson, E. T. Walpole, A. M. Haydon, B. R. Creese, K. L. Roberts, J. R. Zalcberg, R. Gonzalez, *Investigational new drugs* **2008**, *26*, 89-94.

[43] L. Wang, J. R. Brown, A. Varki, J. D. Esko, *The Journal of clinical investigation* **2002**, *110*, 127-136.

[44] R. Schworer, O. V. Zubkova, J. E. Turnbull, P. C. Tyler, *Chemistry* **2013**, *19*, 6817-6823.

[45] J. L. de Paz, C. Noti, F. Bohm, S. Werner, P. H. Seeberger, *Chemistry & biology* **2007**, *14*, 879-887.

[46] J. L. de Paz, E. A. Moseman, C. Noti, L. Polito, U. H. von Andrian, P. H. Seeberger, *ACS chemical biology* **2007**, *2*, 735-744.

[47] K. Dredge, E. Hammond, K. Davis, C. P. Li, L. Liu, K. Johnstone, P. Handley, N. Wimmer, T. J. Gonda, A. Gautam, V. Ferro, I. Bytheway, *Investigational new drugs* **2010**, *28*, 276-283.

C h a p t e r 2

SYNTHESIS OF DIFFERENTIALLY SULFATED HS GLYCOPOLYMERS

Aims and Justification

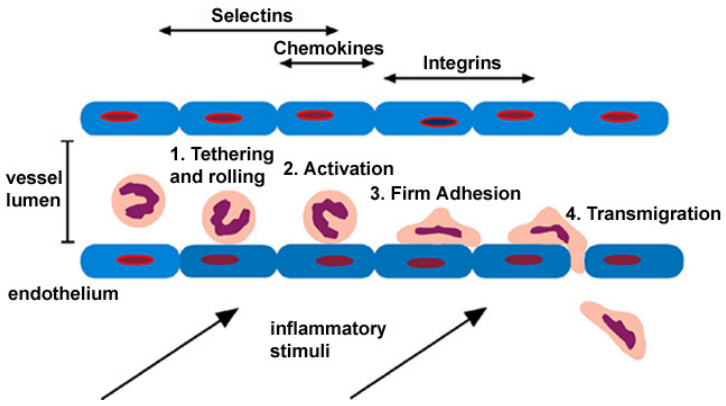

Figure 6. The inflammation cascade for leukocyte extravasation. Leukocytes first make contact with endothelial cells, and are then activated by chemokines to achieve firm adhesion through the expression of integrins. This process allows leukocytes to transmigrate through the vessel wall and subendothelial basement membrane into the inflamed tissue. Each of these steps is mediated in part by the expression of HS proteoglycans (not shown). Adapted from [6].

The inflammatory response is a multi-stage process involving the rapid recruitment of leukocytes in the bloodstream to sites of inflammation, typically through post-capillary venules (Figure 6).[1] First, rolling leukocytes attach to the inflamed endothelium through their expression of three calcium-dependent (C-type) lectins: L-selectin, which is constitutively expressed by leukocytes, and P-selectin and E-selectin, which are expressed on endothelial surfaces upon activation by pro-inflammatory cytokines.[2] These interactions sufficiently reduce the rolling velocity of leukocytes to facilitate: (1) the activation of G protein-coupled receptors (GPCRs) by endothelium-bound chemokines; (2) the upregulation of leukocyte integrins that enable highly stable interactions with the endothelium surface.[3] Once the leukocytes have been activated, they are able to traverse through the endothelial layer and subendothelial basement membrane. This process is facilitated

by the deployment of degradative enzymes, such as matrix metalloproteinases and heparanse.[4] Transmigration *in vivo* typically takes 15-45 minutes,[5] and each step is heavily regulated by the expression of heparan sulfate (HS) proteoglycans on the inflamed vascular endothelium and in the extracellular matrix. The ubiquitous expression of HS proteoglycans is necessary for the establishment of both the acute and chronic inflammatory response of the immune system.

The sugar chains of HS proteoglycans are assembled from disaccharide subunits exhibiting subtle variations in stereochemistry, length, and patterns of sulfation. This structural diversity enables HS proteoglycans to modulate the activity of >400 proteins,[7] including chemokines, integrins, L- and P-selectin, and multiple components of the subendothelial basement membrane. HS has previously been identified as the dominant ligand for L-selectin during leukocyte rolling and adhesion activities, and the targeted deletion of endothelial HS biosynthesis (*Ndst1*) results in impaired neutrophil infiltration for multiple models of inflammation.[8] Here we will focus on a role for HS proteoglycans in modulating chemokine presentation and gradient formation during leukocyte extravasation,[9] as most members of the chemokine family possess a carboxyl terminus stretch of positively charged residues that recognize negatively charged HS chains with moderate affinity.[10] Such interactions have been characterized for both homeostatic and pro-inflammatory chemokines *in vitro* and were recently found to be relevant *in vivo* for the regulation of CCL21, a key mediator of the lymphatic trafficking of dendritic cells and T-cells.[9]

Chemokines control the activation and migration of specific leukocyte populations toward sites of injury and inflammation, and the accumulation of pro-inflammatory chemokines into epithelial spaces contributes to the pathogenesis of allergy, arthritis, psoriasis, and other inflammatory disorders.[11] Although HS proteoglycans are known to establish chemoattractant gradients that promote leukocyte migration,[12] the precise carbohydrate structural determinants involved have yet to be elucidated. A major challenge to understanding the structure-activity relationships of HS

and developing relevant therapeutics is the chemical complexity and heterogeneity of the sugars found *in vivo*. This limitation, often referred to as the "sulfation code" for glycosaminoglycans,[13] has hindered the development of HS-based strategies for targeting the activity of chemokines and other ligands. While genetic ablation of HS biosynthesis enzymes (e.g. *Ndst1*, *Ext1*) can be used to map out the spatial[8] and temporal[9] regulation of HS and to identify functional roles, it lacks the chemical precision to indicate which sequences are involved. However, it is anticipated that homogeneous libraries of well-defined HS oligosaccharides may provide new insights into the molecular mechanisms of chemokine signaling, oligomerization, and receptor activation and their precise interactions with HS.

General glycosaminoglycan libraries can been used to determine which carbohydrate classes are implicated in chemokine binding and activation. In a competitive binding assay for the inhibition of RANTES, heparin (IC_{50} = 25 ng/mL) was found to have the highest affinity, while chondroitin sulfate C (IC_{50} = 50 ng/mL), heparan sulfate (IC_{50} = 150 ng/mL), dermatan sulfate (IC_{50} = 800 ng/mL), and chondroitin sulfate A (IC_{50} = 8 μg/mL) all interacted with the chemokine with lower affinity.[14] Data has also been reported for the binding of IL-8,[15] PF-4,[16] IP-10,[17] MIP-1α,[18] and MIP-1β[19] to heparin polysaccharides, which typically exhibit strong chemokine interactions due to the prevalence of their highly sulfated domains. Not surprisingly, heparin has been shown to have potent anti-inflammatory activity in multiple models of asthma, chronic dermatitis, and ulcerative colitis.[20] However, due to its well-characterized anticoagulant activity and high risk for bleeding, it is not recommended for use as an anti-inflammatory agent. Moreover, heparin polysaccharides isolated from natural sources are prone to undesirable side effects as a result of their structural heterogeneity and potential for external contamination.[21]

As previously described, the development of chemically-defined HS/heparin mimetics lacking the glucosaminyl 3-*O*-sulfate anticoagulant sequence offers a promising solution to these challenges.

Although a few studies have partially modified natural polysaccharides[22] or undertaken the semi-synthesis of glucan sulfate mimetics[23] towards this goal, such approaches lack the precision of chemical synthesis in controlling the sulfation sequence. To our knowledge, only one study[24] has exploited chemical synthesis to generate complex, HS-based oligosaccharides that modulate the activity of pro-inflammatory chemokines; however, this study did not explore the anticoagulant function of the macromolecular structures that they generated. Here, we describe a new class of simplified HS/heparin glycomimetics that have highly tunable structures, controllable lengths, and defined sulfation motifs. Importantly, these molecules possess the ability to inhibit the pro-inflammatory chemokine RANTES with similar efficiency to natural heparin polysaccharides, yet they do not affect the activity of key factors in the coagulation cascade. The ability to control the fine structure within the glycopolymers is significant, as it allows for the generation of mimetics with distinct functions. We envision that this class of glycopolymers can serve as potential tools for dissecting the pleiotropic roles of HS/heparin and other glycosaminoglycans and manipulating their functions *in vivo*.

Rational Design of a RANTES-Targeting Glycopolymer

Chemokines are a superfamily of small proteins (8-10 kDa) with a highly conserved monomeric structure.[25] They can be grouped into four subclasses based on the positioning of their conserved cysteine residues: C, CX_3C, CC, and CXC. While the sequence identity at the primary level can be as low as 20% for some chemokines, their conserved structures are mediated by a common four-cysteine motif that imposes the formation of two disulfide bridges.[26] Most chemokines are highly basic in composition (MIP-1α and MIP-1β being the only two exceptions), exhibiting an isoelectric point of ~9.0 that facilitates their high affinity interactions with heparin, HS, and other

glycosaminoglycans. While all chemokines are able to bind to heparin with varying affinities, a conserved sequence of basic amino acid residues, known as the BBXB motif (B represents either arginine and lysine, X represents any other amino acid) is found in CC chemokines.[26] This key motif was identified in the surface-exposed 40s loop of RANTES (^{44}RKNR^{47}) and has since been recognized as the major heparin-binding site for most chemokines through detailed mutagenesis studies.[14]

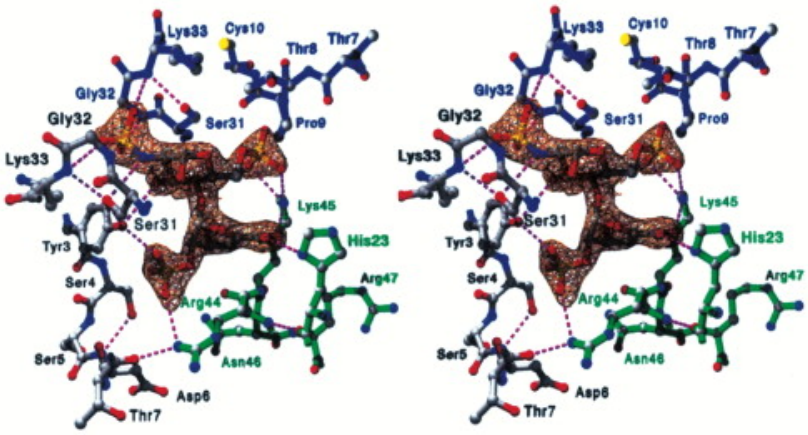

Figure 7. Stereo diagrams of the heparin disaccharide-binding site in crystals of RANTES trimer. Putative hydrogen bonds are shown in violet. Adapted from reference [27].

Based on the plethora of biochemical[14,26] and structural[27] information available for RANTES-heparin interactions, we chose to investigate whether HS glycopolymers could be synthetically tailored to target the BBXB motif of RANTES. Upon examining a co-crystal structure of heparin disaccharide and RANTES oligomers (Figure 7),[27] we envisaged that heparin/HS disaccharide epitopes appended onto a multivalent polymer backbone might be sufficient to target the heparin binding site, provided that the binding affinity of the epitopes could be enhanced through avidity (Scheme 1a). We hypothesized that a trisulfated heparin-based motif would be able to interact efficiently with RANTES (glycopolymer **1**, Scheme 1b), given that all three of its sulfates make contacts with basic clusters including the ^{44}RKNR^{47} site. Mutations to the BBXB motif reduces

the binding affinity of RANTES for heparin and other glycosaminoglycans, and also abrogates its interactions with cognate receptors CCR1 and CCR3, but not CCR5.[26] Based on this data and the known receptor binding domains for RANTES,[28] we anticipate that our HS/heparin mimetic might also be able to disrupt the RANTES-dependent activation of CCR1 and CCR3, but have no such effect on CCR5.

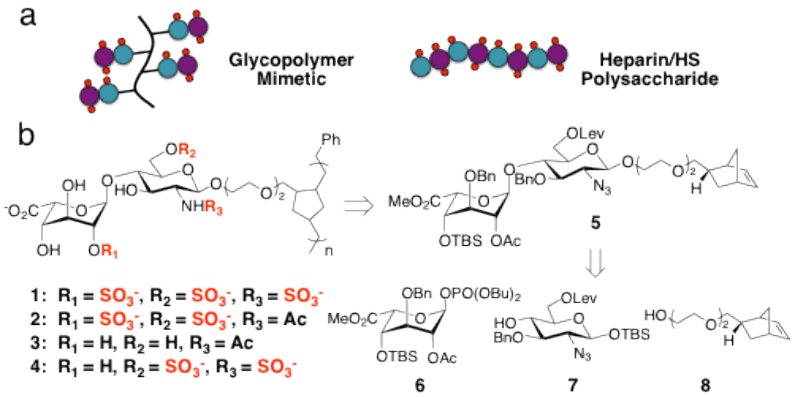

Scheme 1. (a) Synthetic glycopolymers can mimic the macromolecular architecture of heparin/HS polysaccharides. (b) Retrosynthesis of a series of differentially sulfated HS/heparin polymers from three building blocks: phosphate donor **6**, acceptor **7**, and norbornyl-conjugated linker **8**.

Previous work from our group[29] has shown that chondroitin sulfate di- and tetrasaccharides can be amplified on a multiavalent polymer scaffold to recapitulate the activity of natural chondroitin sulfate polysaccharides. These glycopolymers were found to be remarkably potent in neuronal growth inhibition assays, demonstrating the importance of avidity in designing synthetic mimetics of glycosaminoglycans. Inspired by this approach, we sought to design a series of differentially sulfated HS/heparin glycopolymers (**1** – **4**) of the same macromolecular structure. In place of the previously used *cis*-octene scaffold,[29] we chose to utilize a polynorbornene backbone to allow for maximal control over the chain length and polydispersity during ring-opening metathesis polymerization (ROMP) chemistry (Scheme 1b). We chose to reduce the unsaturated backbone at the last stage of the synthesis so that the polymers would be able to emulate the conformational

plasticity found in native HS/heparin, thereby facilitating their binding to RANTES.[30] Finally, by controlling the sulfation pattern prior to polymerization, we sought to increase the specificity of the glycopolymers for RANTES inhibition. Notably, these structures would represent the first example of high-molecular-weight polymers prepared from minimal HS disaccharide units.

Chemical Synthesis

While several strategies[31] have been reported for the preparation of well-defined heparin/HS oligosaccharides, we sought to develop a modified scheme that would allow for the synthesis of a heparin/HS glycopolymer library using a minimum number of protection/deprotection steps. We proposed a divergent scheme that could produce a library of differentially sulfated polymers **1** – **4** from a single precursor, **5** (Scheme 1b). The orthogonal protecting group for disaccharide **5** is distinct from those previously published,[32] as it needs to be compatible with the requirements for ROMP and facilitate deprotection of the glycopolymer in the final stages of the synthesis. In this regard, we chose to install a *tert*-butyldimethylsilyl (TBS) group at the C4'-hydroxyl and benzyl ethers (Bn) at the non-sulfated positions C3' and C3 in order to enhance the solubility of the sulfated HS/heparin monomers during ROMP. Orthogonal acetyl (Ac) and levulinoyl (Lev) ester groups were selected for positions that would ultimately carry the *O*-sulfonate groups (C2' and C6, respectively); the former group would also provide anchimeric assistance in forming the 1,2-*trans* glycosidic linkage in the disaccharide. As indicated in the retrosynthesis analysis (Scheme 1b), we planned to generate core precursor **5** from three building blocks: iduronic acid (IdoA) phosphate donor **6**, glucosamine (GlcN) acceptor **7**,[33] and norbornyl linker **8**.[34]

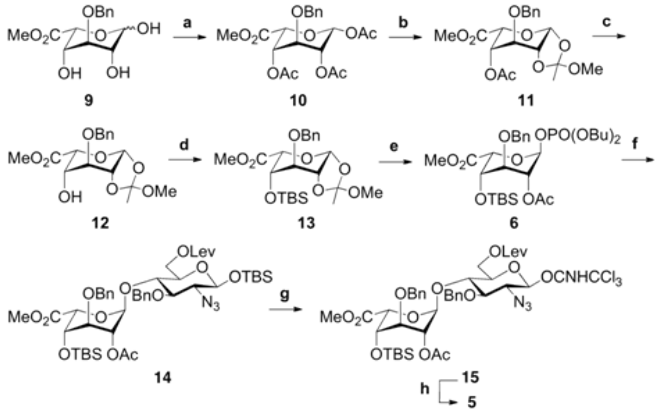

Scheme 2. Synthesis of disaccharide core precursor **5**. Reagents and conditions: (a) AcCl, Py, DMAP, CH_2Cl_2, -40 °C, quant.; (b) (i) $TiBr_4$, CH_2Cl_2, (ii) 2,4,6-collidine, MeOH, CH_2Cl_2, 75%; (c) NaOMe, MeOH, -10 °C, 80%; (d) TBSOTf, Py, 0 °C, 92%; (e) $HOPO(OBu)_2$, CH_2Cl_2, 4 Å MS, quant.; (f) TMSOTf, 7, CH_2Cl_2, 4 Å MS, 93%; (g) (i) TBAF, AcOH, THF, 0 °C, (ii) Cl_3CCN, DBU, CH_2Cl_2, 0 °C, 89%; (h) BF_3OEt_2, 8, CH_2Cl_2, 4 Å MS, 80%.

In previous reports,[33] Seeberger and coworkers developed an efficient route to 1,2,4-triol **9** from commercially available diacetone glucose in six steps. We followed these published procedures without modification to prepare **9**, which was then used to synthesize glycosyl phosphate donor **6** in a highly efficient series of steps (Scheme 2). First, we treated **9** with acetyl chloride (AcCl) and 4-dimethylaminopyridine (DMAP) at -40 °C to afford triacetylated β-isomer **10** in quantitative yield over three cycles of recrystallization.[35] We also tried this reaction using acetic anhydride (Ac_2O) and at higher temperatures;[36] however, these conditions consistently led to a mixture of α/β-pyranose and α/β-furanose isomers that could not be separated from the desired product. Subsequently, anomeric bromination of **10** was accomplished using titanium bromide ($TiBr_4$) to form a glycosyl halide intermediate,[35] which was directly converted into 1,2-orthoester **11** using 2,4,6-collidine as the base in 75% yield. As anticipated, the orthoester moiety locked the pyranose ring into the $^4C_1$ conformation, allowing for selective cleavage of the remaining acetal under Zemplén conditions (NaOMe, MeOH) to deliver **12** in 80% yield.

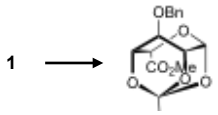

Scheme 3. Intramolecular cyclization of **12** under mild acid conditions.

Table 1. Reagents and conditions for C4' protection of **12**.

Reagents	**Conditions**	**Result**
4-Methoxybenzylether (PMB):		
PMBBr (4 eq), Ag_2O (4 eq), CH_2Cl_2, 4Å MS	24 h, rt	Incomplete
PMBBr (10 eq), Ag_2O (4 eq), CH_2Cl_2, 4Å MS	12 h, rt	Incomplete; desired (minor)
PMBBr (10 eq), Ag_2O (20 eq), DMF, 4Å MS	12 h, rt	Cyclized (major); desired (minor)
PMBBr (10 eq), Ag_2O (20 eq), DMF, 4Å MS	12 h, 5 °C	Cyclized (major); desired (minor)
PMBBr (4 eq), Ag_2O (4 eq), THF, 4Å MS	10 h, 5 °C	Cyclized (major); desired (minor)
PMBBr (10 eq), K_2CO_3 (1 eq), DMF, 4Å MS	6 h, 5 °C	Cyclization byproduct (major)
PMBBr (10 eq), KHMDS (3 eq), THF, 4Å MS	12 h, rt	Incomplete; decomposition
[2-(Trimethylsilyl)ethoxy]methyl Acetal (SEM):		
SEMCl (3 eq), DIPEA (4 eq), CH_2Cl_2	12 h, 5 °C → rt	Incomplete
SEMCl (7 eq), DIPEA (10 eq), CH_2Cl_2	12 h, 5 °C → rt	Incomplete
SEMCl (10 eq), TBAI (3 eq) DIPEA (neat)	14 h, 5 °C → rt	Incomplete; desired (minor)
SEMCl (15 eq), TBAI (3 eq), DIPEA (neat)	16 h, 5 °C → rt	Incomplete; desired (minor)
Allyl Ether:		
AllylBr (5 eq), Ag_2O (3 eq), TBAI (0.5 eq), DMF	24 h, rt	Incomplete; decomposition
AllylBr (5 eq), Ag_2O (3 eq), TBAI (0.5 eq), DMF	24 h, rt	Desired (minor); decomposition
tert-Butydimethylsilyl Ether (TBS):		
TBSCl (10 eq), imidazole (2 eq), DMAP, DMF	24 h, rt	Incomplete

Installing an orthogonal protecting group at the C4' hydroxyl of 1,2-orthoester **12** proved to be a unique challenge. We found this hydroxyl to be a poor nucleophile, likely due to the presence of the electron-withdrawing methyl ester at C5'. Moreover, the orthoester functionality was highly sensitive to acidic conditions and would spontaneously undergo intramolecular cyclization in the presence of a weak acid, thereby limiting the reaction conditions that we could explore (Scheme 3). Some of our unsuccessful attempts at protecting the C4' position with 4-methoxybenzylether (PMB), [2-(trimethylsilyl)ethoxy]methyl acetal (SEM), allyl ether, and TBS are summarized in Table 2. Fortuitously, we discovered two "forcing" conditions that worked efficiently: (1) excess *tert*-butyl-dimethylsilyl trifluoromethanesulfonate (TBSOTf) in neat pyridine at 0 °C delivered **13** in 92% yield; (2) excess SEMCl assisted by tetrabutalammonium iodide (TBAI) in neat *N*,*N*-diisopropylethylamine (DIPEA) delivered the corresponding SEM-protected 1,2-orthoester in 88% yield. We chose to utilize the former set of conditions for the remainder of the synthesis, as we later found TBS-protected 1,2-orthoester **13** to be compatible with the final deprotection steps.

The direct reaction of 1,2-orthoester **13** with acceptor **7** gave low yields of the desired IdoA-GlcN disaccharide **14**. Conversion of **13** to the corresponding trichloroacetimidate donor also delivered unproductive glycosylation reactions. We therefore chose to explore the reactivity of the IdoA phosphate donor, which could be accessed from **13** using dibutyl phosphate ($HOPO(OBu)_2$)[37] in a single quantitative step. We were pleased to discover that phosphate donor **6** reacted quickly with acceptor **7** and trimethylsilyl trifluoromethanesulfonate (TMSOTf, 1.3 eq)[37] to deliver the α-linked disaccharide **14** in 93% yield. We attributed the efficacy of this reaction to the presence of the electron-donating TBS group at C4' in stabilizing the acetoxonium ion transition state, as other protecting groups at this position (e.g. SEM) did not facilitate the same reaction. This hypothesis was further validated by calculating the gas phase Mulliken charge values at the C1'

position, which we found to be 0.27180 and 0.24083 for TBS and SEM, respectively (Wei-Guang Liu, Goddard Lab).

To tether the resulting disaccharide to norbornyl linker **8**, we converted **14** into glycosyl imidate **15** by removing the anomeric TBS and treating the resulting hemiacetal with trichloroacetonitrile and 1,8-diazabicycloundec-7-ene (DBU).[38] We then explored a variety of reaction conditions for the glycosidic coupling of **15** and **8**. While catalytic TMSOTf (typical glycosylation conditions used for such donors) gave a 1:1 mixture of α/β isomers, we were pleased to find that treatment with BF_3OEt_2 (0.34 eq) gave exclusively the β-isomer (δ = 4.34 ppm, J_{12} = 8 Hz) in 80% yield. Interestingly, higher amounts of BF_3OEt_2 promoted the formation of an anomerically-substituted glycosyl fluoride that could not be readily converted into the desired product. At this stage (and for all compounds derived from disaccharide **5**), complete protons assignments necessitated the use of ^1H, ^1H-^1H COSY, ^1H-^1H TOCSY, and ^1H-^{13}C HSQC NMR in order to differentiate the ring protons from the ethylene glycol protons.

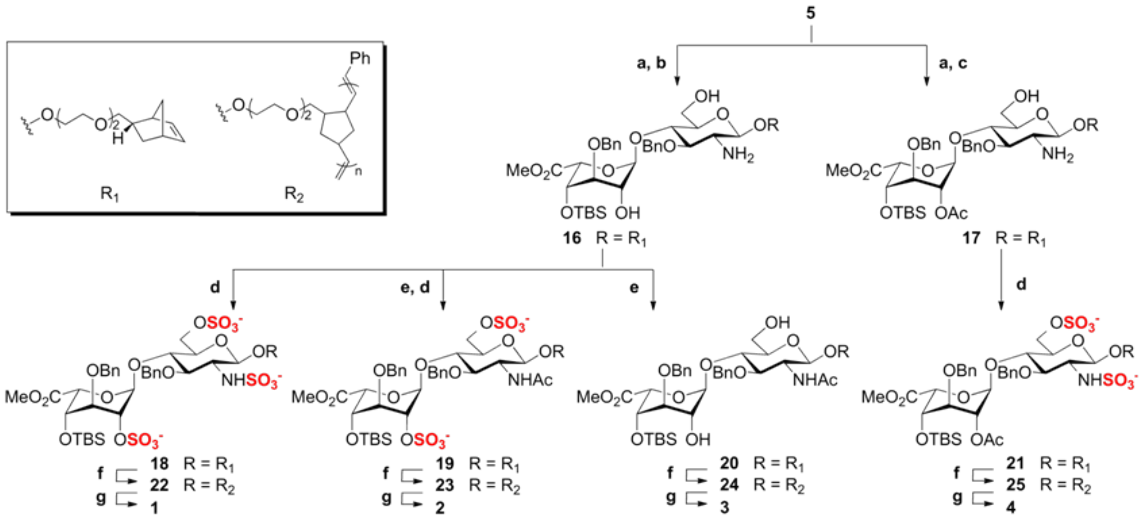

Scheme 4. Synthesis of glycopolymers **1** – **4**. Reagents and conditions: (a) 1,3-propanedithiol, DIPEA, MeOH, 87%; (b) K_2CO_3, MeOH, 78%; (c) $H_2NNH_2{\cdot}H_2O$, AcOH, Py, quant.; (d) SO_3Py, NEt_3, Py, 55 °C, 78 – 85%; (e) Ac_2O, NEt_3, MeOH, quant.; (f) $(H_2IMes)(Py)_2(Cl)_2Ru$=CHPh, DCE, MeOH, quant.; (g) (i) TMSOK, TBAI, THF, 80 – 88%, (ii) $Pd(OH)_2$/charcoal, H_2 (1 atm), phosphate buffer (pH = 7.4), MeOH, 37 – 55%.

To explore the role of sulfate group positioning in chemokine interactions, norbornyl-conjugated disaccharide **5** was diversified into four differentially sulfated glycopolymers (**1** – **4**; Scheme 3). First, we reduced the azide using 1,3-propanedithiol and DIPEA,[39] as we found that the presence of this protecting group quickly catalyzes the decomposition of **5** (presumably through a radical decomposition mechanism involving the norbornene moiety). The resulting intermediate was then treated with either potassium carbonate (K_2CO_3) to deprotect both ester groups, or hydrazine acetate[40] to selectively cleave the Lev ester. Compounds **16** and **17** were regioselectively *N*-sulfated, *O*-sulfated, and *N*-acetylated for their eventual conversion into differentially sulfated glycopolymers. Notably, previous syntheses of HS oligosaccharides have chosen to sulfonate the *N*- and *O*- positions in separate steps using distinct forms of sulfur trioxide (SO_3) salts for each reaction.[33] Here, we found convenient conditions that would enable universal sulfonation at the *O*- and *N*- positions: excess sulfur trioxide pyridine (SO_3Py, 30 eq), freshly distilled pyridine and triethylamine, and mild heating conditions (55 °C) over three days. The resulting monomers (**18** – **21**) were purified by Sephadex LH-20 chromatography to remove excess sulfur trioxide salts prior to polymerization.

In accordance with previous procedures for the synthesis of glycopolymer mimetics,[29] we found that polymerization of the sulfated HS monomers with 5 mol % of Grubbs' fast-initiating catalyst [$(H_2IMes)(Py)_2(Cl)_2Ru$=CHPh][41] led to rapid conversion to the desired glycopolymers (**22** – **25**) within minutes. By varying the amount of catalyst, we could predictably control the polymer lengths within a relatively narrow polydispersity range, affording glycopolymers with lengths comparable to commercial heparin (Table 2). We utilized a 10:1 ratio of dichloroethane (DCE) and methanol (MeOH) for ROMP, as we determined this ratio to represent the minimal amount of MeOH required to dissolve the sulfated monomers (higher levels of MeOH compromised the efficacy of the catalyst and resulted in premature termination of the polymer chain). While

others[29] have reported that mild heating (55 °C) is necessary for the polymerization reaction to achieve complete conversion, we did not find this requirement to be necessary if the DCE and MeOH solvents were thoroughly degassed by multiple freeze-pump-thaw cycles and extended purge by argon, respectively. We also commenced the stirring of the reaction only after the catalyst was added to ensure that the solvents remained thoroughly degassed; this small alteration in our methodology led to considerable improvements in experimental consistency.

Table 2. Properties of glycopolymers **1 – 4**.

	Monomer	mol% Catalyst	M_n[a] (g/mol)	PDI[a]	n (DP[b])
1	**22**	5	27,870	1.22	35
2	**23**	5	36,490	1.02	48
3	**24**	5	53,580	1.16	90
4	**25**	5	32,880	1.03	46

[a]Number average molecular weight (M_n) and polydispersity index (PDI) were determined by size exclusion chromatography multi-angle light scattering (SEC-MALS). [b]Degree of polymerization (DP). Despite equal mol% of catalyst, the DP was notably higher for unsulfated monomer **24**. This was likely due to increased solubility of the unsulfated polymer (**3**) in the polymerization co-solvent (10:1 dichloroethane/methanol) compared to the sulfated polymers (**1**, **2**, and **4**).

In designing the remainder of our synthetic scheme, we reasoned that removing the methyl ester, benzyl ether, and TBS prior to ROMP might compromise the efficacy of the polymerization reaction. However, any late-stage deprotection steps performed on the glycopolymer needed to go to completion to ensure homogeneity of the final compounds. Thus, we decided to first optimize our deprotection conditions using **18** to prepare a monovalent trisulfated disaccharide with the norbornyl linker at the reducing end (**26,** see methods section for structure); identical conditions

were then applied to glycopolymers **22** – **25**. For example, while standard conditions for methyl ester saponification (30% H_2O_2, 1M LiOH, 4N NaOH) were not found to be compatible with our model substrates, we were pleased to find that powerful nucleophile potassium trimethylsilanolate (TMSOK) not only saponified the methyl ester, but also removed the C4' TBS group, likely due to its close proximity to the resulting C5' carboxylate anion. The mechanism of this reaction warrants further investigation, but serves as an elegant example for how the *in situ* generation of a nucleophilic silanolate can be used to streamline the synthesis of HS oligosaccharides.

Finally, we found that catalytic hydrogenation using $Pd(OH)_2$/charcoal in a mixture of phosphate buffer (pH = 7.4) and MeOH[39] delivered final targets **26** and glycopolymers **1** – **4**. The reaction mixture was filtered through a polyethersulfone (PES) membrane to remove excess palladium particles and purified using a Sephadex G-25 column. We then characterized the final polymers by ^{1}H NMR spectroscopy and size exclusion chromatography multi-angle light scattering (SEC-MALS) to determine both chemical homogeneity and molecular weight. Moreover, comparison of the ^{1}H-^{1}H COSY NMR spectrum of trisulfated monomer **26** to that of glycopolymer **1** confirmed that all sulfate groups remained intact during the post-polymerization deprotection steps, given that the two compounds exhibited identical chemical shifts for cross-peaks in the ring proton region. These additional characterization steps allowed us to be confident in our assignments of the chemical structures for all four glycopolymers.

Experimental Methods and Spectral Assignments

Unless stated otherwise, reactions were performed in flame-dried glassware under an argon atmosphere using freshly dried solvents. Solvents were dried via passage through an activated alumina column under argon. All other commercially obtained reagents were used as received

unless otherwise noted. Thin-layer chromatography (TLC) was performed using E. Merck silica gel 60 F254 pre-coated plates (0.25 mm). Visualization of the chromatogram was accomplished by UV, cerium ammonium molybdate, or ninhydrin staining, as necessary. ICN silica gel (particle size 0.032 – 0.063 mm) was used for flash chromatography. Gel filtration chromatography was also used in order to achieve purification of the final products.

^{1}H and ^{13}C NMR experiments were recorded on Varian Mercury 300 (at 300 MHz), Varian Inova 500 (at 500 MHz), or Varian Inova 600 (600 MHz) spectrometers and are reported in parts per million (δ) relative to $CDCl_3$ (7.26 ppm) or CD_3OD (4.80 ppm). Data for ^{1}H are reported as follows: chemical shift (δ ppm), multiplicity (s = singlet, d = doublet, t = triplet, q = quartet, m = multiplet), coupling constant in Hz, and integration. ^{13}C NMR spectra were obtained on Varian Inova 500 (at 125 MHz) or Varian Inova 600 (at 150 MHz) spectrometers and are reported in terms of chemical shift (77.2 ppm for $CDCl_3$; 49.0 for CD_3OD). When necessary, proton and carbon assignments were made by means of ^{1}H-^{1}H gCOSY, ^{1}H-^{1}H TOCSY, and ^{1}H-^{13}C gHSQCAD. Stereochemical assignments are supported by ^{1}H-^{1}H ROESY spectra. Mass spectra were obtained using a Perkin Elmer/Sciex API 365 triple quadrupole/electrospray tandem mass spectrometer or a Waters LCT Premier XE high resolution mass spectrometer.

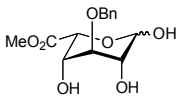

Methyl 3-*O*-benzyl-L-idopyranosyluronate (9). Compound **9** was prepared in six steps from the commercially available diacetone glucose (Sigma Aldrich) using previously reported procedures.[33] The analytical data were in agreement with the reported spectra.

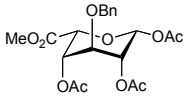

Methyl 1,2,4-tri-*O*-acetyl-3-*O*-benzyl-β-L-idopyranosyluronate (10). Compound **9** (0.30 g, 1.0 mmol) was added to CH_2Cl_2 (5.5 mL) at 0 °C, and the solution was cooled to -40 °C. 4-Dimethylaminopyridine (120 mg, 0.10 mmol) was added, followed by pyridine (700 μL, 10 mmol). Acetyl chloride (470 μL, 6.0 mmol) was then added dropwise to the reaction mixture, which was stirred for 10 h at -40 °C. The reaction was quenched with aqueous $NaHCO_3$ (50 mL), extracted with CH_2Cl_2 (2.0 x 50 mL), and subsequently washed with H_2O, 1M H_2SO_4, and then H_2O (50 mL for each wash). The combined organic layers were dried over $MgSO_4$ and concentrated under reduced pressure. Purification by silica gel flash chromatography (3:1 hexanes:EtOAc) afforded compound **10** (0.40 g) in quantitative yield. The analytical data were in agreement with previously reported spectra.[35] ESI-TOF HRMS: *m/z* calcd for $C_{20}H_{23}O_{10}$ [M+H]-H_2 423.1286; found: 423.1286.

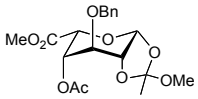

Methyl 4-*O*-acetyl-3-*O*-benzyl-β-L-idopyranuronate 1,2-(methyl-orthoacetate) (11). $TiBr_4$ (8.1 g, 22 mmol) was added to a solution of compound **10** (6.9 g, 16 mmol) in CH_2Cl_2 (360 mL), and the reaction was stirred for 16 h at ambient temperature with exclusion of light. The reaction was quenched with ice-cold H_2O (2.0 x 500 mL), filtered through Celite, and concentrated under reduced pressure. The resulting brown oil was immediately used in the next reaction without

further purification. The crude bromide intermediate (16 mmol) was dissolved in CH_2Cl_2 (220 mL). 2,4,6-Collidine (11 mL, 80 mmol) and methanol (8.0 mL) were added to this solution, and the reaction was stirred for 14 h at room temperature (rt). The reaction mixture was then diluted with CH_2Cl_2 (500 mL), washed with aqueous $NaHCO_3$ and H_2O (200 mL each), dried over $MgSO_4$, and concentrated under reduced pressure. Purification by silica gel flash chromatography (6:1 hexanes:EtOAc + 1% Et_3N) afforded **11** (7.6 g, 75% over 2 steps) as a light yellow oil. ^{1}H NMR (500 MHz; $CDCl_3$): δ 7.44 – 7.30 (m, 5H, OCH_2*Ph*), 5.57 (d, *J* = 2.7 Hz, 1H, H-1), 5.20 (dt, *J* = 2.7, 1.3 Hz, 1H, H-4), 4.82 (d, *J* = 11.7 Hz, 1H, OC*H*$_2$Ph), 4.69 (d, *J* = 11.7 Hz, 1H, OC*H*$_2$Ph), 4.56 (d, *J* = 1.4 Hz, 1H, H-5), 4.15 (dd, *J* = 2.7, 1.9 Hz, 1H, H-3), 4.09 (ddd, *J* = 2.9, 1.9, 1.2 Hz, 1H, H-2), 3.79 (s, 3H, CO_2C*H*$_3$), 3.26 (s, 3H, OC*H*$_3$), 2.05 (s, 3H, OCOC*H*$_3$), 1.74 (s, 3H, C*H*$_3$); ^{13}C NMR (125 MHz; $CDCl_3$): δ 170.1, 168.1, 136.8, 128.6, 128.4, 128.0, 96.6, 77.3, 76.1, 72.9, 71.3, 69.6, 68.9, 52.6, 49.1, 25.0, 20.1; ESI-TOF HRMS: *m/z* calcd for $C_{19}H_{23}O_9$ $[M+H]-H_2$ 395.1342; found: 395.1354.

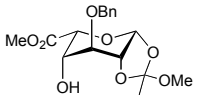

Methyl 3-*O*-benzyl-β-L-idopyranuronate 1,2-(methyl-orthoacetate) (12). Compound **11** (7.2 g, 18 mmol) was dissolved in methanol (90 mL) and cooled to -10 °C. A 0.5 M solution NaOMe (1.8 mL, 0.91 mmol) was added, and the reaction mixture was stirred at -10 °C for 2 h and at 5 °C overnight. The solution was diluted with CH_2Cl_2 (200 mL) at 5 °C, quenched with aqueous $NaHCO_3$ and H_2O (500 mL each), and then extracted with (3.0 x 250 mL). The organic fractions were dried over $MgSO_4$ and concentrated under reduced pressure. Purification by silica gel flash chromatography (4:1 → 1:1 hexanes:EtOAc + 1% Et_3N) yielded **12** (9.5 g, 80%) as a clear oil. ^{1}H

NMR (500 MHz; $CDCl_3$): δ 7.36 – 7.34 (m, 5H, OCH_2Ph), 5.51 (d, J = 2.4 Hz, 1H, H-1), 4.72 (d, J = 11.7 Hz, 1H, OCH_2Ph), 4.62 (d, J = 11.7 Hz, 1H, OCH_2Ph), 4.52 (s, 1H, H-4), 4.15 – 4.08 (m, 3H, H-2, H-5), 3.81 (s, 3H, CO_2CH_3), 3.30 (s, 3H, OCH_3), 2.78 (d, J = 11.4 Hz, 1H, H-3), 1.76 (s, 3H, CH_3); ^{13}C NMR (125 MHz; $CDCl_3$): δ 168.3, 136.8, 128.7, 128.4, 127.9, 96.8, 75.8, 73.0, 72.9, 71.8, 67.0, 52.5, 50.3, 24.4; ESI-TOF HRMS: m/z calcd for $C_{17}H_{21}O_8$ [M+H]-H_2 353.1236; found: 353.1226.

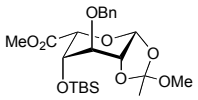

Methyl 3-*O*-benzyl-4-*O*-*tert*-butyldimethylsilyl-β-L-idopyranuronate 1,2-(methyl-orthoacetate) (13). Compound **12** (230 mg, 0.64 mmol) was dissolved in pyridine (7.8 mL) and the solution was cooled to -10 °C. TBSOTf (1.5 mL, 0.65 mmol) was added, and the reaction was stirred overnight at 0 °C. The reaction was diluted with CH_2Cl_2 (100 mL), quenched with aqueous $NaHCO_3$ (100 mL), and extracted with EtOAc (3.0 x 50 mL). The combined organic fractions were dried over $MgSO_4$ and concentrated under reduced pressure. Purification by silica gel flash chromatography (7:1 hexanes:EtOAc + 1% Et_3N) yielded compound **32** (380 mg, 92%) as a clear oil. ^1H NMR (500 MHz; $CDCl_3$): δ 7.47 (m, 5H, OCH_2Ph), 5.62 (d, J = 2.5 Hz, 1H, H-1), 4.80 (d, J = 12 Hz, 1H, OCH_2Ph), 4.75 (d, J = 12 Hz, 1H, OCH_2Ph), 4.51 (s, 1H, H-4), 4.21 (s, 1H, H-5), 4.20 (d, J = 1 Hz, 1H, H-4), 3.98 (s, 1H, H-3), 3.89 (s, 3H, CO_2CH_3), 3.40 (s, 3H, OCH_3), 1.84 (s, 3H, CH_3), 0.94 (s, 9H, $SiC(CH_3)_3$), 0.08 (s, 3H, $SiCH_3$), 0.06 (s, 3H, $SiCH_3$); ^{13}C NMR (125 MHz; $CDCl_3$): δ 169.6, 137.0, 128.9, 128.6, 128.2, 124.6, 97.1, 76.3. 74.6, 72.8, 72.5, 67.9, 52.4, 49.5, 29.9, 25.7, 25.6, -4.4, -5.2; TOF HRMS ES m/z calcd for $C_{23}H_{36}O_8SiNa$ $[M+Na]^+$: 491.2077; found: 491.2070.

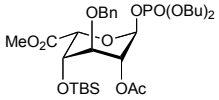

Methyl (dibutylphosphate-2-*O*-acetyl-3-*O*-benzyl-4-*O*-*tert*-butyldimethylsilyl-α-L-idopyranosid)uronate (6). Compound **13** (140 mg, 0.29 mmol) was dissolved in CH_2Cl_2 (7.3 mL) at rt. Freshly activated 4Å molecular sieves (290 mg) were added, and the solution was stirred for 15 min. Dibutylphosphate (0.54 mL, 2.9 mmol) was added slowly, and the reaction mixture was stirred overnight. After confirming that the reaction was complete by TLC, the reaction was quenched with triethylamine (2.0 mL) and concentrated under reduced pressure. Silica gel flash chromatography (5:1 → 3:1 hexanes:EtOAc + 1% Et_3N) afforded the desired product (170 mg) in quantitative yield. ^{1}H NMR (500 MHz; $CDCl_3$): δ 7.36 – 7.35 (m, 5H, OCH_2*Ph*), 5.82 (d, *J* = 7.2 Hz, 1H, H-1), 4.97 (m, 1H, H-2), 4.86 (d, *J* = 2.7 Hz, 1H, H-5), 4.78 (d, *J* = 12 Hz, 1H, OCH_2Ph), 4.62 (d, *J* = 12 Hz, 1H, OCH_2Ph), 4.09 – 3.99 (m, 5H, H-4, $P(OCH_2CH_2CH_3)_2$), 3.77 (s, 3H, CO_2CH_3), 3.62 (m, 1H, H-3), 2.04 (s, 3H, $COCH_3$), 1.64 – 1.60 (m, 4H, $P(OCH_2CH_2CH_2CH_3)_2$), 1.40 – 1.25 (m, 4H, $P(OCH_2CH_2CH_2CH_3)_2$), 0.96 – 0.88 (m, 6H, $P(OCH_2CH_2CH_2CH_3)_2$), 0.81 (s, 9H, $SiC(CH_3)_3$), 0.07 (s, 3H, $SiCH_3$), 0.17 (s, 3H, $SiCH_3$); ^{13}C NMR (125 MHz; $CDCl_3$): δ 169.8, 169.2, 146.6, 137.3, 128.4, 128.0, 95.4, 73.8, 72.0, 68.0, 67.8, 67.0, 66.9, 52.1, 32.1, 25.4, 20.9, 18.6, 17.8, 13.5, -4.7, -5.7; ESI-TOF HRMS *m/z* calcd for $C_{30}H_{52}O_{11}PSi$ $[M+H]^+$: 647.3017; found: 647.3001.

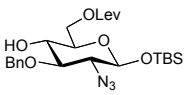

2-*O*-Azido-3-*O*-benzyl-6-*O*-levulinoyl-1-*O*-*tert*-butyldimethylsilyl-2-deoxy-β-D-glucopyranoside (7). Compound **7** was prepared from readily available D-glucosamine (Sigma Aldrich) using previously published procedures, and the analytical data were in agreement with previously reported spectra.[33]

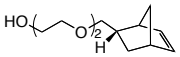

2-(2-((2*S*)-bicyclo[2.2.1]hept-5-en-2-ylmethoxy)ethoxy)ethanol (8). Compound **8** was prepared using a previously published procedure, and the analytical data were in agreement with reported spectra.[34]

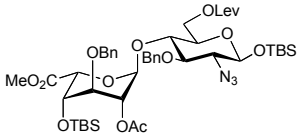

Methyl 2-*O*-acetyl-3-*O*-benzyl-4-*O*-*tert*-butyldimethylsilyl-α-L-idopyranosyluronate-(1→4)-*tert*-butyldimethylsilyl (2-azido-3-*O*-benzyl-6-*O*-levulinoyl-2-deoxy-β-D-glucopyranoside) (14). Compound **6** (92 mg, 0.14 mmol) and **7** (77 mg, 0.17 mmol) were co-evaporated with toluene (3.0 x 1.0 mL) and placed under vacuum overnight. The mixture was dissolved in CH_2Cl_2 (4.2 mL), and freshly activated 4Å molecular sieves (0.21 g) were added. After stirring at rt for 15 min, the temperature was lowered to -10 °C and the mixture stirred for an additional 15 min. TMSOTf (31 μL, 0.18 mmol) was added dropwise to the reaction mixture. The reaction was stirred at -30 °C for 30 min, quenched with Et_3N (1.0 mL), filtered through a silica pad, and

concentrated under reduced pressure. Silica gel flash chromatography (5:1 → 4:1 hexanes:EtOAc) afforded the desired product (120 mg) in 93% yield. ^{1}H NMR (600 MHz; $CDCl_3$): δ 7.37 – 7.24 (m, 10H, OCH_2Ph), 5.20 (d, J = 4.2 Hz, 1H, H-1 of IdoA), 4.85 (t, J = 4.1 Hz, 1H, H-2 of IdoA), 4.82 (d, J = 10.6 Hz, 1H, OCH_2Ph), 4.74 (d, J = 11.8 Hz, 1H, OCH_2Ph), 4.71 (d, J = 10.8 Hz, 1H, OCH_2Ph), 4.69 (d, J = 3.9 Hz, 1H, H-5 of IdoA), 4.64 (d, J = 11.8 Hz, 1H, OCH_2Ph), 4.54 (dd, J = 11.8, 2.1 Hz, 1H, H-1 of GlcN), 4.51 – 4.45 (m, 1H, H-6), 4.20 – 4.03 (m, 1H, H-6), 3.99 (t, J = 4.3 Hz, 1H, H-4 of IdoA), 3.91 – 3.77 (m, 1H, H-4 of GlcN), 3.61 (t, J = 4.3 Hz, 1H, H-3 of IdoA), 3.54 (s, 3H, CO_2CH_3), 3.48 (ddd, J = 9.8, 5.9, 2.2 Hz, 1H, H-5 of GlcN), 3.37 – 3.24 (m, 2H, H-2 and H-3 of GlcN), 2.89 – 2.66 (m, 2H, $COCH_2CH_2COCH_3$), 2.61 (t, J = 6.7 Hz, 2H, $COCH_2CH_2COCH_3$), 2.19 (s, 3H, $COCH_2CH_2COCH_3$), 2.00 (s, 3H, $COCH_3$), 0.92 (s, 9H, $SiC(CH_3)_3$), 0.81 (s, 9H, $SiC(CH_3)_3$), 0.13 (d, J = 4.6 Hz, 6H, $SiCH_3$), -0.06 (s, 3H, $SiCH_3$), -0.12 (s, 3H, $SiCH_3$); ^{13}C NMR (125 MHz; $CDCl_3$): δ 206.5, 172.2, 170.2, 169.9, 138.2, 137.7, 128.5, 128.1, 128.1, 127.9, 127.4, 97.6, 97.1, 80.6, 76.8, 76.5, 75.4, 74.8, 73.4, 72.7, 71.5, 69.9, 68.9, 68.5, 62.6, 51.7, 38.0, 29.9, 28.0, 25.6, 25.5, 20.9, 18.0, 17.8, -4.3, -4.7, -5.2, -5.5; ESI-TOF HRMS m/z calcd for $C_{46}H_{69}N_3O_{14}Si_2$ $[M+Na]^+$: 966.4216; found: 966.4211.

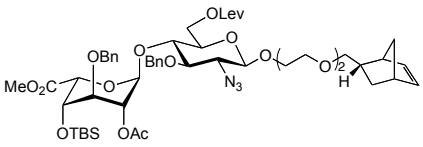

Methyl 2-*O*-acetyl-3-*O*-benzyl-4-*O*-*tert*-butyldimethylsilyl-α-L-idopyranosyluronate-(1→4)-2-azido-3-*O*-benzyl-1-*O*-(2-(2-((2*S*)-bicyclo[2.2.1]hept-5-en-2-yl-methoxy)ethoxy)ethyl)-6-*O*-levulinoyl-2-deoxy-α-D-glucopyranoside (5). Compound **15** (37 mg, 60 μmol) and **8** (33 mg, 70 μmol) were co-evaporated with toluene (3.0 x 1.0 mL) and placed under vacuum overnight. The

mixture was dissolved in CH_2Cl_2 (1.7 mL) and freshly activated 4Å molecular sieves (80 mg) were added. After stirring at rt for 15 min, the temperature was lowered to -30 °C and the mixture stirred for an additional 15 min. TMSOTf (14 μL, 70 μmol) was added to dropwise to the reaction mixture. The reaction was stirred at -10 °C for 10 min, slowly raised to rt over 15 min, quenched with Et_3N (0.50 mL), filtered through a silica pad, and concentrated under reduced pressure. Silica gel flash chromatography (10:1 → 4:1 → 3:1 hexanes:EtOAc) afforded the desired product (35 mg) in 67% yield. ^{1}H NMR (500 MHz; $CDCl_3$): δ 7.38 – 7.25 (m, 10H, OCH_2*Ph*), 6.07 (ddd, *J* = 25.6, 5.7, 3.0 Hz, 2H, C*H*=C*H* of Nb), 5.19 (d, *J* = 4.2 Hz, 1H, H-1 of IdoA), 4.89 – 4.79 (m, 2H, H-2 of IdoA, OC*H*$_2$Ph), 4.72 – 4.68 (m, 3H, H-5 of IdoA, OC*H*$_2$Ph), 4.64 (d, *J* = 11.9 Hz, 1H, OC*H*$_2$Ph), 4.52 (dd, *J* = 12.1, 2.2 Hz, 1H, H-6 of GlcN), 4.34 (d, *J* = 7.9 Hz, 1H, H-1 of GlcN), 4.12 (dd, *J* = 12.1, 2.2 Hz, 1H, H-6 of GlcN), 4.02 – 3.93 (m, 2H, H-4 of IdoA, OC*H*$_2$ of PEG linker), 3.87 (dd, *J* = 9.8, 8.9 Hz, 1H, H-4 of GlcN), 3.82 – 3.55 (m, 5H, H-3 of IdoA, OC*H*$_2$ of PEG linker), 3.54 (s, 3H, CO_2C*H*$_3$), 3.53 – 3.29 (m, 5H, H-5 of GlcN, H-2 of GlcN, H-3 of GlcN, OC*H*$_2$ of PEG linker), 2.88 – 2.67 (m, 4H, C*H*-CH=CH of Nb, $COCH_2CH_2COCH_3$), 2.67 – 2.56 (m, 2H, $COCH_2CH_2COCH_3$), 2.19 (s, 3H, $COCH_2CH_2COCH_3$), 2.00 (s, 3H, OCOC*H*$_3$), 1.75 – 1.66 (m, 1H, C*H* of Nb), 1.39 – 1.15 (m, 4H, C*H*$_2$ of Nb), 0.81 (s, 9H, SiC(C*H*$_3$)), -0.06 (s, 3H, SiC*H*$_3$), -0.11 (s, 3H, SiC*H*$_3$); ^{13}C NMR (125 MHz; $CDCl_3$): δ 136.6, 128.5, 128.2, 127.8, 102.2, 80.9, 76.8, 76.1, 75.0, 73.2, 72.9, 71.6, 70.7, 70.4, 66.0, 45.0, 43.6, 38.8, 38.0, 29.8, 28.1, 25.5; ESI-TOF HRMS *m/z* calcd for $C_{52}H_{73}N_3O_{16}Si$ $[M+Na]^+$: 1046.4658; found: 1046.4670

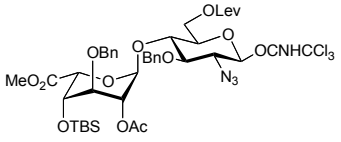

Methyl 2-*O*-acetyl-3-*O*-benzyl-4-*O*-*tert*-butyldimethylsilyl-α-L-idopyranosyluronate-(1→4)-2-azido-3-*O*-benzyl-6-*O*-levulinoyl-2-deoxy-β-D-glucopyranosyl trichloroacetimidate (15). Compound **14** (840 mg, 0.89 mmol) was dissolved in THF (27 mL) and the solution was cooled to 0 °C. 1M TBAF (1.2 mL, 1.2 mmol) and AcOH (60 μL, 1.1 mmol) were added simultaneously, and the reaction was stirred for 30 min at 0 °C. The reaction was quenched with aqueous $NaHCO_3$ (10 mL), extracted with CH_2Cl_2 (2.0 x 10 mL), and subsequently washed with H_2O, 1M H_2SO_4, and then H_2O (10 mL for each wash). After concentrating under reduced pressure, the crude mixture (0.89 mmol) was dissolved in CH_2Cl_2 (27 mL) and cooled to 0 °C. To the reaction mixture, trichloroacetonitrile (1.3 mL, 13 mmol) and DBU (26 μL, 0.18 mmol) were added. The reaction was stirred at 0 °C for 12 h, quenched with Et_3N (1.0 mL), and concentrated under reduced pressure. Silica gel flash chromatography (5:1 → 4:1 → 3:1 hexanes:EtOAc + 1% Et_3N) afforded the desired product (770 mg) in 89% yield over two steps. ^{1}H NMR (600 MHz; $CDCl_3$): δ 8.72 (s, 1H, OCN*H*CCl_3), 7.47 – 7.28 (m, 10H, OCH_2*Ph*), 6.37 (d, *J* = 3.6 Hz, 1H, H-1 of IdoA), 5.24 (d, *J* = 4.7 Hz, 1H, H-1 of GlcN), 4.96 (d, *J* = 10.5 Hz, 1H, OC*H*$_2$Ph), 4.90 (t, *J* = 4.4 Hz, 1H, H-2 of GlcN), 4.75 (d, *J* = 11.7 Hz, 1H, OC*H*$_2$Ph), 4.71 (d, *J* = 10.5 Hz, 1H, OC*H*$_2$Ph), 4.66 (d, *J* = 11.8 Hz, 1H, OC*H*$_2$Ph), 4.63 (d, *J* = 4.2 Hz, 1H, H-5 of GlcN), 4.52 (dd, *J* = 12.3, 1.8 Hz, 1H, H-6 of GlcN), 4.13 (dd, *J* = 12.3, 4.3 Hz, 1H, H-6 of GlcN), 4.08 – 3.98 (m, 3H, H-4 and H-5 of IdoA, H-4 of GlcN), 3.91 (dd, *J* = 10.2, 8.5 Hz, 1H, H-3 of IdoA), 3.69 (dd, *J* = 10.2, 3.6 Hz, 1H, H-2 of IdoA), 3.66 – 3.61 (m, 1H, H-3 of GlcN), 3.57 (s, 3H, CO_2C*H*$_3$), 2.89 – 2.69 (m, 2H, COC*H*$_2CH_2COCH_3$), 2.67 – 2.54 (m, 2H, $COCH_2C$*H*$_2COCH_3$), 2.18 (s, 3H, $COCH_2CH_2COC$*H*$_3$), 2.01 (s, 3H, COC*H*$_3$), 0.82 (d, *J* = 2.5 Hz, 9H, $SiC(C$*H*$_3)_3$), -0.05 (s, 3H, SiC*H*$_3$), -0.09 (s, 3H, SiC*H*$_3$); ^{13}C NMR (125 MHz; $CDCl_3$): δ 206.5, 172.1, 170.2, 170.0, 160.7, 137.7, 137.6, 128.7, 128.2, 128.1, 128.0, 127.9, 127.6, 97.7, 94.4, 78.2, 77.2, 76.7, 75.1, 75.0,

73.0, 72.0, 71.9, 70.2, 69.0, 62.8, 61.9, 51.7, 38.0, 29.9, 28.0, 25.5, 20.1, 17.8, 4.7, 5.4; ESI-TOF HRMS *m/z* calcd for $C_{42}H_{55}N_3O_{15}SiCl_3$ [M+Na]$^+$: 997.2366; found: 997.2415.

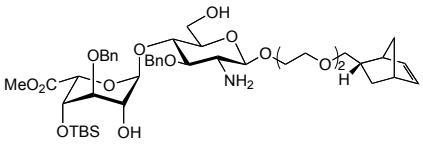

Methyl 3-*O*-benzyl-4-*O*-*tert*-butyldimethylsilyl-α-L-idopyranosyluronate-(1→4)-2-amino-3-*O*-benzyl-1-*O*-(2-(2-((2*S*)-bicyclo[2.2.1]hept-5-en-2-ylmethoxy)ethoxy)ethyl)-2-deoxy-α-D-glu-copyranoside (16). Compound **5** (17 mg, 20 μmol) was dissolved in anhydrous MeOH (0.80 mL), and 1,3-propanedithiol (0.14 mL, 60 μmol) and DIPEA (0.12 mL, 60 μmol) were added dropwise. Upon confirmation of partial disappearance of **5** by TLC, flame-dried K_2CO_3 (2.4 mg, 20 μmol) was added and the reaction mixture was stirred for 24 h at rt. The reaction was quenched with Dowex 5W-X8 (H^+ form), filtered through a pad of Celite, and concentrated under reduced pressure. Silica gel flash chromatography (1:1 hexanes:EtOAc) afforded the desired product (14 mg) in 93% yield. ^{1}H NMR (500 MHz; $CDCl_3$): δ 7.48 – 7.20 (m, 10H, OCH_2Ph), 6.17 – 5.88 (m, 2H, C*H*=C*H* of Nb), 5.25 (d, *J* = 4.5 Hz, 1H, H-1 of IdoA), 4.96 (d, *J* = 11.4 Hz, 1H, OCH_2Ph), 4.83 (d, *J* = 11.4 Hz, 1H, OCH_2Ph), 4.68 – 4.51 (m, 3H, OCH_2Ph, H-5 of IdoA), 4.32 (d, *J* = 8.0 Hz, 1H, H-1 of GlcN), 4.09 – 3.76 (m, 5H, H-6 of IdoA, H-4 of IdoA, H-2 of IdoA, OCH_2 of PEG linker), 3.76 – 3.53 (m, 10H, H-2 of IdoA, H-6 of IdoA, OCH_2 of PEG linker, CO_2CH_3), 3.47 – 3.32 (m, 4H, H-4 of GlcN, OCH_2 of PEG linker, H-5 of GlcN, H-3 of GlcN), 2.84 – 2.68 (m, 3H, H-2 of GlcN, C*H*-CH=CH of Nb), 1.69 – 1.63 (m, 1H, C*H* of Nb), 1.40 – 1.03 (m, 4H, CH_2 of Nb), 0.82 (s, 9H, SiC(CH_3)), -0.03 (d, *J* = 7.3 Hz, 7H, SiCH_3); ^{13}C

NMR (125 MHz; CD_3OD): δ 171.7, 140.1, 139.7, 137.7, 137.5, 129.2, 128.8, 128.4, 104.5, 102.3, 84.1, 79.5, 77.7, 77.0, 75.2, 74.4, 72.8, 71.5, 71.4, 61.8, 57.8, 52.4, 45.8, 44.9, 42.8, 40.1, 30.6, 26.1, 18.7, -4.5, -5.1; ESI-TOF HRMS: *m/z* calcd for $C_{45}H_{66}NO_{13}Si$ $[M-H]^-$ 856.4303; found: 856.4326.

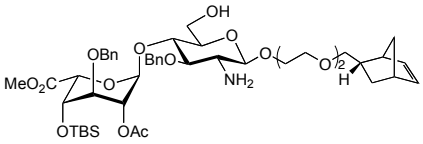

Methyl 2-*O*-acetyl-3-*O*-benzyl-4-*O*-*tert*-butyldimethylsilyl-α-L-idopyranosyluronate-(1→4)-2-acetylamido-3-*O*-benzyl-1-*O*-(2-(2-((2*S*)-bicyclo[2.2.1]hept-5-en-2-ylmethoxy)ethoxy)ethyl)-2-deoxy-α-D-glucopyranoside (17). Compound **5** (190 mg, 0.18 mmol) was dissolved in anhydrous MeOH (11 mL). 1,3-propanedithiol (1.1 mL, 5.4 mmol) and DIPEA (1.1 mL, 6.3 mmol) were added dropwise, and the reaction mixture was stirred for 24 h at rt. The reaction was quenched with Dowex 5W-X8 (H^+ form), filtered through a pad of Celite, and concentrated under reduced pressure. Silica gel flash chromatography (30:2:1 → 20:2:1 EtOAc:MeOH:H_2O) afforded the desired product (150 mg), and the resulting intermediate was dissolved in pyridine (2.8 mL). To this mixture, a solution of hydrazine monohydrate (1.2 mmol) and AcOH (9.9 mmol) in pyridine (17 mL) was added at rt. The reaction mixture was diluted with CH_2Cl_2 (10 mL), washed with cold water (15 mL), saturated $NaHCO_3$ (15 mL), water (15 mL), and saturated brine (15 mL). The combined organic fractions were dried over $MgSO_4$ and concentrated under reduced pressure. Silica gel flash chromatography (20:2:1 EtOAc:MeOH:H_2O) afforded the desired product (140 mg) in 87% yield over two steps. ^1H NMR (500 MHz; $CDCl_3$): δ 7.46 – 7.27 (m, 10H, OCH_2Ph), 6.14 – 5.98 (m, 2H, C*H*=C*H* of Nb), 5.31 (d, *J* = 4.4 Hz, 1H, H-1 of IdoA), 4.99

(d, *J* = 11.2 Hz, 1H, OC*H*$_2$Ph), 4.88 (q, *J* = 3.6 Hz, 1H, H-2 of IdoA), 4.80 – 4.68 (m, 2H, OC*H*$_2$Ph, H-5 of IdoA), 4.67 – 4.55 (m, 2H, OC*H*$_2$Ph), 4.36 (dt, *J* = 8.0, 4.1 Hz, 1H, H-1 of GlcN), 4.05 – 3.85 (m, 4H, H-4 of IdoA, H-6 of GlcN, H-5 of GlcN, OC*H*$_2$ of PEG linker), 3.85 – 3.34 (m, 15H, OC*H*$_2$ of PEG linker, H-6 of GlcN, H-3 of IdoA, CO_2CH_3, H-3 of GlcN, H-4 of GlcN), 2.89 (dd, *J* = 10.0, 7.8 Hz, 1H, H-2 of GlcN), 2.81 – 2.67 (m, 2H, C*H*-CH=CH of Nb), 2.01 (s, 3H, OCOC*H*$_3$), 1.42 – 1.14 (m, 5H, C*H* and C*H*$_2$ of Nb), 0.82 (s, 9H, SiC(C*H*$_3$)), -0.08 (d, *J* = 7.3 Hz, 6H, SiC*H*$_3$); ^{13}C NMR (125 MHz; $CDCl_3$): δ 170.2, 138.7, 137.8, 136.7, 128.5, 128.1, 127.9, 127.6, 97.8, 76.8, 76.2, 75.7, 75.5, 74.2, 72.7, 72.0, 70.7, 70.4, 69.3, 69.0, 61.7, 56.6, 51.9, 45.1, 43.8, 41.7, 38.9, 38.6, 29.9, 25.7, 21.1, 17.9, -4.5, -5.4; ESI-TOF HRMS: *m/z* calcd for $C_{47}H_{70}NO_{14}Si$ $[M-H]^-$ 900.4565; found: 900.4568.

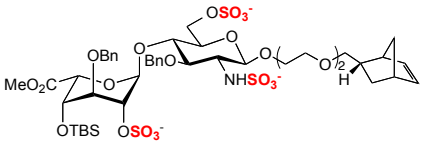

Methyl 3-*O*-benzyl-2-*O*-sulfonato-4-*O*-*tert*-butyldimethylsilyl-α-L-idopyranosyluronate-(1→4)-3-*O*-benzyl-1-*O*-(2-(2-((2*S*)-bicyclo[2.2.1]hept-5-en-2-ylmethoxy)ethoxy)ethyl)-2-deoxy-2-sulfonatamido-6-*O*-sulfonato-α-D-glucopyranoside (18). Compound **16** (9.2 mg, 10 μmol) was dissolved in freshly distilled pyridine (1.0 mL) and to this SO_3•Py (50 mg, 0.32 mmol) and Et_3N (0.20 mL) were added. The reaction mixture was stirred at rt for 24 h, refluxed at 50 °C for 24 h, quenched with MeOH (1.0 mL), and concentrated to afford a golden syrup. Purification by Sephadex LH-20 gel filtration (1:1 CH_2Cl_2:MeOH) followed by silica gel flash chromatography (15:2:1 → 10:2:1 → 8:2:1 EtOAc:MeOH:H_2O) gave the desired product (8.7 mg) in 78% yield. ^{1}H NMR (500 MHz; CD_3OD): δ 7.51 – 7.50 (m, 2H, OCH_2Ph), 7.43 – 7.41 (m, 2H, OCH_2Ph),

7.37 – 7.34 (m, 2H, OCH_2Ph), 7.30 – 7.26 (m, 3H, OCH_2Ph), 7.23 – 7.22 (m, 1H, OCH_2Ph), 6.11 – 6.04 (m, 2H, C*H*=C*H* of Nb), 5.30 (s, H-1 of IdoA), 4.98 (d, *J* = 12.5 Hz, 1H, OCH_2Ph), 4.87 (d, *J* = 11.5 Hz, 1H, OCH_2Ph), 4.78 (d, *J* = 6 Hz, 1H, H-1 of GlcN), 4.67 (d, *J* = 11.5 Hz, 1H, OCH_2Ph), 4.59 (d, *J* = 12.5 Hz, 1H, OCH_2Ph), 4.43 (s, 1H, H-2 of IdoA), 4.37 – 4.28 (m, 2H, H-6, H-6 of GlcN), 4.13 – 4.12 (m, 1H, H-4 of GlcN), 4.05 – 4.03 (m, 1H, H-5 of GlcN), 3.96 – 3.93 (m, 1H, H-4 of IdoA), 3.81 – 3.78 (m, 2H, H-3 of IdoA, OCH_2 of PEG linker), 3.73 – 3.71 (m, 2H, OCH_2 of PEG linker), 3.69 – 3.56 (m, 5H, OCH_2 of PEG linker), 3.54 – 3.51 (m, 1H, H-2 of GlcN), 3.45 – 3.35 (m, 2H, OCH_2 of PEG linker), 3.15 (s, 3H, CO_2CH_3), 2.77 (s, 1H, C*H*-CH=CH of Nb), 2.72 (s, 1H, C*H*-CH=CH of Nb), 2.11 (s, 3H, $OCOCH_3$), 1.98 (s, 3H, $OCOCH_3$), 1.72 – 1.68 (m, 1H, C*H* of Nb), 1.38 – 1.21 (m, 3H, CH_2 of Nb), 1.15 – 1.12 (m, 1H, CH_2 of Nb), 0.76 (s, 9H, $SiC(CH_3)$), -0.17 (s, 3H, $SiCH_3$), -0.24 (s, 3H, $SiCH_3$); ^{13}C NMR (125 MHz; CD_3OD): δ 172.8, 141.1, 140.4, 138.7, 131.6, 131.0, 130.6, 130.4, 130.3, 130.2, 130.0, 129.4, 104.3, 100.1, 80.9, 78.0, 77.0, 72.7, 72.4, 71.0, 70.7, 56.2, 53.5, 46.9, 46.0, 43.8, 41.1, 31.7, 27.4, 19.9, -3.0, -4.4; ESI-TOF HRMS: *m/z* calcd for $C_{45}H_{66}NO_{22}S_3Si$ $[M-H]^-$ 1016.2597; found: 1016.2583.

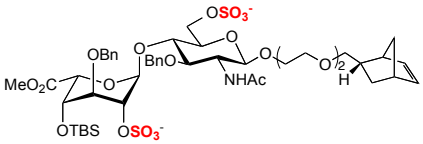

Methyl 2-*O*-sulfonato-3-*O*-benzyl-4-*O*-*tert*-butyldimethylsilyl-α-L-idopyranosyluronate-(1→4)-2-acetylamido-3-*O*-benzyl-1-*O*-(2-(2-((2*S*)-bicyclo[2.2.1]hept-5-en-2-ylmethoxy)ethoxy) ethyl)-2-deoxy-6-*O*-sulfonato-α-D-glucopyranoside (19). To a solution of compound **16** (130 mg, 0.15 mmol) in anhydrous MeOH (8.4 mL) at ambient temperature were added Ac_2O (0.30 mL, 3.0 mmol) and Et_3N (0.50 mL). Additional amounts of Ac_2O (0.30 mL, 3.0 mmol) were

added every hour until complete conversion to the desire product was observed by TLC (at least 4 h). The reaction mixture was directly loaded onto a Sephadex LH-20 gel filtration column and eluted with 1:1 CH_2Cl_2:MeOH. The *N*-acetylated intermediate was dissolved in freshly distilled pyridine (8.1 mL), and SO_3•Py (450 mg, 3.3 mmol) and Et_3N (1.6 mL) were added. The reaction mixture was stirred at rt for 24 h, refluxed at 50 °C for 24 h, quenched with MeOH (5.0 mL), and concentrated to afford a golden syrup. Purification by Sephadex LH-20 gel filtration (1:1 CH_2Cl_2:MeOH) followed by silica gel flash chromatography (10:2:1 EtOAc:MeOH:H_2O) gave the desired product (130 mg) in 85% yield over two steps. ^{1}H NMR (500 MHz; CD_3OD): δ 7.53 – 7.10 (m, 10H, OCH_2*Ph*), 6.12 – 5.95 (m, 2H, C*H*=C*H* of Nb), 5.35 (s, 1H, H-1 of IdoA), 4.84 (m, 2H, H-5 of IdoA, OCH_2*Ph*), 4.73 (d, *J* = 11.2 Hz, 1H, OCH_2*Ph*), 4.60 (d, *J* = 11.6 Hz, 1H, OCH_2*Ph*), 4.55 (d, *J* = 8.3 Hz, 1H, H-1 of GlcN), 4.52 (dd, *J* = 2.1, 1.1 Hz, 1H, H-2 of IdoA), 4.47 (d, *J* = 11.2 Hz, 1H, OCH_2*Ph*), 4.41 (dd, *J* = 11.3, 2.2 Hz, 1H, OCH_2 of PEG linker), 4.29 (dd, *J* = 11.2, 5.0 Hz, 1H, OCH_2 of PEG linker), 4.00 – 3.87 (m, 4H, H-4 of IdoA, H-2 of GlcN, H-3 of GlcN, H-6 of GlcN), 3.86 (t, *J* = 1.8 Hz, 1H, H-3 of IdoA), 3.79 – 3.48 (m, 11H, H-6 of GlcN, OCH_2 of PEG linker, H-4 of GlcN, H-5 of GlcN), 3.46 – 3.36 (m, 1H, OCH_2 of PEG linker), 3.33 (s, 3H, CO_2CH_3), 2.74 (d, *J* = 31.6 Hz, 2H, C*H*-CH=CH of Nb), 1.85 (d, *J* = 1.2 Hz, 3H, NHCOCH_3), 1.67 (d, *J* = 4.5 Hz, 1H, C*H* of Nb), 1.39 – 1.04 (m, 4H, CH_2 of Nb), 0.78 (d, *J* = 1.2 Hz, 9H, SiC(CH_3)), -0.11 (dd, *J* = 47.6, 1.1 Hz, 6H, SiCH_3); ^{13}C NMR (125 MHz; CD_3OD): δ 173.3, 172.1, 139.7, 139.2, 137.7, 137.5, 129.9, 129.5, 129.1, 128.6, 102.6, 99.2, 82.3, 77.1, 76.2, 75.7, 75.3, 74.1, 72.8, 71.5, 71.4, 70.1, 69.7, 67.8, 56.5, 52.4, 45.9, 44.9, 42.8, 40.0, 30.7, 26.2, 23.0, 18.9, -4.2, -5.4; ESI-TOF HRMS: *m/z* calcd for $C_{47}H_{67}NO_{20}NaSiS_2$ $[M+Na]^+$ 1080.3365; found: 1080.3392.

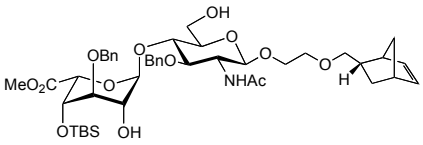

Methyl 3-*O*-benzyl-4-*O*-*tert*-butyldimethylsilyl-α-L-idopyranosyluronate-(1→4)-2-acetyl-amido-3-*O*-benzyl-1-*O*-(2-(2-((2*S*)-bicyclo[2.2.1]hept-5-en-2-ylmethoxy)ethoxy)ethyl)-2-de-oxy-α-D-glucopyranoside (20). To a solution of compound **16** (130 mg, 0.15 mmol) in anhydrous MeOH (8.4 mL) at ambient temperature were added Ac_2O (0.30 mL, 3.0 mmol) and Et_3N (0.50 mL). Additional amounts of Ac_2O (0.30 mL, 3.0 mmol) were added every hour until complete conversion to the desired product was observed by TLC (at least 4 h). Purification by Sephadex LH-20 gel filtration (1:1 CH_2Cl_2:MeOH) followed by silica gel flash chromatography (20:2:1 EtOAc:MeOH:H_2O) gave the desired product (140 mg) in quantitative yield. ^{1}H NMR (600 MHz; $CDCl_3$): δ 7.36 – 7.09 (m, 10H, OCH_2Ph), 6.12 – 5.87 (m, 2H, C*H*=C*H* of Nb), 5.11 (s, 1H, H-1 of IdoA), 4.76 – 4.72 (m, 1H, H-1 of GlcN), 4.70 (t, *J* = 2.7 Hz, 1H, H-4 of IdoA), 4.68 – 4.56 (m, 2H, OCH_2Ph), 4.51 – 4.43 (m, 2H, OCH_2Ph), 4.00 – 3.92 (m, 1H, H-3 of IdoA), 3.91 – 3.80 (m, 2H, OCH_2 of PEG linker, H-6 of GlcN), 3.80 – 3.17 (m, 19H, H-6 of GlcN, H-2 of GlcN, H-3 of GlcN, H-4 of GlcN, H-5 of GlcN, H-2 of IdoA, H-5 of IdoA, OCH_2 of PEG linker, CO_2CH_3), 2.75 – 2.46 (m, 2H, C*H*-CH=CH of Nb), 1.67 (d, *J* = 4.2 Hz, 3H, NHCOCH_3), 1.64 – 1.53 (m, 1H, C*H* of Nb), 1.30 – 1.13 (m, 4H, CH_2 of Nb), 0.71 (s, 9H, SiC(CH_3)), -0.15 (d, *J* = 9.3 Hz, 6H, SiCH_3); ^{13}C NMR (125 MHz; $CDCl_3$): δ 170.4, 169.7, 138.6, 137.5, 136.8, 136.6, 128.8, 128.4, 128.2, 127.4, 107.3, 101.6, 100.9, 78.7, 77.0, 76.4, 75.7, 75.5, 72.6, 72.5, 71.0, 70.7, 70.4, 69.8, 69.1, 68.8, 67.2, 62.7, 52.1, 45.2, 43.8, 41.7, 38.8, 30.0, 29.9, 25.6, 23.3, 17.9, -4.7, -5.4; ESI-TOF HRMS: *m/z* calcd for $C_{47}H_{69}NaNO_{14}Si$ $[M+Na]^+$ 922.4380; found: 922.4385.

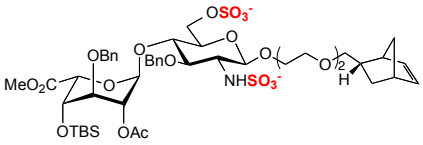

Methyl 2-*O*-acetyl-3-*O*-benzyl-4-*O*-*tert*-butyldimethylsilyl-α-L-idopyranosyluronate-(1→4)-3-*O*-benzyl-1-*O*-(2-(2-((2*S*)-bicyclo[2.2.1]hept-5-en-2-ylmethoxy)ethoxy)ethyl)-2-deoxy-2-sulfonatamido-6-*O*-sulfonato-α-D-glucopyranoside (21). To a solution of compound **17** (22 mg, 0.020 mmol) in freshly distilled pyridine (2.3 mL) were added SO_3•Py (110 mg, 0.60 mmol) and Et_3N (0.5 mL). The reaction mixture was stirred at rt for 24 h and refluxed at 50 °C for 24 h, quenched with MeOH (1.0 mL), and concentrated to afford a golden syrup. Purification by Sephadex LH-20 gel filtration (1:1 CH_2Cl_2:MeOH) followed by silica gel flash chromatography (15:2:1 → 10:2:1 EtOAc:MeOH:H_2O) gave the desired product (26 mg) in 78% yield. ^{1}H NMR (600 MHz; CD_3OD): δ 7.79 - 7.03 (m, 10H, OCH_2Ph), 6.25 – 5.94 (m, 2H, C*H*=C*H* of Nb), 5.31 (d, *J* = 4.4 Hz, 1H, H-1 of IdoA), 5.05 – 4.76 (m, 4H, H-2 of IdoA, H-5 of IdoA, OCH_2Ph), 4.75 – 4.64 (m, 1H, OCH_2Ph), 4.65 – 4.47 (m, 2H, OCH_2Ph, H-1 of GlcN), 4.38 (m, 1H, H-6 of GlcN), 4.20 (m, 1H, H-6 of GlcN), 4.07 – 3.85 (m, 4H, H-2 of IdoA, H-2 of GlcN, H-2 of GlcN, OCH_2 of PEG linker), 3.86 – 3.71 (m, 1H, OCH_2 of PEG linker), 3.71 – 3.45 (m, H, 11H, H-3 of IdoA, H-3 of GlcN, H-5 of GlcN, OCH_2 of PEG linker), 3.40 (s, 3H, CO_2CH_3), 2.81 – 2.74 (m, 2H, C*H*-CH=CH of Nb), 2.07 (s, 3H, $OCOCH_3$), 1.52 – 1.10 (m, 5H, C*H* and CH_2 of Nb), 0.83 (s, 9H, $SiC(CH_3)$), -0.09 (s, 3H, $SiCH_3$), -0.13 (s, 3H, $SiCH_3$); ^{13}C NMR (125 MHz; $CDCl_3$): δ 173.3, 172.0, 171.8, 139.8, 139.1, 137.7, 137.5, 102.8, 99.2, 82.1, 79.8, 77.1, 76.6, 76.2, 75.9, 75.3, 75.2, 73.2, 71.5, 71.4, 71.3, 71.0, 70.1, 69.8, 69.4, 67.3, 56.3, 52.4, 45.9, 44.9, 42.8, 40.0, 37.4, 36.0, 30.7, 23.0, 21.2, 18.7, -4.3, -5.4; ESI-TOF HRMS: *m/z* calcd for $C_{47}H_{67}NO_{20}NaSiS_2$ $[M+Na]^+$ 1080.3365; found: 1080.3392.

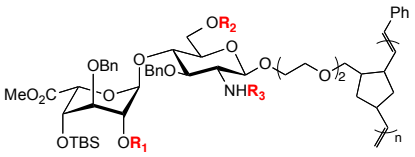

Protected HS glycopolymers (22 – 25). Monomers **18** – **21** were converted into polymers **22** – **25**, which contain the following functional groups: $R_1 = SO_3^-$, $R_2 = SO_3^-$, $R_3 = SO_3^-$ (**1**); $R_1 = SO_3^-$, $R_2 = SO_3^-$, $R_3 = Ac^-$ (**2**); $R_1 = H$, $R_2 = H$, $R_3 = Ac$ (**3**); $R_1 = H$, $R_2 = SO_3^-$, $R_3 = SO_3^-$ (**4**). In a typical polymerization, a small vial was charged with monomer (**18** – **21**; 6.0 mg, 5.0 μmol) and a small stir bar under the flow of argon. To this was added degassed dichloroethane (DCE)/MeOH (10:1, 0.025 M) and *bis*-pyridine Grubbs catalyst $((H_2IMes)(Py)_2(Cl)_2Ru=CHPh)$[4] in DCE (5 mg/mL stock solution, 24 μL, 0.11 μmol) by syringe at rt. The reaction mixture was stirred at rt for 1 h, quenched with ethyl vinyl ether (0.10 mL), and diluted with diethyl ether (1.0 mL) and hexanes (0.50 mL) to obtain a white precipitate. The mixture was centrifuged to remove the organic layer, and the resulting white solid (83 – 98% conversion) was dried *in vacuo*. ^{1}H NMR confirmed disappearance of the norbornene olefinic peaks at 6.04 – 6.11 ppm. The protected polymers were characterized by size exclusion chromatography multi-angle light scattering (SEC-MALS) using a system equipped with an MZ-Gel SDplus organic column (10E5Å, MZ Analysentechnik), a light scattering detector (miniDAWN, Wyatt Technology), and a refractive index detector (TREOS, Wyatt Technology), and 0.2 M LiBr in DMF as the mobile phase. ^{1}H NMR (500 MHz; D_2O): δ 7.49 – 7.15 (m, 10H), 5.42 (br, 1H), 5.18 (br, 1H), 4.75 (br, 1H), 4.65 – 4.51 (m, 2H), 4.38 (br, 1H), 4.05 – 3.84 (m, 4H), 3.86 (br, 1H), 3.79 – 3.50 (m, 13H), 3.46 (br, 1H), 3.31 (br, 3H) 3.30 – 3.25 (m, 2H), 2.49 (br, 2H), 1.94 (br, 3H), 1.79 – 1.07 (m, 5H), 0.77 (br, 9H), -0.07 (br, 3H), -0.17 (br, 3H).

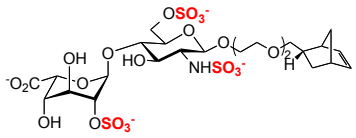

2-*O*-Sulfonato-α-L-idopyranosyluronate-(1→4)-1-*O*-(2-(2-((2*S*)bicyclo[2.2.1]hept-5-en-2-ylmethoxy)ethoxy)ethyl)-2-deoxy-2-sulfonatamido-6-*O*-sulfonato-α-D-glucopyranoside (26). Compound **18** (14 mg, 0.013 mmol) was dissolved in THF (1.3 mL), and TMSOK (33 mg, 0.26 mmol) was added to the reaction mixture. The reaction was stirred for 24 h at rt and quenched with MeOH (1.0 mL). The crude reaction mixture was loaded directly onto a Sephadex G-25 gel filtration column and eluted with 100% H_2O, and fractions were combined, lyophilized, and subjected to hydrogenation. The intermediate was dissolved in a 3:2 mixture of 80 mM phosphate buffered saline (2.4 mL, pH = 7.0) and MeOH (0.80 mL). To this, $Pd(OH)_2$/charcoal (80 mg, 8x by weight of starting material) was added, and the reaction was carried out under 1 atm H_2 gas for 3 d. The reaction mixture was filtered using a vacuum filtration system (0.45 μm PES membrane, VWR) and desalted on a Sephadex G-25 column in 100% H_2O to obtain the desired product 60% yield after lyophilization. ^{1}H NMR (500 MHz, D_2O) δ 5.24 (s, 1H, H-1 of IdoA), 4.83 (d, J = 2.7 Hz, 1H, H-5 of IdoA), 4.73 (d, J = 8.2 Hz, 1H, H-1 of GlcN), 4.44 (m, 1H, H-6 of GlcN), 4.34 (m, 2H, H-6 of GlcN, H-2 of IdoA), 4.10 (m, 2H, H-3 of IdoA, H-4 of IdoA), 4.01 – 3.71 (m, 11H, OCH_2 of PEG linker, H-3 of GlcN, H-4 of GlcN, H-5 of GlcN), 3.44 – 3.31 (m, 2H, OCH_2 of PEG linker), 3.16 (m, 1H, H-2 of GlcN), 2.28 – 2.20 (m, 2H, bridgehead CH_2 of Nb), 1.82 (s, 2H, CH_2 of Nb), 1.59 (s, 2H, CH_2 of Nb), 1.48 – 1.36 (m, 2H, CH of Nb), 1.27 – 1.19 (m, 2H, CH_2 of Nb), 1.08 (s, 1H, CH of Nb); ESI-TOF HRMS: m/z calcd for $C_{24}H_{37}Na_3NO_{22}S_3$ $[M+3Na-H]^{2+}$ 856.0662; found: 856.0624.

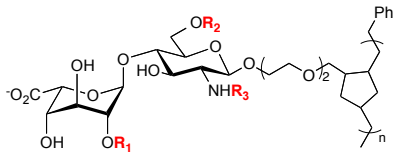

Deprotected glycopolymers (1 – 4). Polymers **22** – **25** were deprotected to obtain final polymers **1** – **4**, which contain the following functional groups: $R_1 = SO_3^-$, $R_2 = SO_3^-$, $R_3 = SO_3^-$ (**1**); $R_1 = SO_3^-$, $R_2 = SO_3^-$, $R_3 = Ac^-$ (**2**); $R_1 = H$, $R_2 = H$, $R_3 = Ac$ (**3**); $R_1 = H$, $R_2 = SO_3^-$, $R_3 = SO_3^-$ (**4**). In a typical reaction, polymer (11 mg, 10 μmol per unit) was dissolved in THF (1.0 mL), and TBAI (7.0 mg, 20 μmol) and TMSOK (25 mg, 0.20 mmol) were added. The reaction was stirred for 24 h at rt and quenched with MeOH (1.0 mL). The crude reaction mixture was loaded directly onto a Sephadex G-25 gel filtration column and eluted with 100% H_2O. The polymer-containing fractions were combined, lyophilized, and subjected to hydrogenation. In a typical hydrogenation reaction, the polymer from the previous reaction was dissolved in a 3:2 mixture of 80 mM phosphate buffered saline (0.9 mL, pH = 7.0) and MeOH (0.60 mL). To this, $Pd(OH)_2$/charcoal (84 mg, 8x weight of polymer) was added, and the reaction was carried out under 1 atm H_2 gas for 3 d. Samples were filtered using a vacuum filtration system (0.45 μm PES membrane, VWR) and desalted on a Sephadex G-25 column in 100% H_2O to obtain the desired polymers in 35 – 55% yield after lyophilization. ^{1}H NMR showed disappearance of the benzyl and methyl ester peaks at 7.79 – 7.03 ppm and 3.40 ppm, respectively. Deprotected polymers were characterized by SEC-MALS using a system equipped with an OHpak water column (SB-804 HQ, Shodex), a light scattering detector (miniDAWN, Wyatt Technology), and a refractive index detector (TREOS, Wyatt Technology), and 3 mM NaN_3 and 6 mM $NaNO_3$ in H_2O as the mobile phase. ^{1}H NMR (500 MHz; D_2O): δ 5.03 (br, 1H), 4.44 (br, 1H), 4.25 – 4.20 (m, 1H), 4.18 – 4.11 (m, 2H), 3.92 (br, 1H), 3.84 (br, 2H), 3.75 – 3.40 (m, 12H), 3.34 (br, 1H), 3.19 (br, 1H), 1.91 (br, 3H), 1.72 (br, 1H), 1.48 – 0.88 (m, 6H).

reri28.2
Std Proton parameters

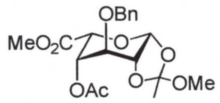

11

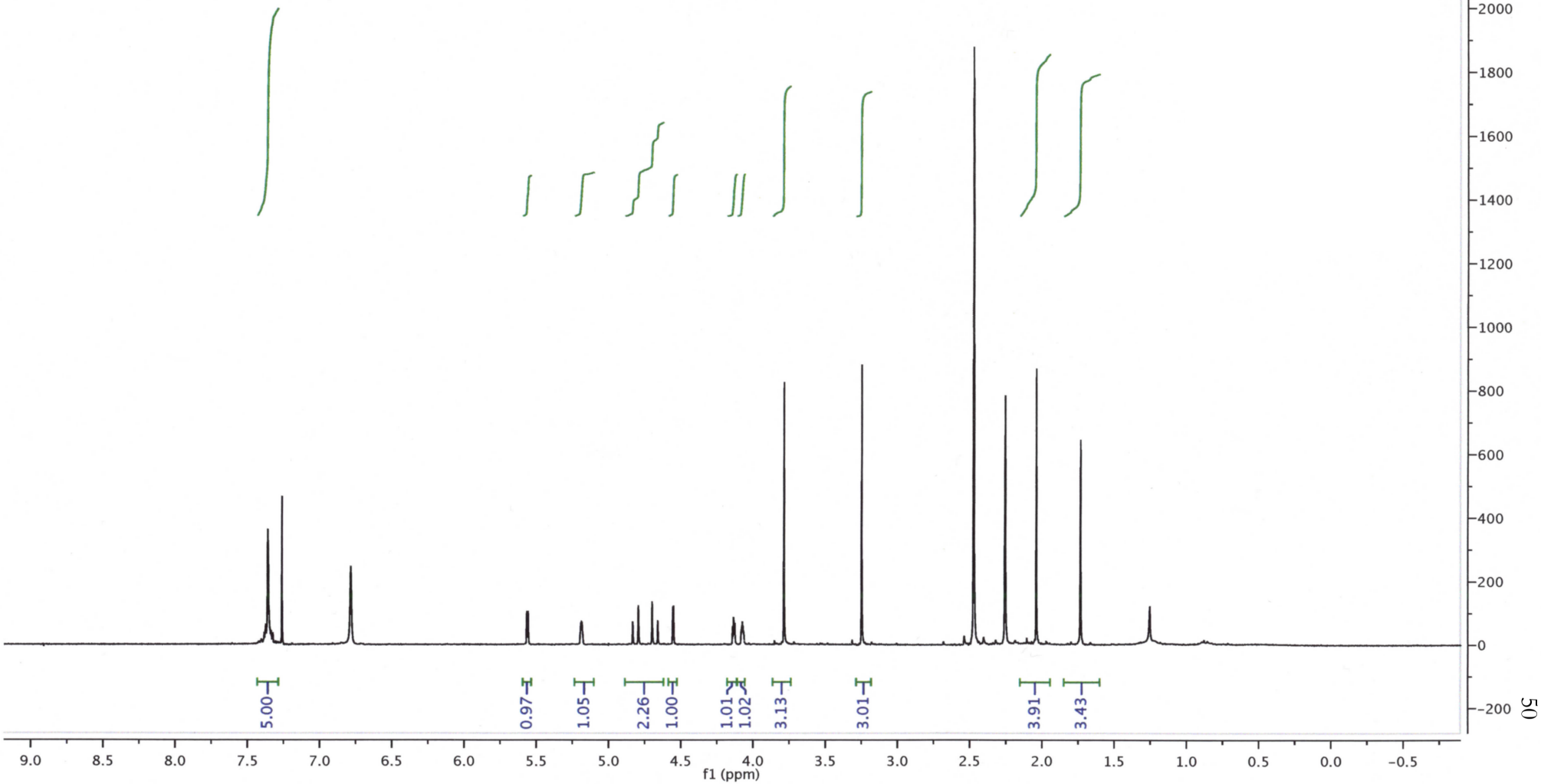

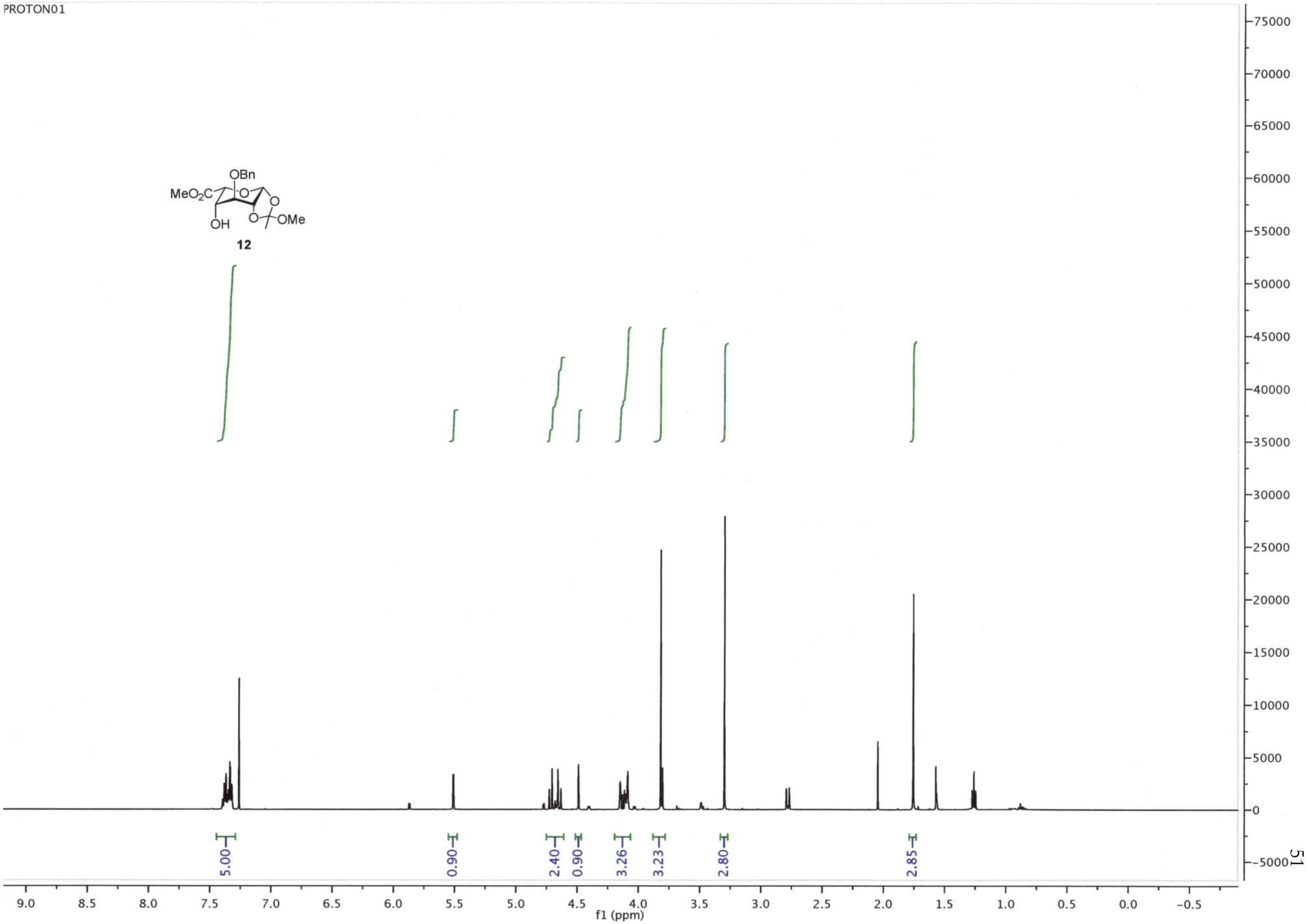
PROTON01
OBn
MeO2C
OH
OMe
12
5.00
0.90
2.40
0.90
3.26
3.23
2.80
2.85
f1 (ppm)

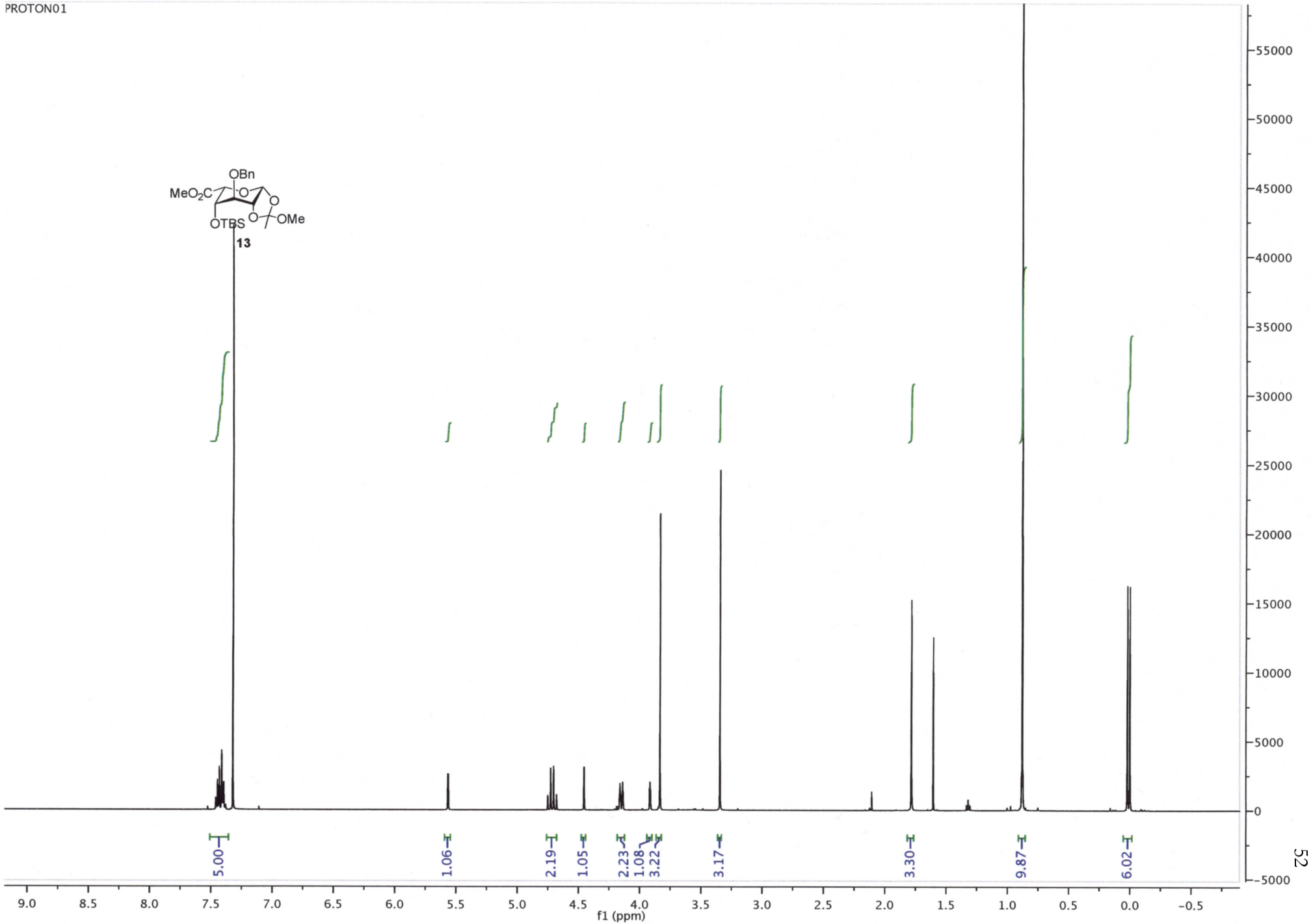
PROTON01
OBn
MeO2C
OTBS
OMe
13
5.00
1.06
2.19
1.05
2.23
1.08
3.22
3.17
3.30
9.87
6.02
f1 (ppm)

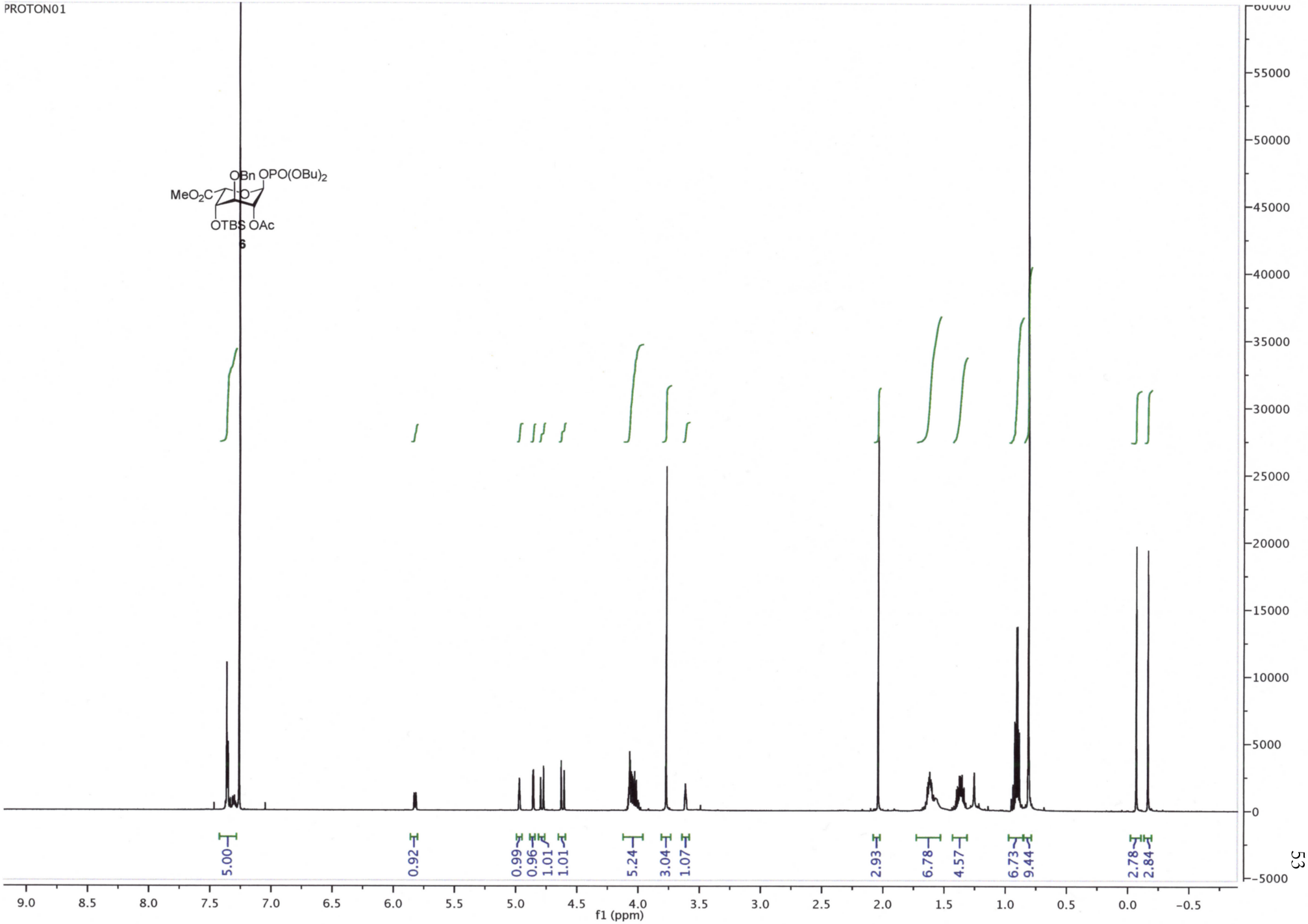
PROTON01
OBn OPO(OBu)2
MeO2C
OTBS OAc
6
5.00
0.92
0.99
0.96
1.01
1.01
5.24
3.04
1.07
2.93
6.78
4.57
6.73
9.44
2.78
2.84
f1 (ppm)

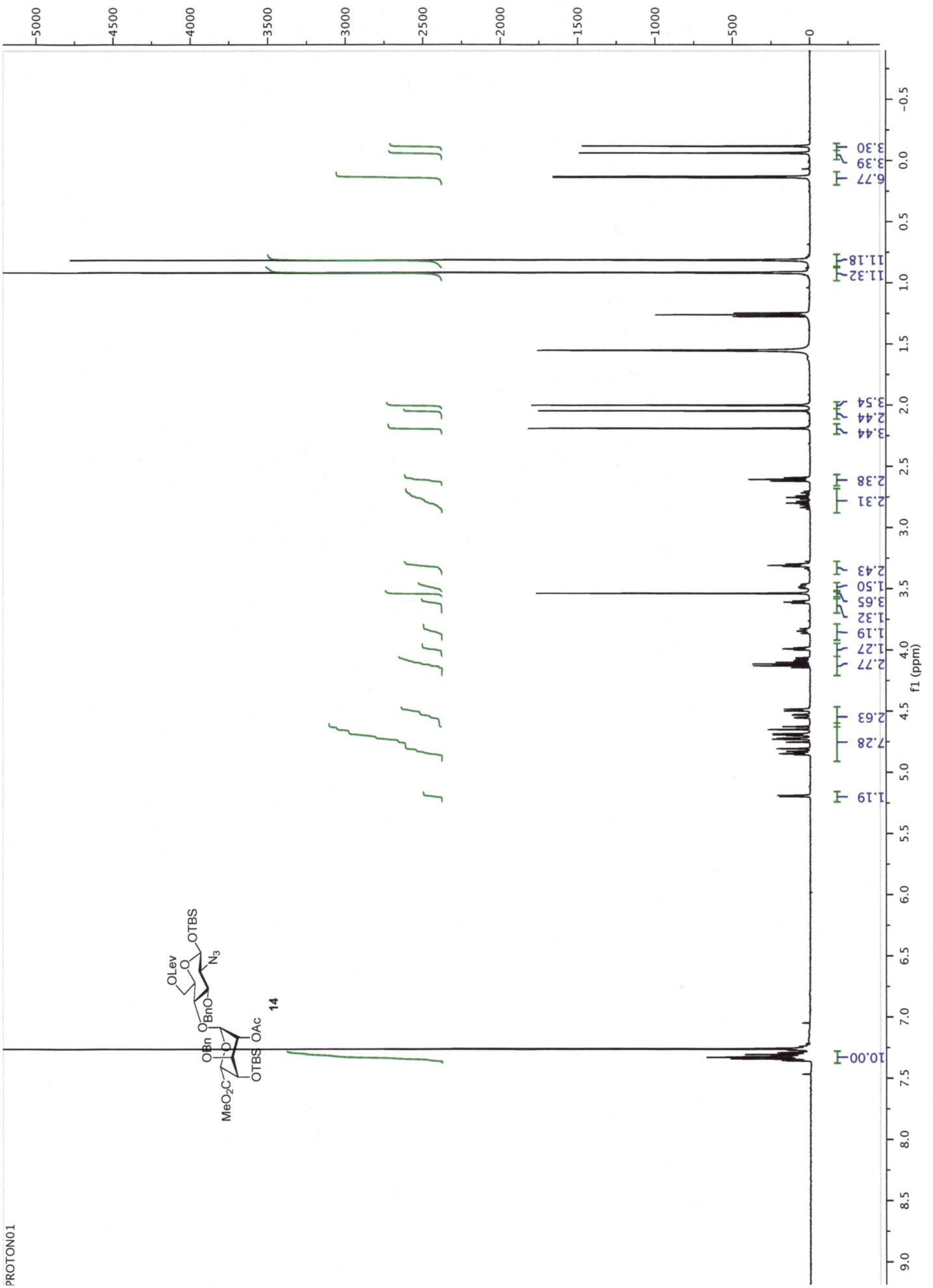
PROTON01
f1 (ppm)
14
OLev
OTBS
N_3
BnO
OBn
OAc
OTBS
MeO_2C
10.00
1.19
7.28
2.63
2.77
1.27
1.19
1.32
3.65
1.50
2.43
2.31
2.38
3.44
2.44
3.54
11.32
11.18
6.77
3.39
3.30

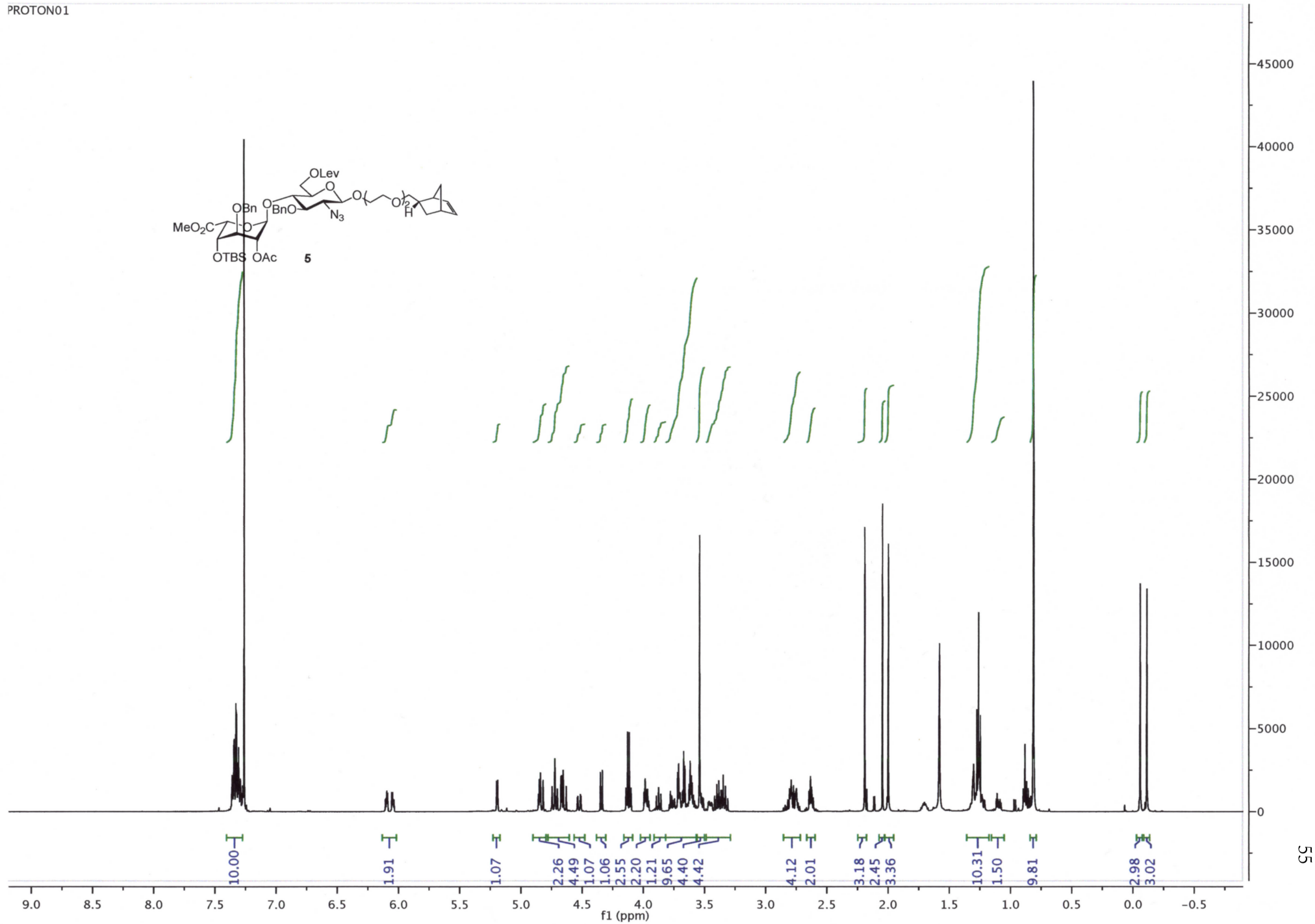
PROTON01
OLev
OBn
BnO
N_3
MeO_2C
OTBS
OAc
5
45000
40000
35000
30000
25000
20000
15000
10000
5000
0
10.00
1.91
1.07
2.26
4.49
1.07
1.06
2.55
2.20
1.21
9.65
4.40
4.42
4.12
2.01
3.18
2.45
3.36
10.31
1.50
9.81
2.98
3.02
9.0
8.5
8.0
7.5
7.0
6.5
6.0
5.5
5.0
4.5
4.0
3.5
3.0
2.5
2.0
1.5
1.0
0.5
0.0
-0.5
f1 (ppm)

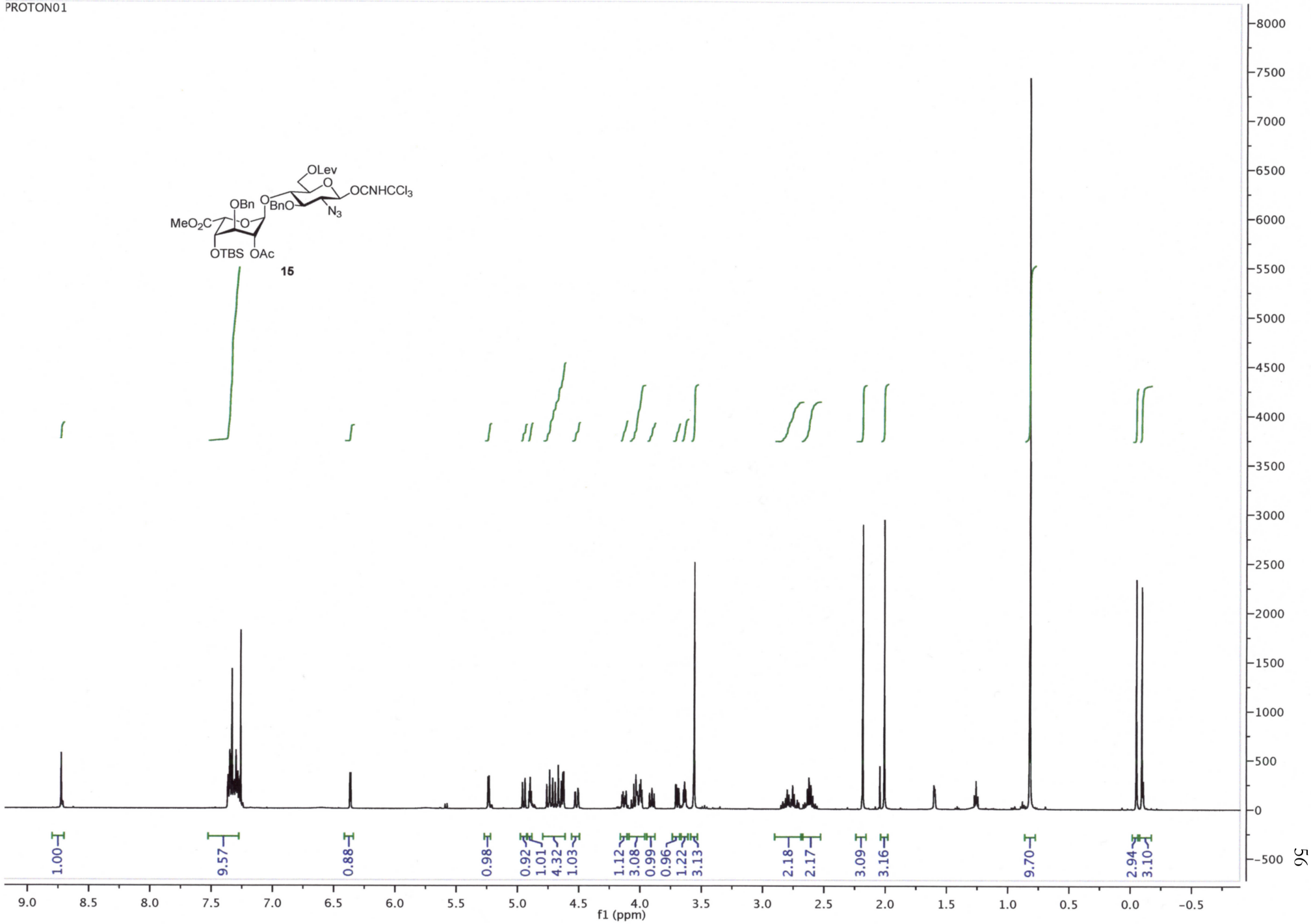
PROTON01
OLev
OCNHCCl3
OBn
BnO
N3
MeO2C
OTBS OAc
15
1.00
9.57
0.88
0.98
0.92
1.01
4.32
1.03
1.12
3.08
0.99
0.96
1.22
3.13
2.18
2.17
3.09
3.16
9.70
2.94
3.10
f1 (ppm)

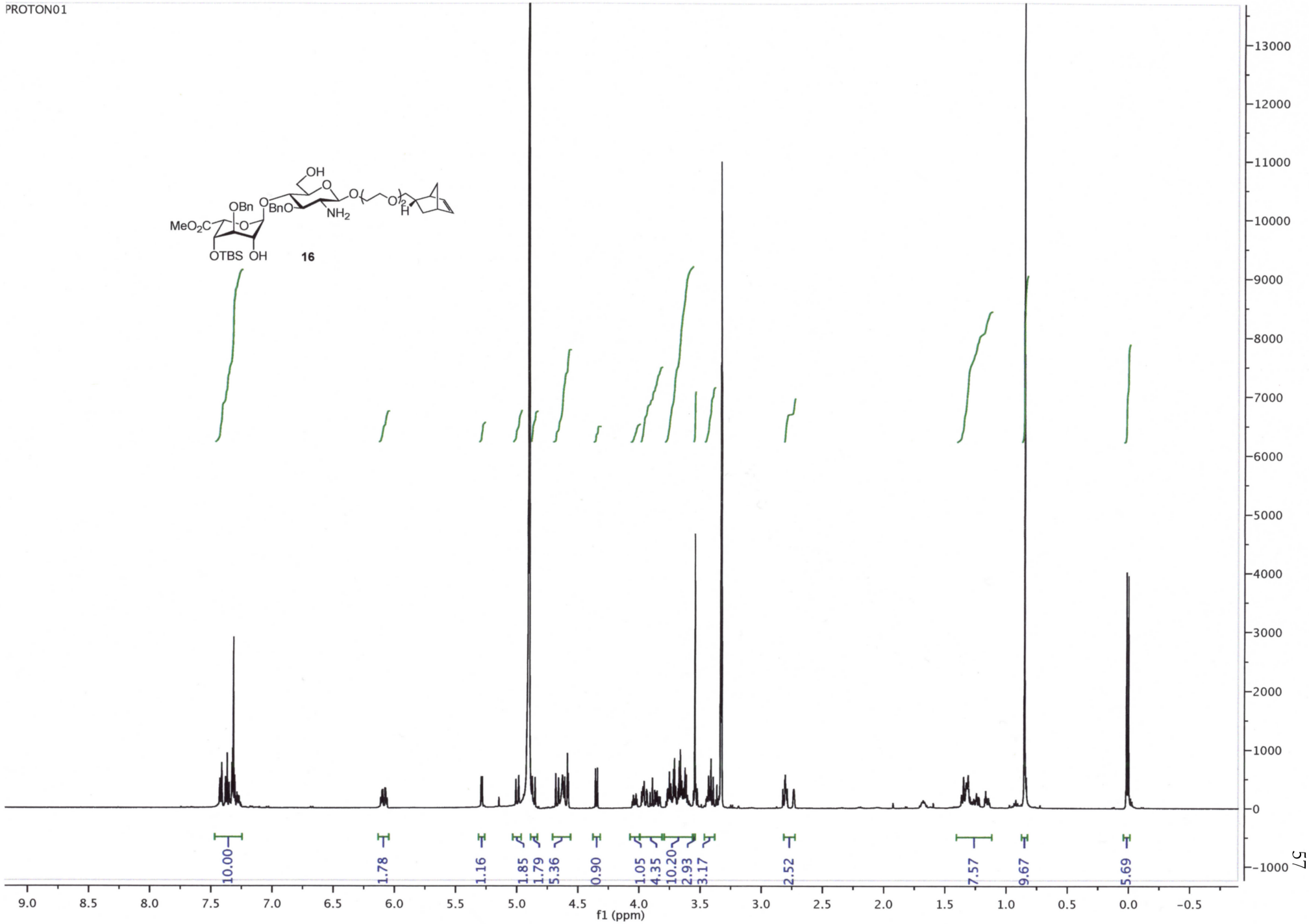
PROTON01
OH
OBn
BnO
NH2
MeO2C
OTBS OH
16
10.00
1.78
1.16
1.85
1.79
5.36
0.90
1.05
4.35
10.20
2.93
3.17
2.52
7.57
9.67
5.69
f1 (ppm)

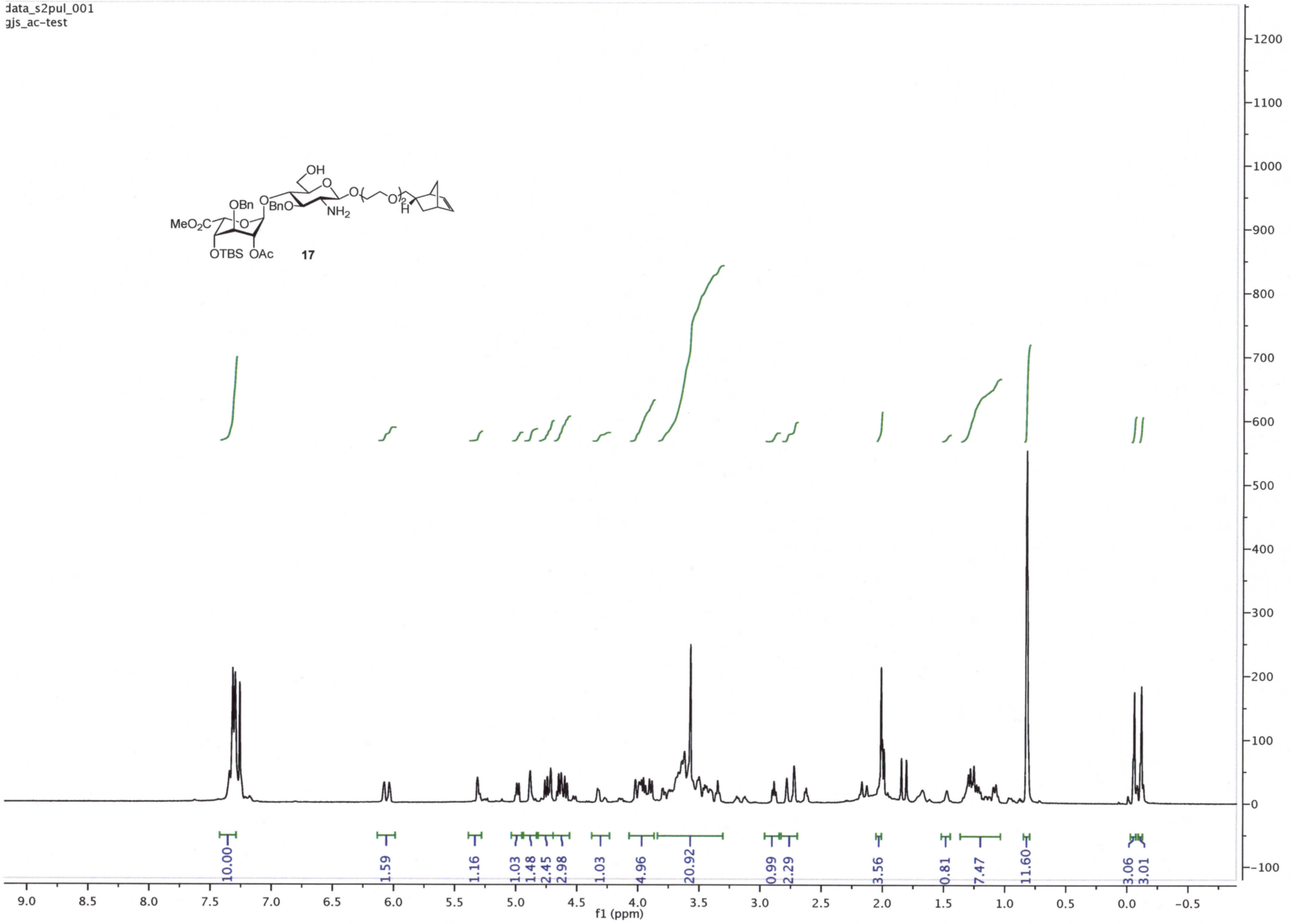
data_s2pul_001
gjs_ac-test
OH
O
OBn
O
BnO
NH2
O
O
O
2
H
MeO2C
O
OTBS OAc
17
10.00
1.59
1.16
1.03
1.48
2.45
2.98
1.03
4.96
20.92
0.99
2.29
3.56
0.81
7.47
11.60
3.06
3.01
9.0
8.5
8.0
7.5
7.0
6.5
6.0
5.5
5.0
4.5
4.0
3.5
3.0
2.5
2.0
1.5
1.0
0.5
0.0
-0.5
f1 (ppm)
1200
1100
1000
900
800
700
600
500
400
300
200
100
0
-100

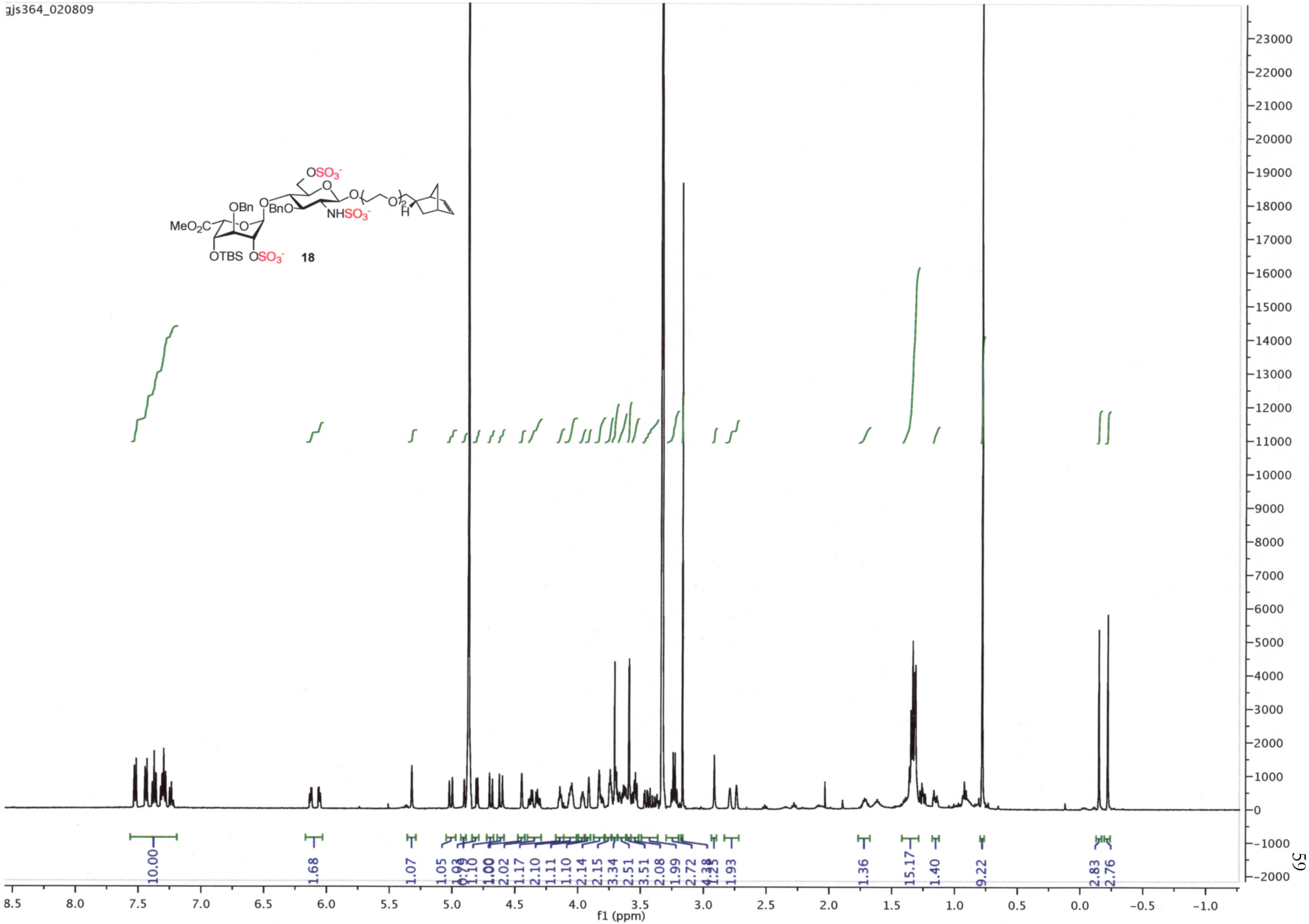
gjs364_020809
OSO3-
OBn
BnO
NHSO3-
MeO2C
OTBS
OSO3-
18
f1 (ppm)

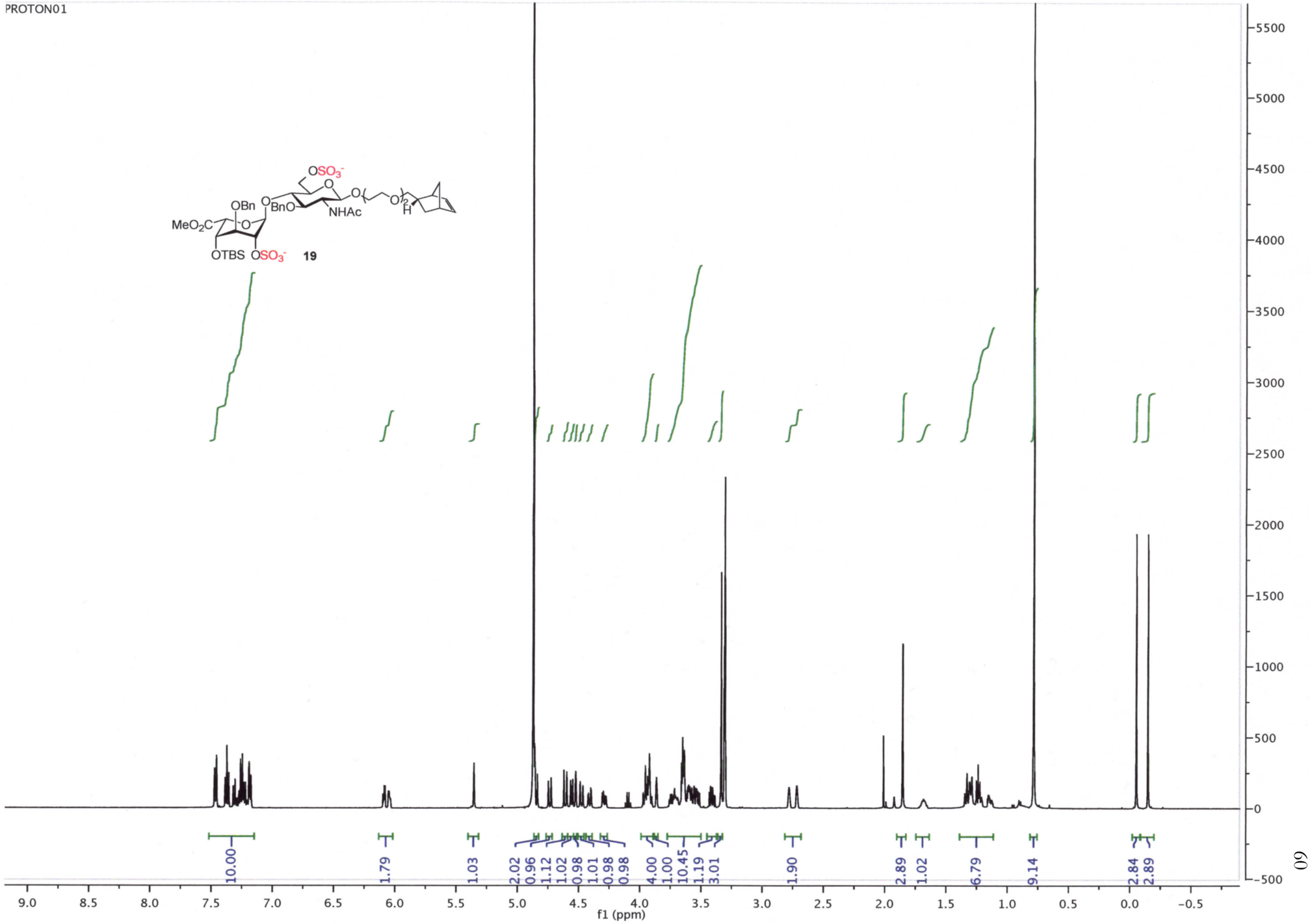
PROTON01
OSO3-
OBn
BnO
NHAc
MeO2C
OTBS
OSO3-
19
10.00
1.79
1.03
2.02
0.96
1.12
1.02
0.98
1.01
0.98
0.98
4.00
1.00
10.45
1.19
3.01
1.90
2.89
1.02
6.79
9.14
2.84
2.89
f1 (ppm)

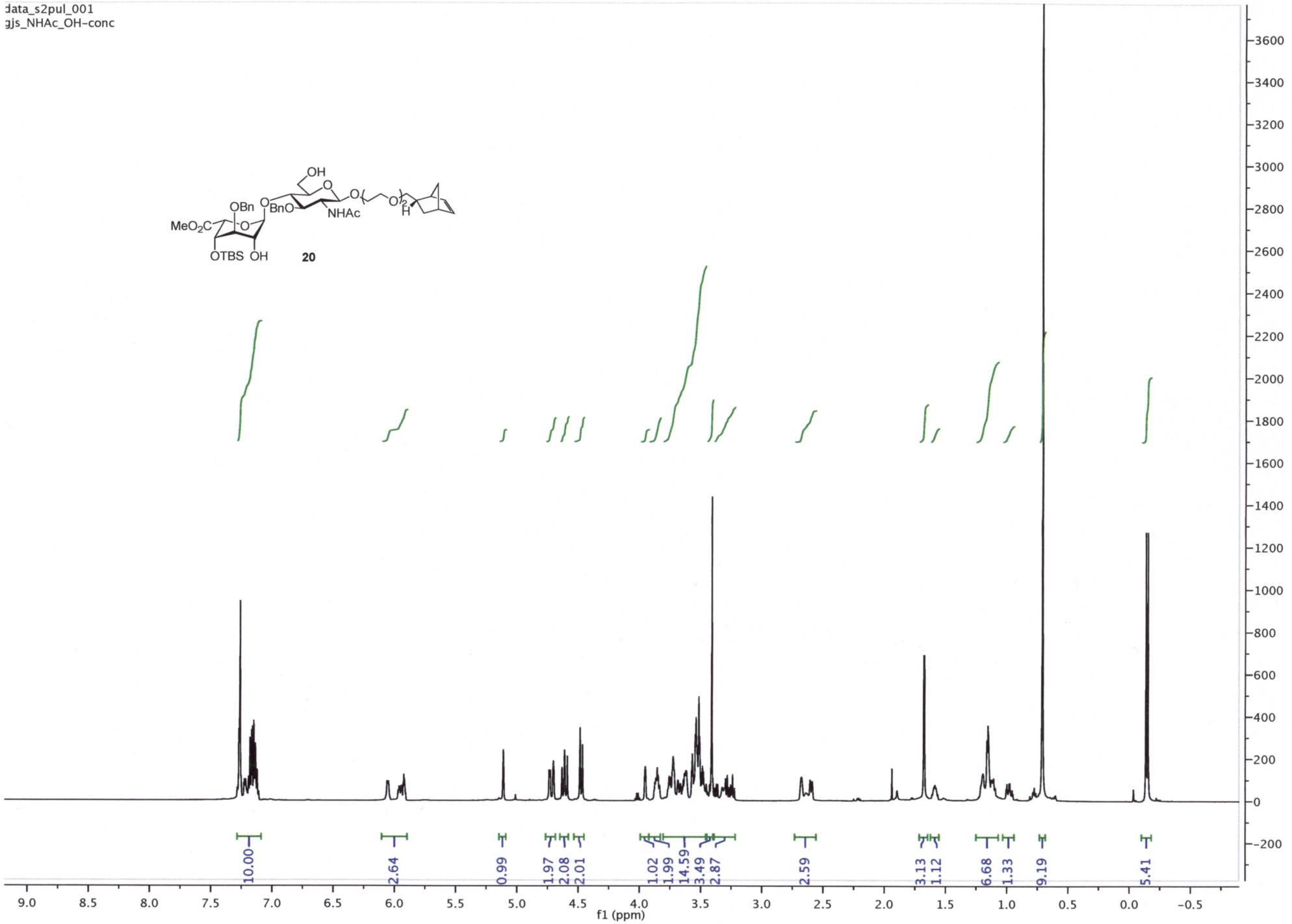
data_s2pul_001
gjs_NHAc_OH-conc
OBn
BnO
NHAc
MeO2C
OTBS OH
20
10.00
2.64
0.99
1.97
2.08
2.01
1.02
1.99
14.59
3.49
2.87
2.59
3.13
1.12
6.68
1.33
9.19
5.41
f1 (ppm)

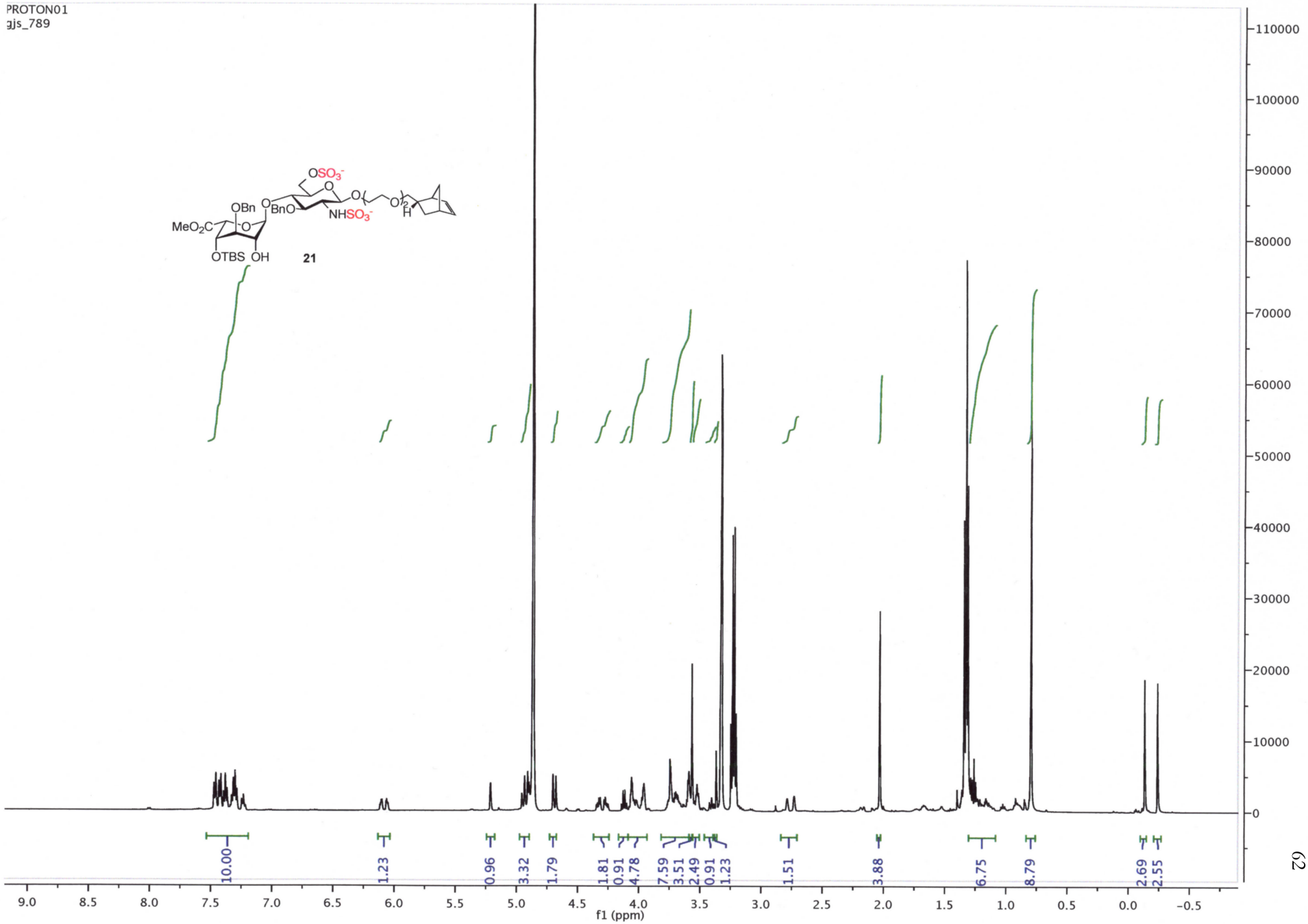
PROTON01
gjs_789
OSO3-
OBn
BnO
NHSO3-
MeO2C
OTBS OH
21
10.00
1.23
0.96
3.32
1.79
1.81
0.91
4.78
7.59
3.51
2.49
0.91
1.23
1.51
3.88
6.75
8.79
2.69
2.55
f1 (ppm)

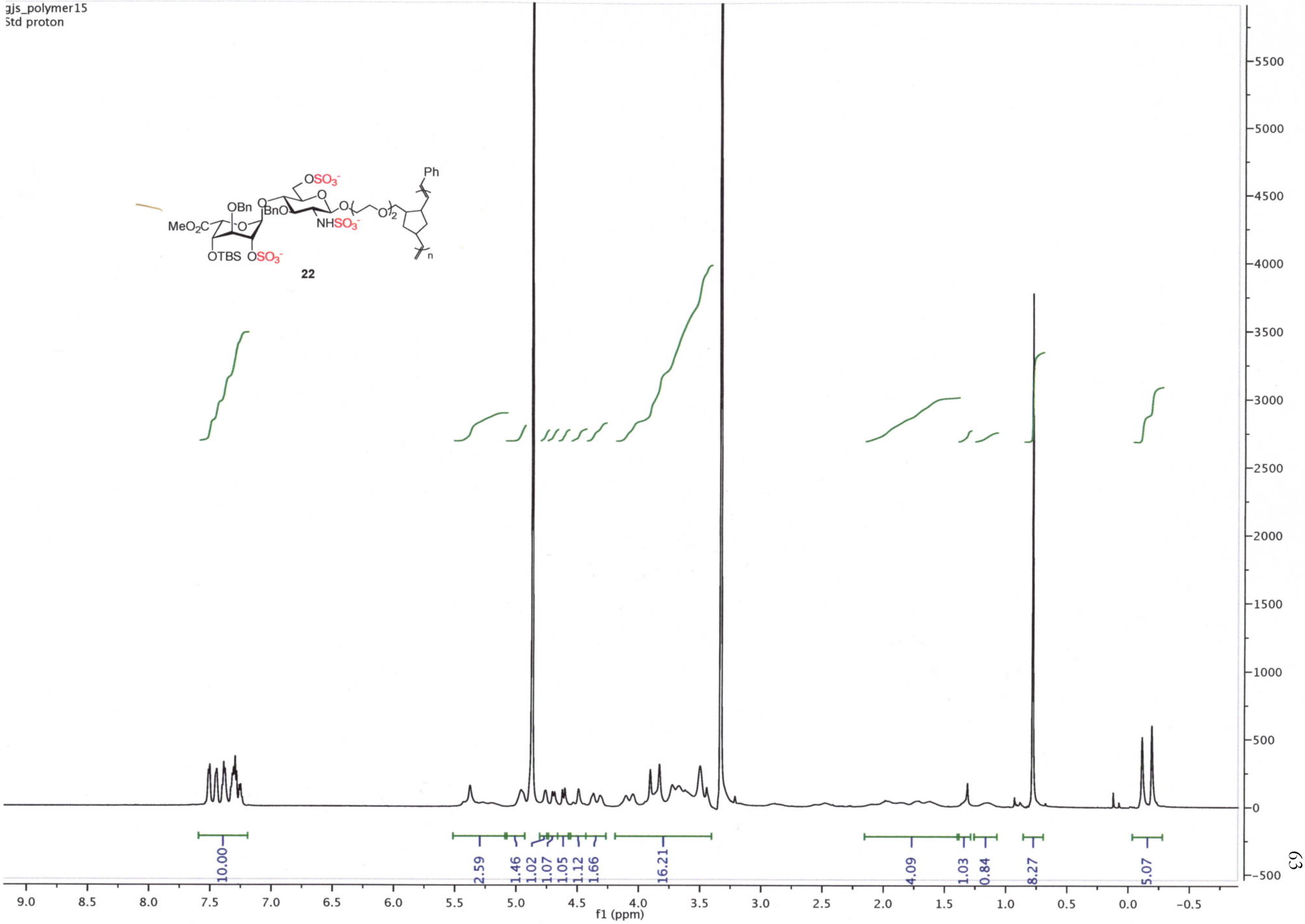
gjs_polymer15
Std proton
OSO3-
Ph
OBn
BnO
NHSO3-
MeO2C
OTBS
OSO3-
22
10.00
2.59
1.46
1.02
1.07
1.05
1.12
1.66
16.21
4.09
1.03
0.84
8.27
5.07
f1 (ppm)

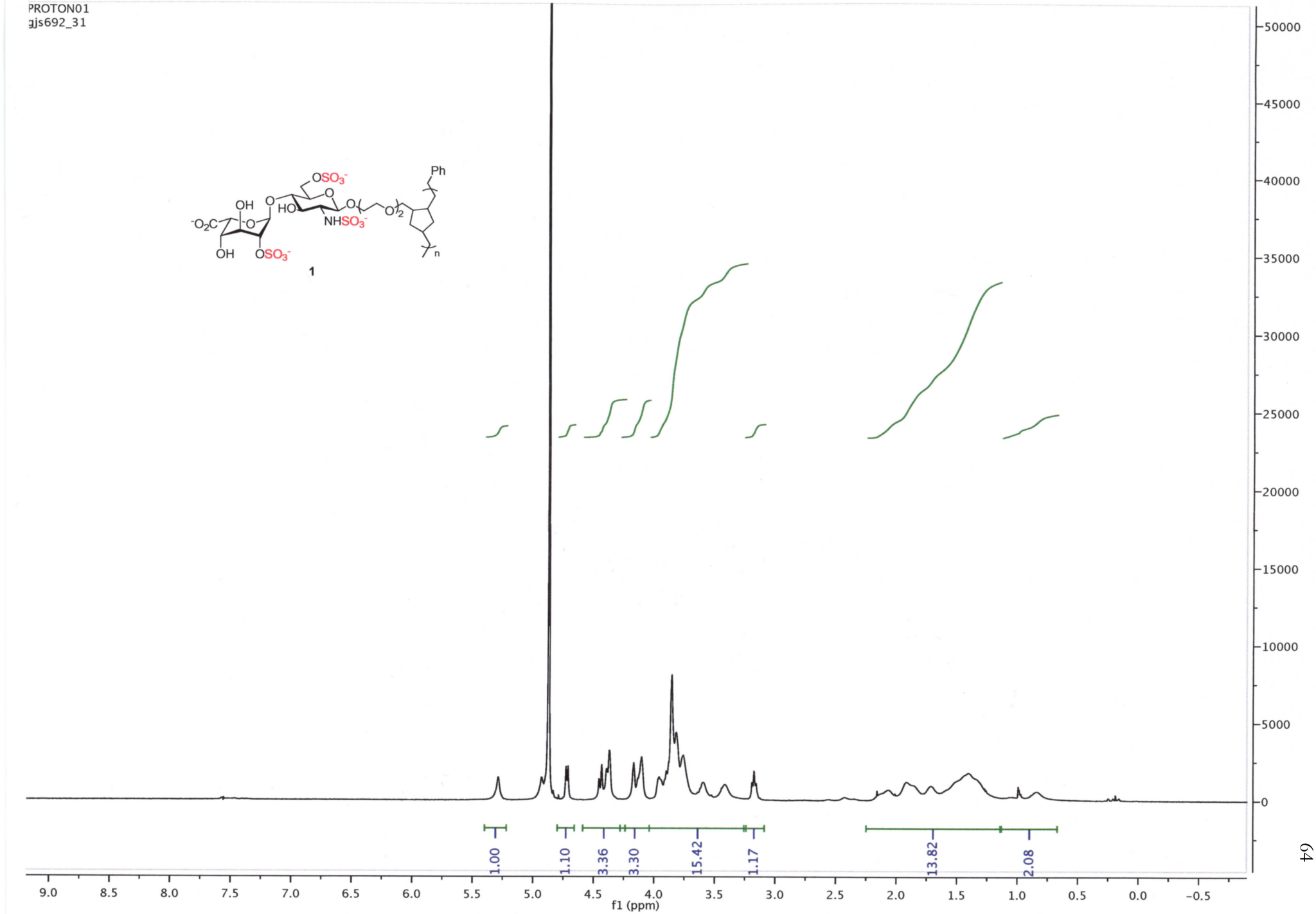
PROTON01
gjs692_31
OSO3-
Ph
OH
O
HO
O
O
O2
NHSO3-
-O2C
O
OH
OSO3-
n
1
50000
45000
40000
35000
30000
25000
20000
15000
10000
5000
0
1.00
1.10
3.36
3.30
15.42
1.17
13.82
2.08
9.0
8.5
8.0
7.5
7.0
6.5
6.0
5.5
5.0
4.5
4.0
3.5
3.0
2.5
2.0
1.5
1.0
0.5
0.0
-0.5
f1 (ppm)

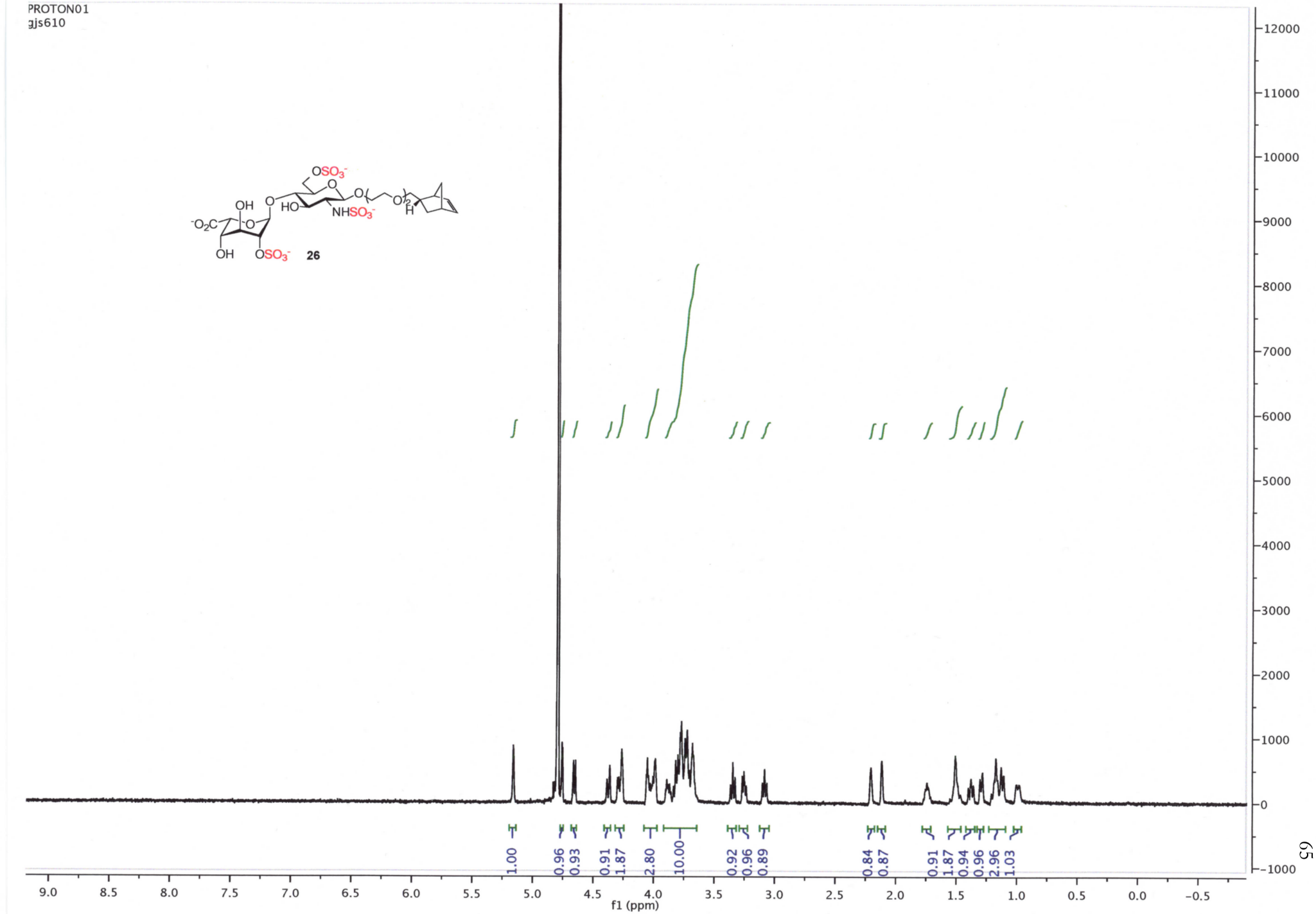
PROTON01
gjs610
26
1.00
0.96
0.93
0.91
1.87
2.80
10.00
0.92
0.96
0.89
0.84
0.87
0.91
1.87
0.94
0.96
2.96
1.03
f1 (ppm)

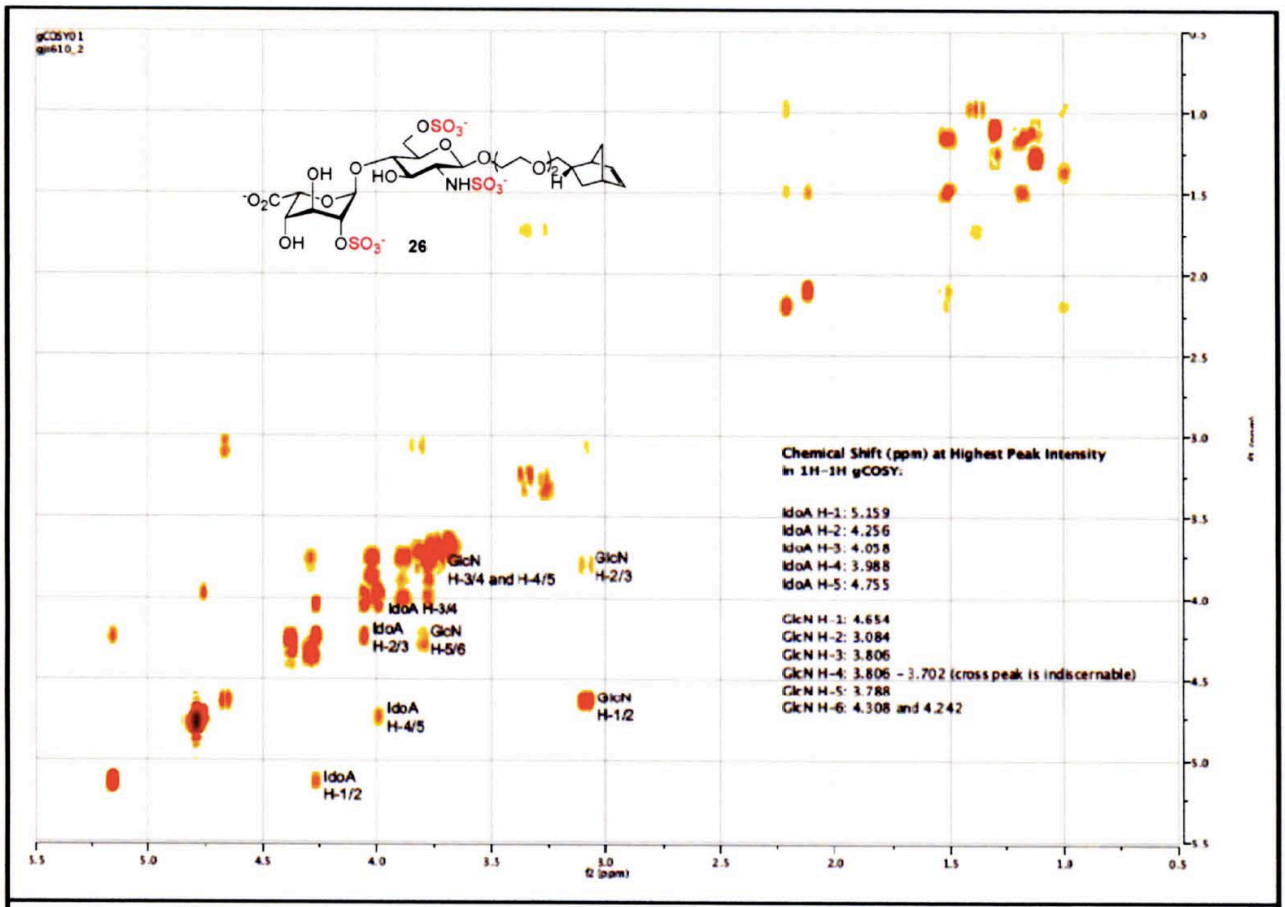
gCOSY01
gs610_2
26
Chemical Shift (ppm) at Highest Peak Intensity
in 1H-1H gCOSY:
IdoA H-1: 5.159
IdoA H-2: 4.256
IdoA H-3: 4.058
IdoA H-4: 3.988
IdoA H-5: 4.755
GlcN H-1: 4.654
GlcN H-2: 3.084
GlcN H-3: 3.806
GlcN H-4: 3.806 - 3.702 (cross peak is indiscernable)
GlcN H-5: 3.788
GlcN H-6: 4.308 and 4.242
GlcN H-3/4 and H-4/5
GlcN H-2/3
IdoA H-3/4
IdoA H-2/3
GlcN H-5/6
IdoA H-4/5
GlcN H-1/2
IdoA H-1/2
f2 (ppm)

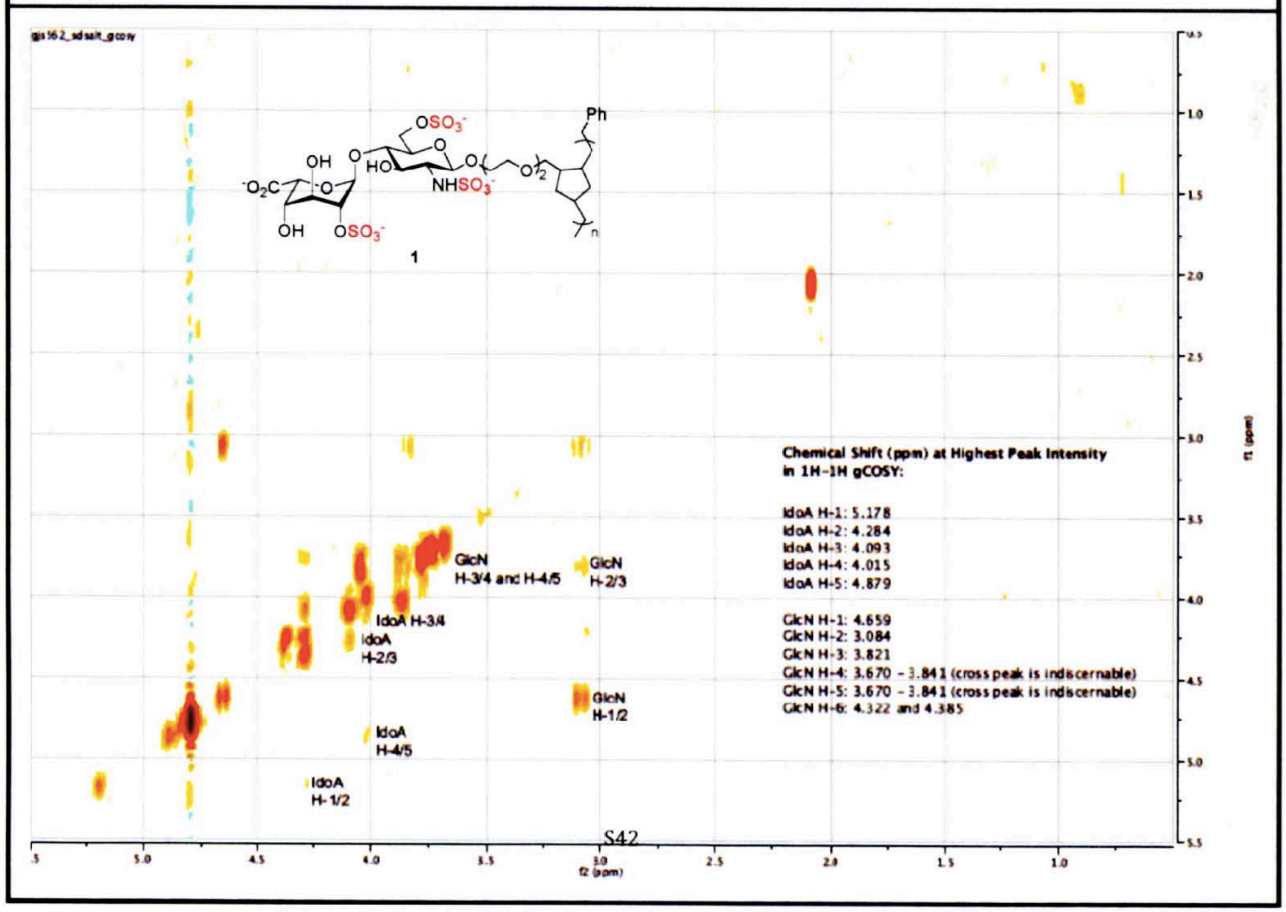
gs162_sdsalt_gcosy
1
Chemical Shift (ppm) at Highest Peak Intensity
in 1H-1H gCOSY:
IdoA H-1: 5.178
IdoA H-2: 4.284
IdoA H-3: 4.093
IdoA H-4: 4.015
IdoA H-5: 4.879
GlcN H-1: 4.659
GlcN H-2: 3.084
GlcN H-3: 3.821
GlcN H-4: 3.670 - 3.841 (cross peak is indiscernable)
GlcN H-5: 3.670 - 3.841 (cross peak is indiscernable)
GlcN H-6: 4.322 and 4.385
GlcN H-3/4 and H-4/5
GlcN H-2/3
IdoA H-3/4
IdoA H-2/3
GlcN H-1/2
IdoA H-4/5
IdoA H-1/2
f2 (ppm)

REFERENCES

[1] W. A. Muller, *Trends in immunology* **2003**, *24*, 327-334.

[2] J. B. Lowe, *Current opinion in cell biology* **2003**, *15*, 531-538.

[3] A. Rot, U. H. von Andrian, *Annual review of immunology* **2004**, *22*, 891-928.

[4] C. R. Parish, E. J. Hindmarsh, M. R. Bartlett, M. A. Staykova, W. B. Cowden, D. O. Willenborg, *Immunology and cell biology* **1998**, *76*, 104-113.

[5] R. Yadav, K. Y. Larbi, R. E. Young, S. Nourshargh, *Thrombosis and haemostasis* **2003**, *90*, 598-606.

[6] L. Raffaghello, V. Pistoia, *Journal of leukocyte biology* **2009**, *86*, 1271-1273.

[7] A. Ori, M. C. Wilkinson, D. G. Fernig, *Frontiers in bioscience : a journal and virtual library* **2008**, *13*, 4309-4338.

[8] L. Wang, M. Fuster, P. Sriramarao, J. D. Esko, *Nature immunology* **2005**, *6*, 902-910.

[9] X. Bao, E. A. Moseman, H. Saito, B. Petryniak, A. Thiriot, S. Hatakeyama, Y. Ito, H. Kawashima, Y. Yamaguchi, J. B. Lowe, U. H. von Andrian, M. Fukuda, *Immunity* **2010**, *33*, 817-829.

[10] A. E. Proudfoot, *Biochemical Society transactions* **2006**, *34*, 422-426.

[11] C. Gerard, B. J. Rollins, *Nature immunology* **2001**, *2*, 108-115.

[12] A. E. Proudfoot, T. M. Handel, Z. Johnson, E. K. Lau, P. LiWang, I. Clark-Lewis, F. Borlat, T. N. Wells, M. H. Kosco-Vilbois, *Proceedings of the National Academy of Sciences of the United States of America* **2003**, *100*, 1885-1890.

[13] C. I. Gama, S. E. Tully, N. Sotogaku, P. M. Clark, M. Rawat, N. Vaidehi, W. A. Goddard, 3rd, A. Nishi, L. C. Hsieh-Wilson, *Nature chemical biology* **2006**, *2*, 467-473.

[14] L. Martin, C. Blanpain, P. Garnier, V. Wittamer, M. Parmentier, C. Vita, *Biochemistry* **2001**, *40*, 6303-6318.

[15] L. M. Webb, M. U. Ehrengruber, I. Clark-Lewis, M. Baggiolini, A. Rot, *Proceedings of the National Academy of Sciences of the United States of America* **1993**, *90*, 7158-7162.

[16] K. H. Mayo, E. Ilyina, V. Roongta, M. Dundas, J. Joseph, C. K. Lai, T. Maione, T. J. Daly, *The Biochemical journal* **1995**, *312 (Pt 2)*, 357-365.

[17] A. D. Luster, S. M. Greenberg, P. Leder, *The Journal of experimental medicine* **1995**, *182*, 219-231.

[18] W. Koopmann, M. S. Krangel, *The Journal of biological chemistry* 1997, *272*, 10103-10109.

[19] D. Gilat, R. Hershkoviz, Y. A. Mekori, I. Vlodavsky, O. Lider, *Journal of Immunology* **1994**, *153*, 4899-4906.

[20] E. Young, *Thrombosis research* **2008**, *122*, 743-752.

[21] M. Petitou, L. P. Herault, A. Bernat, P. A. Driguez, P. Duchaussoy, J. C. Lormeau, J. M. Herbert, *Nature* **1999**, *398*, 417-422.

[22] L. C. Wang, J. R. Brown, A. Varki, J. D. Esko, *Journal of Clinical Investigation* **2002**, *110*, 127-136.

[23] S. Alban, R. J. Ludwig, G. Bendas, M. P. Schon, G. J. Oostingh, H. H. Radeke, J. Fritzsche, J. Pfeilschifter, R. Kaufmann, W. H. Boehncke, *The Journal of investigative dermatology* **2009**, *129*, 1192-1202.

[24] J. L. de Paz, E. A. Moseman, C. Noti, L. Polito, U. H. von Andrian, P. H. Seeberger, *ACS chemical biology* **2007**, *2*, 735-744.

[25] T. N. Wells, A. E. Proudfoot, *Inflammation research : official journal of the European Histamine Research Society ... [et al.]* **1999**, *48*, 353-362.

[26] A. E. Proudfoot, S. Fritchley, F. Borlat, J. P. Shaw, F. Vilbois, C. Zwahlen, A. Trkola, D. Marchant, P. R. Clapham, T. N. Wells, *The Journal of biological chemistry* **2001**, *276*, 10620-10626.

[27] J. P. Shaw, Z. Johnson, F. Borlat, C. Zwahlen, A. Kungl, K. Roulin, A. Harrenga, T. N. Wells, A. E. Proudfoot, *Structure* **2004**, *12*, 2081-2093.

[28] D. R. Pakianathan, E. G. Kuta, D. R. Artis, N. J. Skelton, C. A. Hebert, *Biochemistry* **1997**, *36*, 9642-9648.

[29] M. Rawat, C. I. Gama, J. B. Matson, L. C. Hsieh-Wilson, *Journal of the American Chemical Society* **2008**, *130*, 2959-2961.

[30] A. Canales, J. Angulo, R. Ojeda, M. Bruix, R. Fayos, R. Lozano, G. Gimenez-Gallego, M. Martin-Lomas, P. M. Nieto, J. Jimenez-Barbero, *Journal of the American Chemical Society* **2005**, *127*, 5778-5779.

[31] M. Weiwer, F. Huang, R. J. Linhardt, *Abstr Pap Am Chem S* **2007**, *234*.

[32] A. Prabhu, A. Venot, G. J. Boons, *Org Lett* **2003**, *5*, 4975-4978.

[33] H. A. Orgueira, A. Bartolozzi, P. Schell, R. E. Litjens, E. R. Palmacci, P. H. Seeberger, *Chemistry* **2003**, *9*, 140-169.

[34] S. G. Lee, J. M. Brown, C. J. Rogers, J. B. Matson, C. Krishnamurthy, M. Rawat, L. C. Hsieh-Wilson, *Chemical science* **2010**, *1*, 322-325.

[35] O. Gavard, Y. Hersant, J. Alais, V. Duverger, A. Dilhas, A. Bascou, D. Bonnaffe, *Eur J Org Chem* **2003**, 3603-3620.

[36] A. Dilhas, D. Bonnaffe, *Carbohydrate research* **2003**, *338*, 681-686.

[37] A. Ravida, X. Liu, L. Kovacs, P. H. Seeberger, *Org Lett* **2006**, *8*, 1815-1818.

[38] R. R. Schmidt, W. Kinzy, *Advances in carbohydrate chemistry and biochemistry* **1994**, *50*, 21-123.

[39] Y. P. Hu, S. Y. Lin, C. Y. Huang, M. M. Zulueta, J. Y. Liu, W. Chang, S. C. Hung, *Nature chemistry* **2011**, *3*, 557-563.

[40] R. H. Fan, J. Achkar, J. M. Hernandez-Torres, A. Wei, *Organic letters* **2005**, *7*, 5095-5098.

[41] M. Scholl, S. Ding, C. W. Lee, R. H. Grubbs, *Organic letters* **1999**, *1*, 953-956.

C h a p t e r 3

EVALUATION OF ANTI-CHEMOKINE ACTIVITY

Binding Affinity of the Glycopolymer for RANTES

With our library of differentially sulfated glycopolymers in hand, we sought to characterize their specificities for RANTES (CCL5), a small basic chemokine that induces leukocyte migration by binding to specific members of the G-protein coupled receptor (GPCR) family, namely CCR1, CCR3, and CCR5.[1] Specifically, RANTES is able to induce the migration of T cells, monocytes, natural killer cells, dendritic cells, eosinophils, basophils, and several other types of leukocytes.[2] RANTES is typically produced by $CD8^+$ T cells and is a hallmark feature of >100 inflammatory conditions, such as allogeneic transplant rejection, atherosclerosis, arthritis, atopic dermatitis, asthma, delayed-type hypersensitivity reactions, and endometriosis.[3] RANTES is also known to be involved in the pathogenesis of several neurological disorders, such as Alzheimer's disease.[4] In the aforementioned disorders, RANTES is thought to act as a pro-inflammatory chemokine that promotes the infiltration of leukocytes to sites of inflammation.[5] More recently, RANTES was also found to be a potent suppressor of replication in non-syncitum-inducing (NSI) HIV-1 strains, leading to the identification of CCR5 as a major co-receptor for NSI HIV-1 viral entry.[6] The precise mechanism for RANTES-induced suppression of HIV-1 replication is currently not known, but may involve the dimerization of RANTES and internalization of its receptor CCR5.[7]

In addition to its cognate receptors, RANTES associates with cell surface proteoglycans such as syndecan-1 and syndecan-4,[8] and its chemotactic activities can be directly inhibited by soluble glycosaminoglycans.[9] Furthermore, deletion of the glycosaminoglycan-binding site on RANTES (^{44}RKNR^{47}) abrogates the chemokine's ability to form higher-order oligomers and generates a dominant-negative inhibitor of cell migration induced by endogenous RANTES.[10] It is well

established that RANTES preferentially recognizes heparin (or the trisulfated motif found in HS) over other glycosaminoglycan classes.[11] However, the effects of HS sulfation on binding to RANTES have not yet been examined using homogeneously sulfated molecules. Our synthetic glycopolymer library represents four distinct sulfation sequences that could potentially interact with RANTES with varying potencies and differentially affect its cellular activities *in vitro*. Here, we sought to compare the relative ability of each glycopolymer (**1** – **4**) in antagonizing RANTES binding to heparin polysaccharides using a competitive enzyme-linked immunosorbent assay (ELISA).

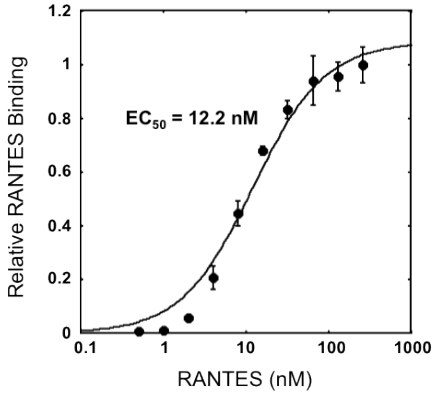

Figure 8. Binding of RANTES to heparin, as determined by ELISA. Heparin-binding 96-well plates were coated with heparin (25 μg/mL; 20-kDa). Human RANTES (1 – 1024 nM; ●) was serially diluted and then incubated in the heparin-coated plates. For ELISA analysis, RANTES was first incubated with a mouse anti-RANTES primary antibody and then with a goat anti-mouse IgG antibody conjugated to horseradish peroxidase (HRP). Levels of plate-bound RANTES were measured by detecting HRP activity at 450 nm. Data were fitted to a sigmoidal curve to determine the half-maximal effective concentration (EC_{50}) for RANTES binding to heparin. Experiments were conducted in quadruplicate, and the standard error is depicted.

We chose to use a competitive ELISA format based on its physiological relevance (representing the ability of our synthetic polymers to disrupt endogenous RANTES activities) and amenability to high-throughput screens. First, we evaluated the half maximal effective concentration (EC_{50}) of human recombinant RANTES binding to heparin-coated (25 μg/mL) 96-well plates. We prepared a serial dilution of RANTES (0.50 – 1024 nM) and incubated the heparin-coated plates with each

solution, followed by the corresponding primary and secondary antibodies. Levels of plate-bound chemokine were measured by detection of horseradish peroxidase (HRP), which was conjugated to our choice of secondary antibody. By fitting the relative values for RANTES binding to a Hill equation using KaleidaGraph software, we determined the EC_{50} to be 12.2 nM (Figure 8).

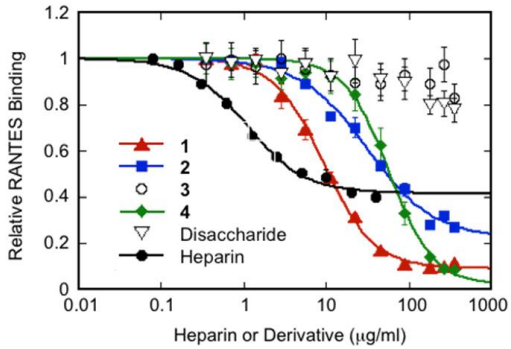

Figure 9. Comparison of the ability of glycopolymers **1 – 4** to compete with heparin for binding to RANTES. $P < 0.05$ for IC_{50} values of glycopolymers **2** and **4** compared to **1**; $P < 0.05$ for IC_{50} value of **2** compared to glycopolymer **4**. IC_{50} values corrected for ligand valence are reported in Table 3.

We used this concentration of RANTES to conduct all competitive ELISA experiments with the synthetic glycopolymers. We followed the same experimental format, except that RANTES was first preincubated with either heparin or glycopolymer, allowing us to determine the individual ability of each compound to inhibit RANTES binding to the heparin-bound plates. The half maximal inhibitory concentrations (IC_{50}) were calculated by fitting the relative binding values to the Michaelis-Menten equation (Kaleidagraph software). We found that trisulfated glycopolymer **1** bound very strongly to RANTES (IC_{50} = 9.3 ± 1.1 mg/mL (334 ± 39 nM)), albeit with reduced affinity in comparison to natural heparin polysaccharides of similar lengths (IC_{50} = 0.90 ± 0.03 mg/mL (45.0 ± 1.5 nM); Figure 9). However, glycopolymer **1** was a more efficient competitor for RANTES at its concentration of maximum inhibition: whereas heparin exhibited a maximum inhibition of 58.4%, glycopolymer **1** inhibited RANTES binding by up to 90.8% under the same

assay conditions. Maximum inhibition values were also determined from the Michaelis-Menten equation.[12] As expected, trisulfated disaccharide **26** (the monovalent version of glyocopolymer **1**) failed to compete with heparin for RANTES binding in the competitive ELISA assay (Figure 9). Thus, our results provide the first demonstration that an HS disaccharide epitope is indeed sufficient for chemokine binding when presented in a multivalent framework and underscore the importance of avidity in the recognition of glycosaminoglycan structures.

Next, we tested whether site-defined modifications to the glycopolymer sulfation pattern would alter its affinity for RANTES. Removal of the *N*-sulfate group of GlcN (glycopolymer **2**) or the 2-*O*-sulfate group of IdoA (glycopolymer **4**) decreased the binding to RANTES (IC_{50} = 31.1 ± 6.2 mg/mL (852 ± 170 nM) and 58.0 ± 5.7 mg/mL (1760 ± 170 nM), respectively), and negative control glycopolymer **3** showed no appreciable activity (Figure 9). Our observation that removal of 2-*O*-sulfation has a greater effect than removal of *N*-sulfation implies that precise positioning of the sulfate groups (in addition to overall electrostatic charge) is important for determining the affinity of the glycopolymers for RANTES. However, this result does not determine from an absolute standpoint that a trisulfated motif is required for RANTES, and also does not rule out that other HS/heparin sequences can interact with RANTES. Further biochemical and biophysical experiments are still needed to determine if a precise sequence dictates the binding of HS/heparin to RANTES and the subsequent activation of its corresponding chemokine receptors.

To validate the IC_{50} values from the competitive ELISA assay, we calculated the valence-adjusted IC_{50} values for heparin and glycopolymers **1**, **2**, and **4** (Table 3). Since heparin contains a different number of sugar units per chain compared to the glycopolymers, this calculation allowed us to calibrate the IC_{50} values so that it would represent the activity of each bioactive epitope. For each of the glycopolymers, we accounted for the mass percentage of sugar contributing to the disaccharide-norbornyl linker unit; this value allowed us to calculate the valence-adjusted IC_{50}

values. We then used the molecular mass of the differentially sulfated disaccharide units to determine the valence-adjusted IC_{50} values according to the molar concentration of disaccharide. As indicated in Table 3, the overall trends in RANTES inhibition for heparin and glycopolymers **1**, **2**, and **4** remains the same after adjusting for valency; however, the potency of activity for glycopolymer **1** relative to heparin does improve by a modest factor. Fortuitously, by knowing the precise chemical structure of the molecules in hand, we were able to bypass the use of the carbazole assay[13] to calculate valence-adjusted concentration values.

Table 3. Half maximal inhibitory concentration (IC_{50}) for antagonists of RANTES.

Antagonist	IC_{50} (μg/mL)[a]	IC_{50} (nM)[b]	IC_{50} (μg/mL of disac)[c]	IC_{50} (μM of disac)[d]
1	9.30 ± 1.1	335 ± 39	6.79 ± 0.80	11.7 ± 1.4
2	31.1 ± 6.2	852 ± 170	21.8 ± 4.4	40.3 ± 8.0
4	58.0 ± 5.7	1760 ± 170	40.6 ± 4.0	81.3 ± 8.0
Heparin	0.900 ± 0.030	45.0 ± 1.5	0.900 ± 0.030	1.50 ± 0.050

[a] Values were determined from Figure 9 using KaleidaGraph software. Data represent the mean ± standard error for quadruplicate assays.
[b] Values were calculated from Figure 9 based on molar concentration of antagonist (see Table 1 for molecular weights of glycopolymers **1**-**4**).
[c] Values were corrected for ligand valence after taking into account the mass percentage of disaccharide contributing to each disaccharide-norbornyl linker unit.
[d] Values were corrected for ligand valence based on molar concentration of disaccharide.

Anticoagulant Activity of the Glycopolymers

After evaluating the ability of heparin and glycopolymers **1** – **4** to antagonize RANTES, we then evaluated their anticoagulant activities (in collaboration with Dr. Young In Oh). The binding of heparin polysaccharides to antithrombin III (ATIII) induces a conformational change that enables ATIII to inhibit the serine protease Factor Xa (FXa) in the coagulation cascade.[14] Specifically,

heparin binds to ATIII through a high-affinity glucosaminyl 3-*O* sulfated pentasaccharide that is found in one third of all heparin chains.[15] A methylated derivative of this pentasaccharide is now widely distributed as the drug Arixtra (GlaxoSmithKline), and the addition of an additional glucosaminyl 3-*O*-sulfate group has been shown to confer greater specificity for ATIII activation (Figure 10). Given that our glycopolymers lack the glucosaminyl 3-*O* sulfate modification, we hypothesized they would not be able to potentiate ATIII in an anticoagulant assay as heparin polysaccharides do.

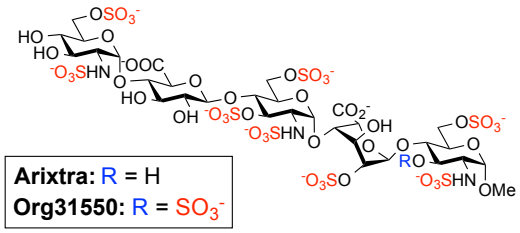

Figure 10. Chemical structures of pentasaccharide-based anticoagulant drugs Arixtra and Org31550.

To measure anticoagulant activity, we incubated heparin or glycopolymer (10^{-5} – 500 μg/mL) in a purified system with ATIII and an excess of FXa. A conformational change in the structure of ATIII increases the protein's inhibitory activity for FXa and can be evaluated *in vitro* using a chromogenic substrate specific for the proteolytic activity of FXa. By measuring the absorbance (405 nm) to determine the levels of residual chromogenic substrate, we could evaluate the ability of heparin or glycopolymers **1** – **4** to potentiate the inhibitory activity of ATIII. Importantly, none of the glycopolymers possessed any anti-FXa activity, while heparin was expectedly shown to be active in the same assay (Figure 11a). We also evaluated the ability of ATIII to inhibit Factor IIa (FIIa or Thrombin), which is activated downstream of FXa in the coagulation cascade as part of the common pathway. Unlike FXa, which utilizes a specific pentasaccharide sequence for ATIII activation, FIIa necessitates longer, highly sulfated template in order to form an inhibitory ternary

complex with ATIII.[16] In agreement with this molecular mechanism, we found that only heparin had significant anti-FIIa activity, while none of the glycopolymers were active (Figure 11b).

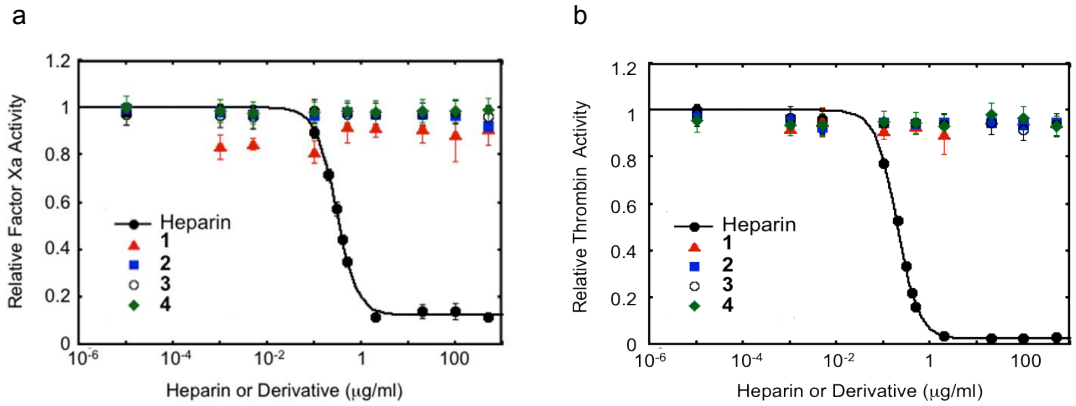

Figure 11. Glycopolymers **1** – **4** do not potentiate inhibition of thrombin in a purified system with antithrombin III. Human antithrombin III (1 IU/mL) was incubated with an excess of (a) Factor Xa or (b) Factor IIa (Thrombin) (24 IU/mL) in the presence of either heparin or glycopolymer (10^{-5} – 500 μg/mL). Heparin is known to bind to and induce a conformational change in the structure of antithrombin III, thereby increasing its inhibitory activity for Factor Xa or Factor IIa (as observed in this assay). A chromogenic substrate (1.25 umol/mL) specific for the proteolytic activity of Factor Xa or Factor IIa was added to measure residual levels of coagulation factor. The absorbance was measured at 405 nm and is inversely proportional to the ability of heparin or glycopolymer to potentiate the inhibitory activity of antithrombin III. Data represent the mean ± standard error for quadruplicate assays.

Finally, we measured the *ex vivo* clotting times of the glycopolymers in comparison to heparin using human plasma samples. As the presence of other proteins in complex serum can potentially interfere with anticoagulant activity, these assays represent a more stringent test of anticoagulant efficacy. We measured the activated partial thromboplastin time (APTT) and prothrombin time (PT) of each compound to determine if the intrinsic and extrinsic pathways of the coagulation cascade are inhibited, respectively. While heparin (150 μg/mL) increased both the APTT and PT for blood clotting, glycopolymer **1** at the same concentration showed no appreciable change in APTT or PT (Table 4). Interestingly, the addition of glucosaminyl 3-*O* sulfation to glycopolymer **1** drastically increased its APTT and PT values (data not shown; see Dr. Young In Oh's thesis for experimental details), thus reinforcing the importance of this specific sulfate modification in the

context of glycosaminoglycan anticoagulant activity. Altogether, our results demonstrate that controlling the positioning of sulfate groups within the glycopolymer enables one to dissect the anti-inflammatory function of HS/heparin glycosaminoglycans from its anti-coagulant function. Furthermore, modifications to the sulfation motif can be distinctly exploited to adjust the affinity of the glycopolymers for specific HS/heparin-binding proteins. These efforts may facilitate the development of novel glycosaminoglycan-based therapeutic agents with fewer off-target side effects.

Table 4. *Ex vivo* clotting times for heparin and glycopolymer **1**.

Compound	**APTT**[a] (s)	**PT**[a] (s)
None	31.2	13.3
Heparin	>180	12.7
1	46.1	84.2

[a] For 150 mg/mL of compound in citrated human plasma, *n*=3.

Glycopolymer Activity in Cellular Assays

The chemotactic activity of RANTES, which is essential to the clinical pathogenesis of allergic inflammatory responses such as asthma, is mediated in part by the chemokine receptor CCR3.[17] To test whether glycopolymer **1** can interfere with RANTES-induced chemotaxis via CCR3, we probed the migration of murine L1.2 pre-B cells that were stably transfected with CCR3 receptor (gift from Prof. Osamu Yoshi, Kinki University Faculty of Medicine, Japan).[18] Stable expression of CCR3 (and all other chemokine receptors mentioned in this study) was routinely confirmed by flow cytometry analysis. Using a modified Boyden chamber, we observed that the directional migration of L1.2-CCR3 cells (but not wild-type L1.2 cells lacking the expression of chemokine receptors) was dependent on RANTES concentration (0.5 – 1024 nM). In establishing the optimal

conditions for the migration assay, we systematically varied the incubation period (0.5 – 8 h), filter pore size (5 or 8 μm), and cell concentration (10^5 – 10^7 cells per pore). We discovered that a robust maximal response was elicited at 10 nM of RANTES (Figure 12a) upon placing 10^6 cells on a 5 μm filter pore and incubating the setup for four hours. While other conditions also elicited dose-dependent migration curves, the aforementioned parameters yielded the most consistent results in our hands.

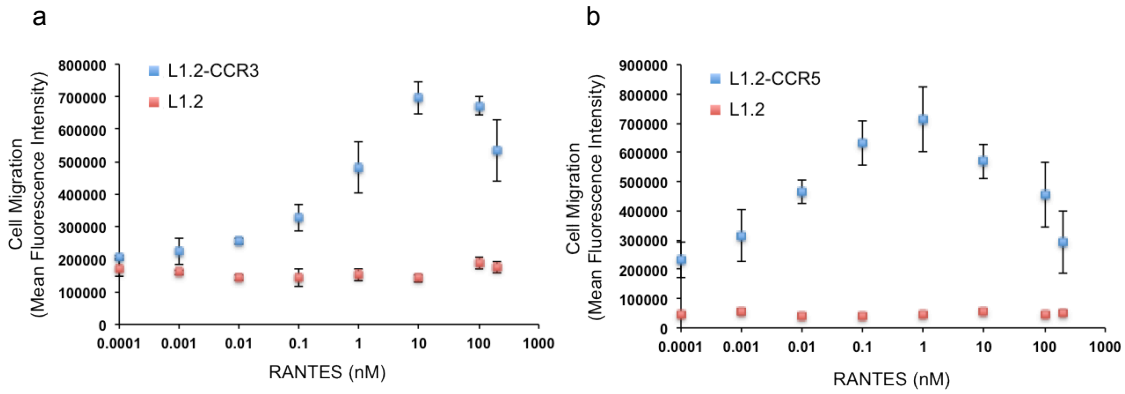

Figure 12. RANTES-induced migration of CCR3- and CCR5-expressing cells. Chemotactic response to RANTES is maximal at (a) 10 nM for CCR3-stably transfected L1.2 cells and (b) 1 nM for CCR5-stably transfected L1.2 cells. In both experiments, wild-type L1.2 cells did not migrate in response to RANTES as expected. Chemotaxis was measured using a 96-well Boyden chamber, and the relative number of migrated cells was determined using a fluorescent nucleic acid dye. Data represent the mean ± standard error for two independent experiments conducted in quadruplicate.

Using the same experimental conditions, we found that preincubation of RANTES (10 nM) with glycopolymer **1** or heparin (0.020 – 4.0 μg/mL) diminished the chemotactic activity of RANTES in a dose-dependent manner (Figure 13a). Further corroborating these observations, lower levels of RANTES were also detected on the surface of L1.2-CCR3 cells after the chemokine (100 nM) was pretreated with glycopolymer **1** or heparin, as determined by flow cytometry analysis (Figure 14). Both glycopolymer **1** and heparin failed to block the migration of L1.2 cells transfected with CCR5 (see Figure 12b for migration curve, exhibiting a maximal response at 1 nM of RANTES), an alternative receptor for RANTES activity (Figure 13b). Consistent with these findings, the

reported binding sites for HS and RANTES exhibit considerable overlap on CCR3, whereas the two binding sites share no overlap on CCR5.[11] Altogether, our results show that glycopolymer **1** effectively antagonizes the CCR3-dependent chemotactic activity of RANTES in various cellular assays, with comparable potency as heparin polysaccharides of the same length. Furthermore, we demonstrate the ability of these glycomimetics to selectively target specific chemokine-receptor interactions in the context of RANTES activation of the chemokine receptors CCR3 and CCR5.

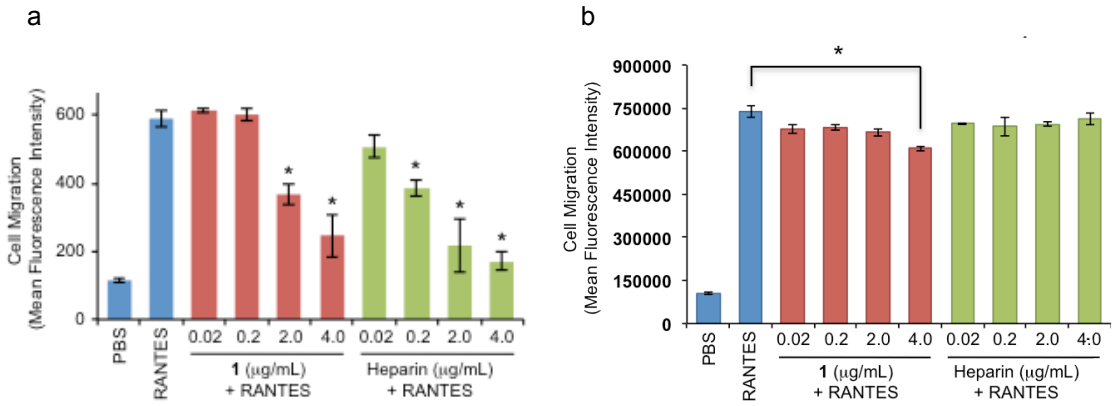

Figure 13. RANTES-induced migration of (a) CCR3 and (b) CCR5-expressing L1.2 cells. RANTES (1 nM or 10 nM) was added to the bottom half of a 96-well modified Boyden chamber and preincubated with various concentrations of heparin or glycopolymer **1** prior to chemotaxis induction. The relative number of migrated cells was measured using a fluorescent nucleic acid dye. Heparin and glycopolymer **1** antagonizes the RANTES-induced migration of L1.2-CCR3 cells, but did not affect the migration of L1.2-CCR5 cells except at the highest concentration of glycopolymer **1** (4 μg/mL; *, $P < 0.01$; means were compared to RANTES treatment alone using a Student's *t* test). Experiments were conducted in quadruplicate, and the standard error is depicted.

In conclusion, we have developed a new class of HS mimetics that are synthetically accessible and highly tunable in structure and sulfation sequence. By controlling the sulfation sequence and exploiting the principles of multivalency to enhance glycan recognition, the binding affinity of HS disaccharides for protein binding partners can be amplified to target chemokines and their receptor interactions. We demonstrate that a trisulfated HS glycopolymer binds to RANTES with nanomolar affinity and inhibits the CCR3-dependent cellular response to this therapeutically

important chemokine, without affecting key components of the blood coagulation cascade. We envision that variations of these glycomimetics can be synthetically tailored in future studies to antagonize a wide range of HS/heparin-binding proteins with clinical relevance to atherosclerosis, cancer, and autoimmune disorders.

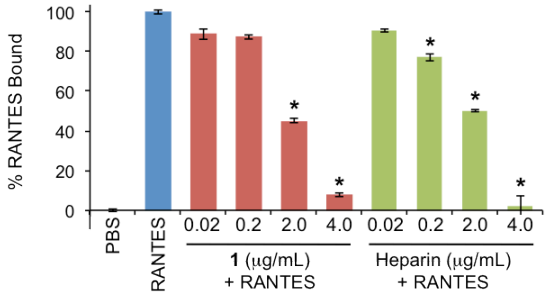

Figure 14. RANTES binding to the surface of CCR3-expressing L1.2 cells. RANTES (100 nM) was preincubated with varying concentrations of heparin or glycopolymer **1** (0.02 – 2 μg/mL). Heparin or **1** inhibits the binding of RANTES to L1.2-CCR3 cells, as determined by flow cytometry (*, $P < 0.05$; means were compared to RANTES treatment alone using a Student's *t* test). Data represent the mean ± standard error for three independent experiments, each conducted in quadruplicate.

Experimental Methods

Direct and Competitive Enzyme-Linked Immunosorbent Assay (ELISA) for RANTES. A 96-well heparin-binding plate (BD Biosciences) was coated with 25 μg/mL of heparin (Neoparin) for 12 h at rt. Wells were rinsed with phosphate-buffered saline (PBS) and blocked with 10% fetal bovine serum (FBS) in PBS for 1 h at 37 °C. For the direct ELISA, various concentrations of RANTES (0.50 – 1024 nM; R&D Systems) were serially diluted in 1% BSA in PBS and incubated in each well for 1.5 h at 37 °C. For the competitive ELISA, RANTES (at 12.2 nM, the pre-determined EC_{50}; Figure 12) was preincubated (3 h, 37 °C) with various concentrations of heparin (0.010 – 40 μg/mL) or glycopolymers **1** – **4** (0.10 – 180 μg/mL), and the co-mixture was

added to the 96-well plate for 1.5 h at 37 °C. Wells were washed three times with PBST (PBS + 0.1% Tween-20), incubated with a mouse anti-RANTES antibody (R&D Systems) for 1 h at 37 °C, washed three times with PBST, and incubated with a horseradish peroxidase (HRP)-conjugated anti-mouse IgG antibody (GE Healthcare Life Sciences) for 1 h at 37 °C. After three washes with PBST, RANTES binding was detected using a 3,3',5,5'-tetramethylbenzidine (TMB) substrate kit (Thermo Scientific) according to the manufacturer's instructions. Absorbance was measured at 450 nm using a Victor 3 plate reader (PerkinElmer). The half-maximal effective concentration (EC_{50}) and half maximal inhibitory concentration (IC_{50}) were calculated using KaleidaGraph software (Synergy). IC_{50} values reported in the paper are for both the mass and molar concentrations of antagonist. IC_{50} values were also corrected for ligand valence (Table 3) by calculating the mass percentage of the disaccharide epitope contributing to each disaccharide-norbornyl linker unit, and then dividing by the molecular weight of the disaccharide epitope.

Cell Culture. L1.2 cells (mouse pre-B lymphocytes) stably transfected with CCR3, CCR5, or vector only, were kindly provided by Dr. Osamu Yoshie (Kinki University, School of Medicine, Japan). Cells were maintained in RPMI 1640 (Invitrogen) supplemented with 10% FBS, 100 μg/mL penicillin/streptomycin (Invitrogen), and 50 μM 2-mercaptoethanol (Sigma Aldrich). Cells were routinely analyzed by flow cytometry (FACSCalibur, Beckman Dickenson) to verify that cultures expressed adequate levels of chemokine receptor (>90%) for migration and cell binding assays.

Cell Migration Assay. Experiments were performed using ChemoTx chambers (Neuroprobe). L1.2 cells (wild-type or stably-transfected with CCR3 or CCR5) were harvested and washed twice in flow cytometry buffer (Hank's Balanced Salt Solution (HBSS) with 2.5 mg/mL bovine

serum albumin (BSA) and 10 mM HEPES). Human RANTES (R&D Systems) was serially diluted in flow cytometry buffer (0.5 – 1024 nM), and 30 μL of each dilution was added to the bottom wells of the ChemoTx chamber. Alternatively, in competitive migration assays, 1 or 10 nM of RANTES was preincubated with various concentrations of heparin or glycopolymer **1** (0.020 – 4.0 μg/mL) for 30 min at rt, and the same volume of each solution was added to the bottom wells. The sample plate was fitted with a 5-μm pore filter, and 10^6 cells (50 μL) were placed on top of each well. Cells were allowed to migrate through the filter for 4 h at 37 °C and 5% CO_2. Subsequently, non-migrating cells were removed from the top of the filter by manual scraping; cells adhering to the filter were dislodged using 20 μL of 2.5 mM EDTA for 30 min at rt. Migrated cells were transferred (500 x *g*, 5 min) to a 96-well black-walled clear-bottomed plate (Corning) using a funnel plate (Neuroprobe). Cells were lysed at -80 °C and stained with CyQUANT dye (Invitrogen) as described in the product literature. Fluorescence was measured at 535 nm using a Victor 3 plate reader (PerkinElmer).

Chemokine Cell Binding Assay. 3 x 10^6 L1.2 cells (wild-type or stably-transfected with CCR3) were washed twice with flow cytometry buffer and incubated with RANTES (100 nM in flow cytometry buffer) for 45 min at rt. Alternatively, cells were incubated with RANTES (100 nM in flow cytometry buffer) previously treated with various concentrations of heparin or glycopolymer 1 (0.02 – 2 μg/mL) for 30 min at rt. Cells were spun twice (500 x g, 5 min) through 100% FBS (1.0 mL) to remove excess reagent and stained with phycoerythrin (PE)-conjugated anti-RANTES (1 test) in FACS buffer (100 μL) for 1 h at 4 °C. Cells were again spun twice through 100% FBS (1.0 mL) and resuspended in flow cytometry buffer (500 μL) for flow cytometry analysis. Immediately before analysis, 7-amino-actinomycin-D (7-AAD, 5 μL, eBioscience) was

added to evaluate cell viability. Cells were analyzed for PE intensity on a FACSCalibur flow cytometer (Beckman Dickenson, Caltech Flow Cytometry Facility) with 10,000 cell events per sample. Data analysis was performed using FlowJo (Tree Star Inc.).

Chromogenic Assay for the Measurement of Antithrombin Activity. Factor Xa (FXa) Activity: The BIOPHEN Heparin Anti-FXa (2 stages) USP/EP kit (Aniara) was used to evaluate FXa activity. This chromogenic anti-FXa method for measuring homogeneous heparin in purified systems is in compliance with Pharmacopoeias (USP, EP) and FDA guidelines. All reagents were prepared according to manufacturer's instructions and incubated at 37 °C for 15 min. Varying concentrations of heparin (Neoparin) or glycopolymers **1** – **4** (40 uL) and antithrombin (40 uL) were added to a microcentrifuge tube, mixed, and incubated at 37 °C for 2 min. FXa (40 uL) was added to the solution, incubated at 37 °C for exactly 2 min, and then the FXa chromogenic substrate (40 μL) was added. After 2 min, the reaction was quenched with citric acid (20 g/L, 240 μL), and the absorbance was measured at 405 nm. The sample blank was obtained by mixing the reagents in reverse order, and the resulting value was deducted from the absorbance values measured in the assay.

Factor IIa (FIIa) Activity: The BIOPHEN Heparin Anti-FIIa (2 stages) USP/EP kit (Aniara) was used to determine FIIa activity. This chromogenic anti-FIIa method was conducted according to the same procedure used for FXa.

Activated Partial Thromboplastin Time (APTT) and Prothrombin Time (PT) Analysis. Flash frozen, platelet-poor human plasma with 3.2% citrate was purchased from Valley Biomedical

(Winchester, VA) for the coagulation assay. Samples were thawed at room temperature for 30 min and used immediately for APTT and PT assays.

For APTT analysis, samples were prepared by mixing 300 μL of heparin or glycopolymer in 0.9% saline with 2.7 mL citrated human plasma. The tube was inverted three times to mix the sample thoroughly. Dade® Actin® activated cephaloplastin reagent was used as a plasma activator. To 100 μL of the plasma/anticoagulant sample, 100 μL of prewarmed APTT reagent (0.2% ellagic acid) was added. After incubation for 4 min, clotting was initiated by adding 100 μL of 25 mM $CaCl_2$ at 37 ºC and the time required for clot formation was measured. Clotting time in the absence of an anticoagulant was determined using 300 μL of saline solution. Each clotting assay was performed in triplicate.

For PT analysis, samples were prepared by mixing 300 μL of heparin or glycopolymer in 0.9% saline with 2.7 mL citrated human plasma. The tube was inverted three times to mix the sample thoroughly. Dade® Innovin® reagent was reconstituted according to the manufacturer's directions and warmed to 37 °C. 100 μL of the plasma/anticoagulant sample was incubated for 3 min at 37 °C, followed by the addition of 200 μL of prewarmed thromboplastin reagent. The time required for clot formation was measured. Clotting time in the absence of an anticoagulant was determined using 300 μL of saline solution. Each clotting assay was performed in triplicate.

REFERENCES

[1] A. Zlotnik, O. Yoshie, *Immunity* **2000**, *12*, 121-127.

[2] M. Baggiolini, *Nature* **1998**, *392*, 565-568.

[3] V. Appay, S. L. Rowland-Jones, *Trends in immunology* **2001**, *22*, 83-87.

[4] M. Q. Xia, S. X. Qin, L. J. Wu, C. R. Mackay, B. T. Hyman, *The American journal of pathology* **1998**, *153*, 31-37.

[5] R. Meurer, G. Van Riper, W. Feeney, P. Cunningham, D. Hora, Jr., M. S. Springer, D. E. MacIntyre, H. Rosen, *The Journal of experimental medicine* **1993**, *178*, 1913-1921.

[6] F. Cocchi, A. L. DeVico, A. Garzino-Demo, S. K. Arya, R. C. Gallo, P. Lusso, *Science* **1995**, *270*, 1811-1815.

[7] S. G. Ward, J. Westwick, *The Biochemical journal* **1998**, *333 (Pt 3)*, 457-470.

[8] F. Charni, V. Friand, O. Haddad, H. Hlawaty, L. Martin, R. Vassy, O. Oudar, L. Gattegno, N. Charnaux, A. Sutton, *Biochimica et biophysica acta* **2009**, *1790*, 1314-1326.

[9] J. M. Burns, G. K. Lewis, A. L. DeVico, *Proceedings of the National Academy of Sciences of the United States of America* **1999**, *96*, 14499-14504.

[10] Z. Johnson, M. H. Kosco-Vilbois, S. Herren, R. Cirillo, V. Muzio, P. Zaratin, M. Carbonatto, M. Mack, A. Smailbegovic, M. Rose, R. Lever, C. Page, T. N. Wells, A. E. Proudfoot, *Journal of immunology* **2004**, *173*, 5776-5785.

[11] L. Martin, C. Blanpain, P. Garnier, V. Wittamer, M. Parmentier, C. Vita, *Biochemistry* **2001**, *40*, 6303-6318.

[12] A. E. Proudfoot, T. M. Handel, Z. Johnson, E. K. Lau, P. LiWang, I. Clark-Lewis, F. Borlat, T. N. Wells, M. H. Kosco-Vilbois, *Proceedings of the National Academy of Sciences of the United States of America* **2003**, *100*, 1885-1890.

[13] M. Cesaretti, E. Luppi, F. Maccari, N. Volpi, *Carbohyd Polym* **2003**, *54*, 59-61.

[14] B. Casu, P. Oreste, G. Torri, G. Zoppetti, J. Choay, J. C. Lormeau, M. Petitou, P. Sinay, *The Biochemical journal* **1981**, *197*, 599-609.

[15] J. Choay, M. Petitou, J. C. Lormeau, P. Sinay, B. Casu, G. Gatti, *Biochemical and biophysical research communications* **1983**, *116*, 492-499.

[16] W. Li, D. J. Johnson, C. T. Esmon, J. A. Huntington, *Nature structural & molecular biology* **2004**, *11*, 857-862.

[17] L. C. Borish, J. W. Steinke, *The Journal of allergy and clinical immunology* **2003**, *111*, S460-475.

[18] M. Kitaura, T. Nakajima, T. Imai, S. Harada, C. Combadiere, H. L. Tiffany, P. M. Murphy, O. Yoshie, *The Journal of biological chemistry* **1996**, *271*, 7725-7730.

Chapter 4

DISCOVERY OF A SPECIFIC MODULATOR OF SDF-1 ACTIVITY

Chemokine Binding to Synthetic Glycopolymers

Our previous experiments showed that trisulfated glycopolymer **1** has the highest affinity (IC_{50} = 9.30 ± 1.1 μg/mL (335 ± 39 nM)) for the pro-inflammatory chemokine RANTES compared to the other sulfated glycopolymers in our synthetic library. While heparin polysaccharide of the same length (IC_{50} = 0.900 ± 0.03 μg/mL (45.0 ± 1.5 nM) bound to RANTES more efficiently than glycopolymer **1**, both antagonists exhibited similar potencies in cell migration and binding assays. As cell migration and chemotactic gradients play an essential role during angiogenesis, here we sought to compare the relative binding affinities of glycopolymer **1** and heparin for a series of chemokines strongly implicated in angiogenesis.[1] Specifically, we chose to examine growth related oncogene-α (Gro-α; CXCL1), interleukin 8 (IL-8; CXCL8), and stromal cell-derived factor 1 (SDF-1; CXCL12), three members of the CXC subfamily.

CXC chemokines are known for their ability to regulate angiogenesis,[2] the physiological process by which new blood vessels are derived from existing capillaries. All CXC chemokines have four highly conserved cysteine residues, and the first two cysteines are separated by a nonconserved residue.[3] A second structural domain in these chemokines dictates their angiogenic capacity: that is, a tripeptide sequence (Glu-Leu-Arg; also designed the ELR motif) at the N-terminus preceding the first cysteine residue in the CXC domain.[4] Typically, members that have the ELR motif (ELR^+) are potent inducers of angiogenesis, while those lacking the motif (ELR^-) are inhibitors.[5] Thus, the local expression of specific CXC chemokines can serve as an important regulator of angiogenesis; likewise, an imbalance in chemokine expression can have dire consequences, such as the promotion of tumor growth or the induction of chronic fibroproliferative disorders.[6] Two

of the chemokines that we chose to investigate, Gro-α and IL-8, are distinctly pro-angiogenic (ELR^+) and can act as ligands for CXCR2,[7] a chemokine receptor upregulated in several cancers of high metasatic index (breast cancer,[8] head and neck cancer,[9] melanoma,[10] ovarian cancer,[11] pancreatic cancer[12]). We also chose to evaluate SDF-1, the only ELR^- chemokine that is able to potentiate angiogenesis and other growth promoting activities. In fact, SDF-1 has been shown to play a major role in recruiting CXCR4-positive bone marrow and tumor cells to neo-angiogenic niches to support the revascularization of ischemic tissues[13] and tumor microenvironments.[14]

Table 5. Half maximal inhibitory concentration (IC_{50}) for antagonists of Gro-α, IL-8, and SDF-1.

Antagonist	IC_{50} (μg/mL)[a]	IC_{50} (nM)[b]	IC_{50} (μg/mL of disac)[c]	IC_{50} (μM of disac)[d]
		Gro-α		
1	77.4	2780	56.5	97.6
Heparin	2.41	121	2.41	4.17
		IL-8		
1	5.66	203	4.13	7.13
Heparin	22.8	1140	22.8	39.4
		SDF-1		
1	2.70	97.0	1.97	3.41
2	16.4	449	11.5	21.3
Heparin	44.3	2210	44.3	76.4

[a] Values were determined from Figure 15 using KaleidaGraph software. Data represent the mean ± standard error for quadruplicate assays.
[b] Values were calculated from Figure 15 based on molar concentration of antagonist (see Table 1 for molecular weights of glycopolymers **1**-**4**).
[c] Values were corrected for ligand valence after taking into account the mass percentage of disaccharide contributing to each disaccharide-norbornyl linker unit.
[d] Values were corrected for ligand valence based on molar concentration of disaccharide.

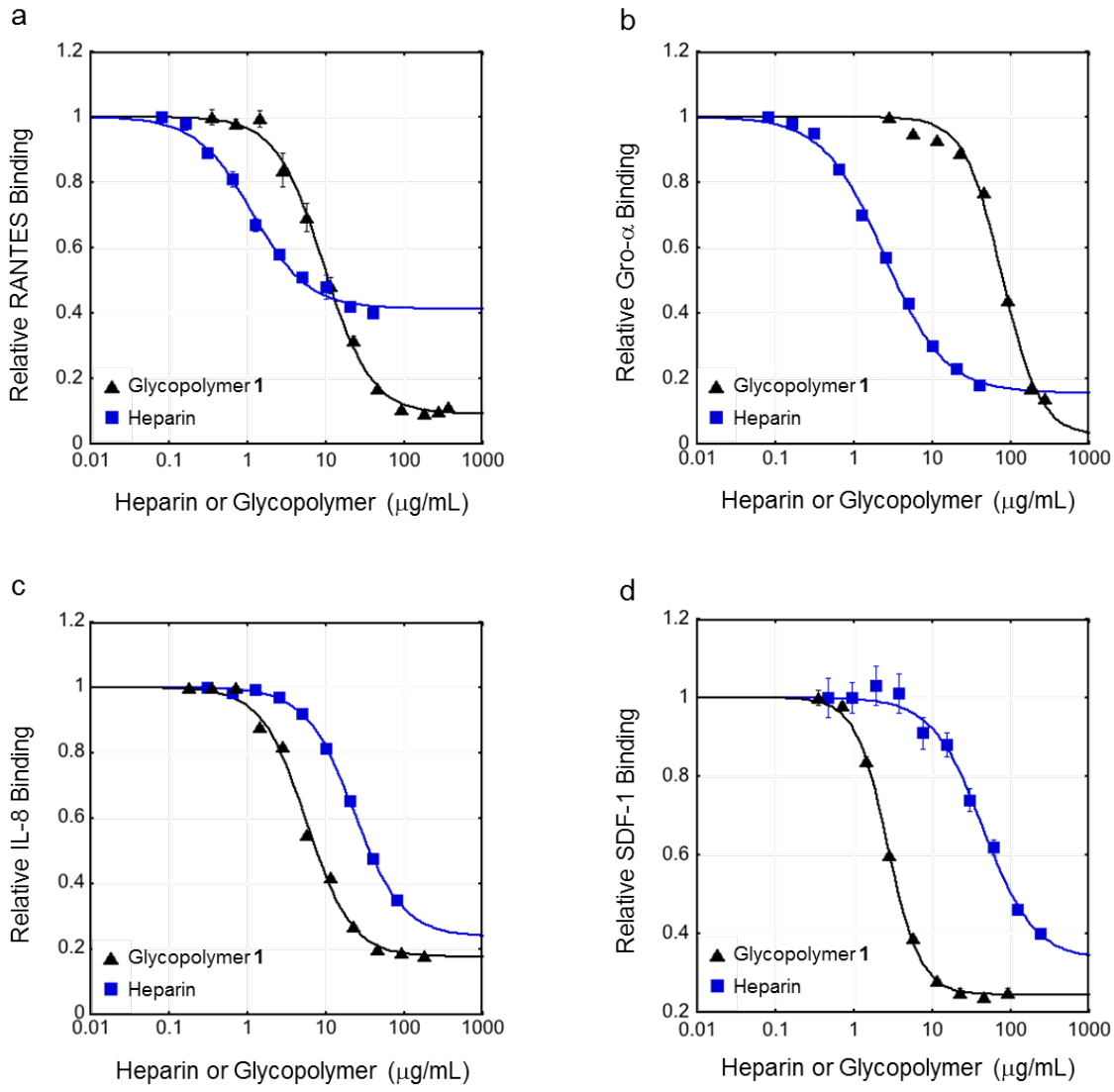

Figure 15. Comparison of the ability of glycopolymer **1** and heparin to compete for binding to (a) RANTES; (b) Gro-α; (c) IL-8; (d) SDF-1. IC_{50} values corrected for ligand valence are reported in Table 5.

First, we determined the EC_{50} values of Gro-α, IL-8, and SDF-1 binding to heparin-coated (25 μg/mL) 96-well plates using a direct ELISA format (166 nM, 38 nM, and 315 nM, respectively). We then evaluated the ability of glycopolymer **1** or heparin to inhibit each of the chemokines at its EC_{50} value using the same competitive ELISA procedure developed for RANTES. While the IC_{50} values for heparin-mediated chemokine inhibition reflected the EC_{50} values from the direct ELISA, we were surprised to find that the IC_{50} values for glycopolymer-mediated chemokine

inhibition were drastically different from the EC_{50} values (Table 5 and Figure 15). For example, heparin inhibited Gro-α (EC_{50} = 166 nM) with expected nanomolar affinity (IC_{50} = 2.41 μg/mL or 121 nM), while glycopolymer **1** was found to be 30-fold less effective (IC_{50} = 77.4 μg/mL or 2780 nM). In contrast, heparin exhibited slightly reduced affinity for IL-8 (EC_{50} = 38 nM; IC_{50} = 22.8 μg/mL or 1140 nM) in comparison to glycopolymer **1** (IC_{50} = 5.66 μg/mL or 203 nM). Despite these discrepancies, we were pleased to discover that glycopolymer **1** bound to SDF-1 (EC_{50} = 315 nM; IC_{50} = 2.70 μg/mL or 97.0 nM) with tight nanomolar affinity, while heparin was notably less efficient (IC_{50} = 44.3 μg/mL or 2210 nM). This result suggests that structural features unique to glycopolymer **1** (unrelated to sulfation) endowed it with the ability to act as a more specific antagonist of SDF-1.

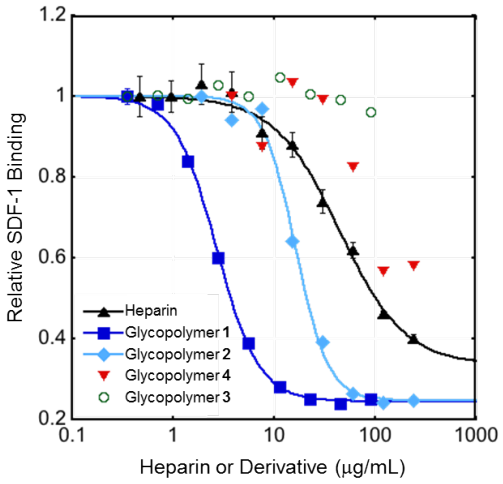

Figure 16. Comparison of the ability of glycopolymers **1 – 4** and heparin to compete for binding to SDF-1. IC_{50} values corrected for ligand valence are reported in Table 1.

We also investigated whether modifications to the sulfation motif would alter the glycopolymer's ability to inhibit SDF-1. Similar to our observations with RANTES, we found that removal of the 2-*O* sulfate group on IdoA (glycopolymer **4**; IC_{50} = 16.4 μg/mL or 449 nM) had a more drastic effect

on SDF-1 binding affinity than removal of the *N*-sulfate group on GlcN (glycopolymer **2**; IC_{50} undeterminable) (Table 5 and Figure 16). As expected, the unsulfated control (glycopolymer **3**) did not exhibit any appreciable binding to SDF-1. Interestingly, glycopolymer **2** was determined to be a more effective inhibitor of SDF-1 than heparin itself, despite possessing fewer sulfate groups per sugar unit. These findings suggest that the macromolecular architecture of the glycopolymer is inherently favorable for SDF-1 interactions and may even promote the formation of higher-order SDF-1 oligomers. However, further structural insights (such as molecular docking simulations) are still needed for one to be able to predict the biochemical behavior of the synthetic glycopolymers. The development of such efforts would greatly facilitate the design of highly specific antagonists for targeting chemokine activity.

Glycopolymer Modulation of SDF-1 Activity

Given the remarkable and unexpected affinity of glycopolymer **1** for SDF-1, we sought to examine how glycopolymer modulated SDF-1 activity in a cellular context. As previously mentioned, SDF-1 signaling through its primary receptor CXCR4 has been strongly linked to cancer metastasis in the context of tumor-associated immune cells, neo-angiogenesis, invasion, and proliferation. At least 23 types of cancers have been shown to upregulate CXCR4 within the tumor microenvironment and are highly sensitized to SDF-1 gradients originating from distant tissues (e.g. bone marrow, lung, liver).[15] Current efforts to block the metastatic dissemination of malignant cancers have primarily focused on the development of small molecule CXCR4 antagonists; unfortunately, such compounds have proven to be remarkably difficult to transfer into the clinic.[15] Thus, alternative strategies are still needed for targeting SDF-1 mediated metastatic homing of invasive cancer cells, such as direct inhibition of SDF-1 itself and/or alterations to its oligomerization state.

Both SDF-1 and cognate receptor CXCR4 are known to play vital roles in leukocyte trafficking,[16] hematopoiesis,[17] and development.[18] While gene knockouts of most chemokines and chemokine receptors exhibit no apparent phenotype due to the inherent redundancy of the chemokine system, SDF-$1^{-/-}$ and $CXCR4^{-/-}$ mice both display significant defects in B-cell lymphopoiesis, bone marrow myelopoiesis, vascularization of the gastrointestinal tract, cardiac ventral septum formation, and cerebellar development.[19] In addition to normal physiological functions, SDF-1 and CXCR4 also contribute to the pathogenesis of several types of cancer[20] by controlling the metastasis of CXCR4-expressing tumor cells towards SDF-1-secreting organs. Given the multifunctional and diverse roles of SDF-1 and CXCR4, we sought to determine if glycopolymer **1** could effectively disrupt the migration of CXCR4-expressing cells towards a SDF-1 chemoattractant gradient.

We chose to use the Jurkat T cell line, as it is known to express high levels of endogenous CXCR4 and respond accordingly to SDF-1-mediated chemotaxis.[21] Using a modified Boyden chamber, we observed that maximal migration of Jurkat cells occurred at 5 nM of SDF-1 using assay conditions previously optimized for L1.2 cells (5 μm filter pore, 4 hour incubation at 37 °C, 10^6 cells per pore). We found that the percentage of cells migrating in response to SDF-1 gradients could be further improved by reducing the number of cells per pore to 10^5. Using these modified conditions, we found that precinbuation of SDF-1 (5 nM) with glycopolymer **1** (0.02 – 10 μg/mL) blocked the chemotactic activity of SDF-1 in a dose-dependent manner, while heparin administered at the same concentrations had no appreciable effect (Figure 17). The potent inhibition of SDF-1 mediated cell migration by glycopolymer **1** is consistent with the IC_{50} value that we measured in the competitive ELISA and implicates the potential use of synthetic glycomimetics as anti-metastasis agents in CXCR4-expressing tumor microenvironments. Furthermore, the distinct ability of glycopolymer **1** to recognize of SDF-1 over other chemokines in the competitive ELISA suggests that glycopolymer

1 could serve as a specific inhibitor of SDF-1 at effective concentrations for which heparin/HS polysaccharides show no activity.

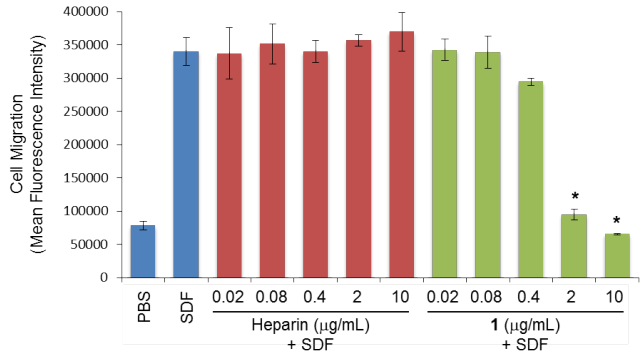

Figure 17. SDF-1-induced migration of CXCR4-expressing Jurkat cells. SDF-1 (5 nM) was added to the bottom half of a 96-well modified Boyden chamber and preincubated with various concentrations of heparin or glycopolymer **1** prior to chemotaxis. The relative number of migrated cells was measured using a fluorescent nucleic acid dye. Glycopolymer **1** antagonizes the SDF-1-induced migration of Jurkat cells (*, $P < 0.01$; means were compared to SDF-1 treatment alone using a Student's *t* test), while heparin at the same concentrations exhibited no effect. Experiments were conducted in quadruplicate, and the standard error is depicted.

Under physiological conditions, SDF-1 exists in a monomer-dimer equilibrium that can be altered by chemokine concentration, pH, the presence of anions (phosphate, sulfate, citrate), and heparin. Acidic pH is known to promote the monomeric state by destabilizing the dimeric structure, while negatively charged species have been shown to shift the equilibrium towards dimer formation.[22] Furthermore, the monomeric form of SDF-1 is responsible for mobilization of intracellular calcium, inhibition of cAMP signaling, recruitment of β-arrestin, stimulation of actin polymerization, and cellular migration, and thus is highly linked to mechanisms of cancer metastasis dictated by SDF-1 gradients.[23] Conversely, dimeric SDF-1 is able to induce G-protein-dependent calcium flux, inhibit adenylyl cyclase, and rapidly activate ERK1/2, mechanisms that are associated instead with cell survival.[23] Micromolar amounts of heparin are typically required to induce SDF-1 dimerization; thus, the heparin concentrations (0.02 – 10 μg/mL) used in the migration assay would not have been sufficient to block SDF-1-mediated chemotaxis by promoting dimer formation. However, we did

observe full inhibition of SDF-1 activity for 2 μg/mL of glycopolymer **1** in the same assay (Figure 17). This observation led us to reason that relatively low concentrations of glycopolymer **1** might be sufficient to block SDF-1-mediated cell migration due to a shift in the monomer-dimer equilibrium towards the latter species.

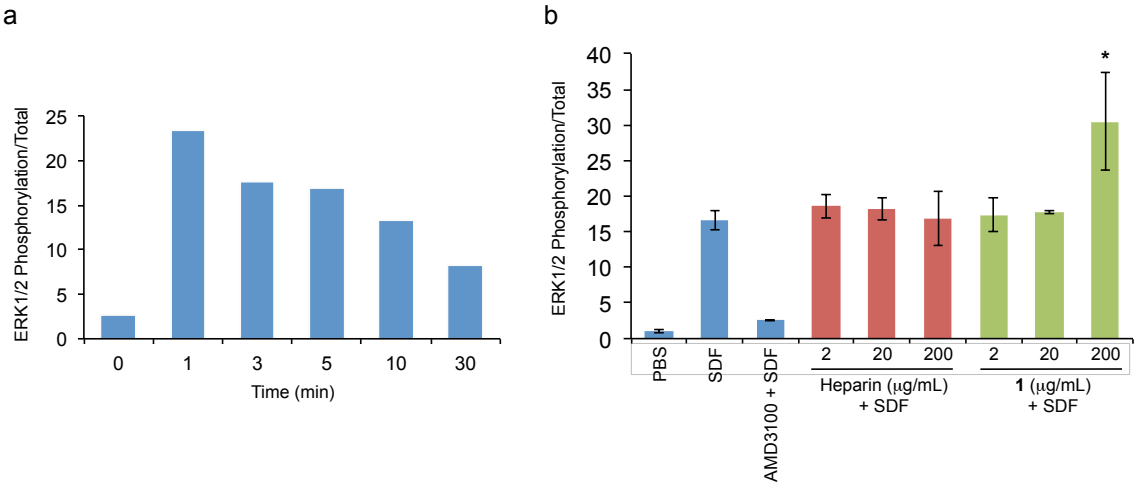

Figure 18. SDF-1-induced ERK1/2 phosphorylation of CXCR4-expressing Jurkat cells. ERK1/2 phosphorylation levels are measured by immunoblotting for phosphorylated and total ERK1/2, and the ratio of their relative intensities is plotted. (a) SDF-1 (0.5 ng/mL) induces a maximal response in ERK1/2 phosphorylation at 1 minute, which gradually decreases over 30 minutes. (b) Glycopolymer **1** potentiates the ERK1/2 phosphorylation after 5 min (*, $P < 0.05$; means were compared to SDF-1 treatment alone using a Student's *t* test), while heparin at the same concentrations has no effect. Experiments were conducted in triplicate, and the standard error is depicted.

To further explore this hypothesis, we examined the intracellular signaling pathways modulated by SDF-1 and CXCR4 in Jurkat cells. The dimer form of SDF-1 has been shown to preferentially induce downstream activation of ERK1/2 to control cell proliferation and cell death.[24] To verify that SDF-1 can activate the ERK1/2 pathway in Jurkat cells, we measured phosphorylation levels of ERK1/2 after exposure to the chemokine. Immunoblotting with phospho-ERK1/2 antibody revealed that SDF-1 treatment (0.5 ng/mL) led to rapid activation of ERK1/2, with phosphorylation levels peaking at 1 min after SDF-1 exposure (Figure 18a). ERK1/2 phosphorylation was sustained for at least 30 min and was completely abrogated upon pretreatment of the cells with CXCR4-specific

antagonist AMD3100 (100 ng/mL; Figure 18b). No significant changes were observed in total ERK expression during the same time period. Next we evaluated the ability of glycopolymer **1** or heparin to alter the phosphorylation status of ERK1/2 at 5 min after exposure to SDF-1. Notably, we found that glycopolymer **1** (200 μg/mL) potentiated the activation of ERK1/2 by 1.8-fold, while the same concentration of heparin had no effect (Figure 18b), thus further validating our hypothesis that the glycopolymer promotes the dimer form of SDF-1. However, detailed biophysical experiments are still warranted to demonstrate that natural glycosaminoglycans and synthetic glycomimetics induce differential changes in SDF-1 structure and CXCR4 signaling.

The ability to differentially activate CXCR4 pathways by modulating the oligomerization status of its ligand would provide an exciting new strategy for therapeutic invention of many diseases. For example, the monomer form of SDF-1 is believed to be cardioprotective, as an obligate monomer of SDF-1 has recently been proposed to potentially treat ischemia-reperfusion injuries and myocardial infarctions.[25] In the context of cancer metastasis, however, an obligate dimer of SDF-1 has been shown to preferentially inhibit the metastasis of colonic carcinoma and pulmonary melanoma cells *ex vivo*, presumably due to the formation of nonmotogenic SDF-1 dimers. Our experiments here show that trisulfated glycopolymer **1** bound to SDF-1 with high affinity, and the resulting complex recapitulated the inhibitory activity of the SDF-1 dimer in two preliminary *in vitro* assays. In contrast, similar complexes formed by heparin and SDF-1 did not show any activity. If additional biophysical experiments are able to demonstrate that glycopolymer **1** does preferentially bias the SDF-1 equilibrium towards the dimer form, we propose that this synthetic mimetic could potentially be used as a treatment for several types of invasive cancers relying on SDF-1 gradients, including breast carcinoma,[26] liver carcinoma,[27] and highly malignant cases of glioblastoma multiforme.[28] We anticipate that this strategy will have several advantages over current efforts to block the CXCR4 receptor, since it would allow for direct disruption of local SDF-1 gradients at the tissue

harboring the tumor microenvironment and the preservation of SDF-1 dimer signaling necessary for cell proliferation and other homeostatic functions. Furthermore, the highly tunable nature of the glycopolymer structure will enable the eventual development of tissue-specific inhibitors of SDF-1 in the context of specific metastatic cancers.

Experimental Methods

Direct and Competitive Enzyme-Linked Immunosorbent Assay (ELISA) for SDF-1. A 96-well heparin-binding plate (BD Biosciences) was coated with 25 μg/mL of heparin (Neoparin) for 12 h at rt. Wells were rinsed with phosphate-buffered saline (PBS) and blocked with 10% fetal bovine serum (FBS) in PBS for 1 h at 37 °C. For the direct ELISA, various concentrations of SDF-1 (0.50 – 1024 nM; R&D Systems) were serially diluted in 1% BSA in PBS and incubated in each well for 1.5 h at 37 °C. For the competitive ELISA, SDF-13 (at 315 nM, the pre-determined EC_{50} value) was preincubated (3 h, 37 °C) with various concentrations of heparin (0.010 – 40 μg/mL) or glycopolymers **1** – **4** (0.10 – 270 μg/mL), and the co-mixture was added to the 96-well plate for 1.5 h at 37 °C. Wells were washed three times with PBST (PBS + 0.1% Tween-20), incubated with a mouse anti-SDF-1 antibody (R&D Systems) for 1 h at 37 °C, washed three times with PBST, and incubated with a horseradish peroxidase (HRP)-conjugated anti-mouse IgG antibody (GE Healthcare Life Sciences) for 1 h at 37 °C. After three washes with PBST, SDF-1 binding was detected using a 3,3',5,5'-tetramethylbenzidine (TMB) substrate kit (Thermo Scientific) according to the manufacturer's instructions. Absorbance was measured at 450 nm using a Victor 3 plate reader (PerkinElmer). The half-maximal effective concentration (EC_{50}) and half maximal inhibitory concentration (IC_{50}) were calculated using KaleidaGraph software (Synergy). IC_{50} values reported in the paper are for both the mass and molar concentrations of antagonist. IC_{50}

values were also corrected for ligand valence (Table 5) by calculating the mass percentage of the disaccharide epitope contributing to each disaccharide-norbornyl linker unit, and then dividing by the molecular weight of the disaccharide epitope.

Cell Culture. CXCR4-expressing Jurkat T cells were maintained in RPMI 1640 (Invitrogen) supplemented with 10% FBS, 100 μg/mL of penicillin/streptomycin (Invitrogen), and 50 μM of 2-mercaptoethanol (Sigma Aldrich). Cells were routinely analyzed by flow cytometry *(FACSCalibur, Beckman Dickenson) to verify adequate expression of the chemokine receptor*.

Cell Migration Assay. Experiments were performed using ChemoTx chambers (Neuroprobe). CXCR4-expressing Jurkat cells were harvested and washed twice in flow cytometry buffer (Hank's Balanced Salt Solution (HBSS) with 2.5 of mg/mL bovine serum albumin (BSA) and 10 mM of HEPES). Human SDF-1 (R&D Systems) was serially diluted in flow cytometry buffer (0.5 – 1024 nM), and 30 μL of dilution was added to the bottom wells of the ChemoTx chamber. Alternatively, in competitive migration assays, 5 nM of SDF-1 was preincubated with various concentrations of heparin or glycopolymer **1** (0.020 – 10 μg/mL) for 30 min at rt, and the same volume of each solution was added to the bottom wells. The sample plate was fitted with a 5-μm pore filter, and 10^5 cells (50 μL) were placed on top of each well. Cells were allowed to migrate through the filter for 4 h at 37 °C and 5% CO_2. Subsequently, non-migrating cells were removed from the top of the filter by manual scraping; cells adhering to the filter were dislodged using 20 μL of 2.5 mM EDTA for 30 min at rt. Migrated cells were transferred (500 x *g*, 5 min) to a 96-well black-walled clear-bottomed plate (Corning) using a funnel plate (Neuroprobe). Cells were

lysed at -80 °C and stained with CyQUANT dye (Invitrogen) as described in the product literature. Fluorescence was measured at 535 nm using a Victor 3 plate reader (PerkinElmer).

ERK1/2 Phosphorylation Assay. A total of 10^7 cells in 1 ml of RPMI 1640 media were equilibrated for 5 min at 37 °C and then stimulated with SDF-1 (0.5 ng/mL) alone or SDF-1 preincubated with various concentrations of heparin or glycopolymer **1** (1 – 100 ng/mL). Reactions were terminated by the addition of ice-cold PBS (1 mL). Cells were pelleted in a microcentrifuge for 45 s, followed by aspiration of the supernatant and the addition of 0.5 mL of ice-cold cell lysis buffer (10 mM Tris–HCl, pH 7.4, 150 mM NaCl, 1% Triton X-100, 0.5% NP-40, 0.5%SDS, 1 mM EDTA, 1 mM EGTA, 1 mM Na_3VO_4, and 1 mM NaF) containing protease and phosphatase inhibitor cocktail (Roche). Lysates were clarified by centrifugation at 10,000 x *g* for 10 min, and the total protein concentrations were determined by BCA Protein Assay (Pierce). Equal amounts (30 μg) of total protein were separated by SDS-PAGE on 4-12% Bis-Tris gels (Invitrogen) and transferred to PVDF membranes. After blocking in 5% BSA for 1 h at rt, the membranes were incubated overnight at 4 °C with primary antibodies to ERK42/44 and phospho-ERK42/p44 (Cell Signaling Technology). After excessive washing with TBS containing 0.1% Tween 20, the membranes were probed with IR-labeled secondary Antibodies (Rockland Immunochemicals) for 1 h at rt. Membranes were then washed with TBS containing 0.1% Tween and scanned under both the 700 and 800 channels using the Odyssey Infrared Imaging System (LI-COR Bioscience).

REFERENCES

[1] F. Kiefer, A. F. Siekmann, *Cellular and molecular life sciences : CMLS* **2011**, *68*, 2811-2830.

[2] J. A. Belperio, M. P. Keane, D. A. Arenberg, C. L. Addison, J. E. Ehlert, M. D. Burdick, R. M. Strieter, *Journal of leukocyte biology* **2000**, *68*, 1-8.

[3] B. J. Rollins, *Blood* **1997**, *90*, 909-928.

[4] A. D. Luster, *The New England journal of medicine* **1998**, *338*, 436-445.

[5] R. M. Strieter, P. J. Polverini, S. L. Kunkel, D. A. Arenberg, M. D. Burdick, J. Kasper, J. Dzuiba, J. Van Damme, A. Walz, D. Marriott, et al., *The Journal of biological chemistry* **1995**, *270*, 27348-27357.

[6] R. M. Strieter, J. A. Belperio, M. D. Burdick, M. P. Keane, *Current drug targets. Inflammation and allergy* **2005**, *4*, 23-26.

[7] M. Burger, T. Hartmann, J. A. Burger, I. Schraufstatter, *Oncogene* **2005**, *24*, 2067-2075.

[8] L. J. Miller, S. H. Kurtzman, Y. Wang, K. H. Anderson, R. R. Lindquist, D. L. Kreutzer, *Anticancer research* **1998**, *18*, 77-81.

[9] B. L. Richards, R. J. Eisma, J. D. Spiro, R. L. Lindquist, D. L. Kreutzer, *Am J Surg* **1997**, *174*, 507-512.

[10] J. Norgauer, B. Metzner, I. Schraufstatter, *Journal of immunology* **1996**, *156*, 1132-1137.

[11] H. Takamori, Z. G. Oades, R. C. Hoch, M. Burger, I. U. Schraufstatter, *Pancreas* **2000**, *21*, 52-56.

[12] G. Venkatakrishnan, R. Salgia, J. E. Groopman, *Journal of Biological Chemistry* **2000**, *275*, 6868-6875.

[13] D. J. Ceradini, A. R. Kulkarni, M. J. Callaghan, O. M. Tepper, N. Bastidas, M. E. Kleinman, J. M. Capla, R. D. Galiano, J. P. Levine, G. C. Gurtner, *Nat Med* **2004**, *10*, 858-864.

[14] I. Petit, D. Jin, S. Rafii, *Trends Immunol* **2007**, *28*, 299-307.

[15] F. Balkwill, *Seminars in Cancer Biology* **2004**, *14*, 171-179.

[16] A. E. Proudfoot, T. M. Handel, Z. Johnson, E. K. Lau, P. LiWang, I. Clark-Lewis, F. Borlat, T. N. Wells, M. H. Kosco-Vilbois, *Proceedings of the National Academy of Sciences of the United States of America* **2003**, *100*, 1885-1890.

[17] Y. R. Zou, A. H. Kottmann, M. Kuroda, I. Taniuchi, D. R. Littman, *Nature* **1998**, *393*, 595-599.

[18] K. A. Molyneaux, H. Zinszner, P. S. Kunwar, K. Schaible, J. Stebler, M. J. Sunshine, W. O'Brien, E. Raz, D. Littman, C. Wylie, R. Lehmann, *Development* **2003**, *130*, 4279-4286.

[19] C. T. Veldkamp, F. C. Peterson, A. J. Pelzek, B. F. Volkman, *Protein science : a publication of the Protein Society* **2005**, *14*, 1071-1081.

[20] A. Muller, B. Homey, H. Soto, N. F. Ge, D. Catron, M. E. Buchanan, T. McClanahan, E. Murphy, W. Yuan, S. N. Wagner, J. L. Barrera, A. Mohar, E. Verastegui, A. Zlotnik, *Nature* **2001**, *410*, 50-56.

[21] J. Hesselgesser, M. Liang, J. Hoxie, M. Greenberg, L. F. Brass, M. J. Orsini, D. Taub, R. Horuk, *J Immunol* **1998**, *160*, 877-883.

[22] C. T. Veldkamp, J. J. Ziarek, J. Su, H. Basnet, R. Lennertz, J. J. Weiner, F. C. Peterson, J. E. Baker, B. F. Volkman, *Protein science : a publication of the Protein Society* **2009**, *18*, 1359-1369.

[23] L. J. Drury, J. J. Ziarek, S. Gravel, C. T. Veldkamp, T. Takekoshi, S. T. Hwang, N. Heveker, B. F. Volkman, M. B. Dwinell, *Proceedings of the National Academy of Sciences of the United States of America* **2011**, *108*, 17655-17660.

[24] R. K. Ganju, S. A. Brubaker, J. Meyer, P. Dutt, Y. Yang, S. Qin, W. Newman, J. E. Groopman, *The Journal of Biological Chemistry* **1998**, *273*, 23169-23175.

[25] S. Kanki, V. F. M. Segers, W. Wu, R. Kakkar, J. Gannon, S. U. Sys, A. Sandrasagra, R. T. Lee, *Circulation Heart Failure* **2011**, *4*, 509-518.

[26] F. Jin, U. Brockmeier, F. Otterbach, E. Metzen, *Molecular Cancer Research* **2012**, *10*, 1021-1031.

[27] B. Wang, W. Wang, W. Niu, E. Liu, X. Liu, J. Wang, C. Peng, S. Liu, L. Xu, L. Wang, J. Niu, *Carcinogenesis* **2014**, *35*, 282-291.

[28] S. A. Rempel, S. Dudas, S. Ge, J. A. Gutierrez, *Clinical Cancer Research* **2006**, *2*, 102-111.